

LI

LABORATORY INVESTIGATION

THE BASIC AND TRANSLATIONAL PATHOLOGY RESEARCH JOURNAL

ABSTRACTS

(218-291)

CYTOPATHOLOGY

2022



USCAP 111TH ANNUAL MEETING

REAL INTELLIGENCE



MARCH 19-24, 2022 LOS ANGELES, CALIFORNIA

Published by

SPRINGER NATURE

www.ModernPathology.org

 **USCAP**
Creating a Better Pathologist

AN OFFICIAL JOURNAL OF THE
UNITED STATES AND CANADIAN
ACADEMY OF PATHOLOGY

EDUCATION COMMITTEE

Rhonda K. Yantiss
Chair

Kristin C. Jensen
Chair, CME Subcommittee

Laura C. Collins
Chair, Interactive Microscopy Subcommittee

Yuri Fedoriw
Short Course Coordinator

Ilan Weinreb
Chair, Subcommittee for Unique Live Course Offerings

Carla L. Ellis
Chair, DEI Subcommittee

Adebowale J. Adeniran

Kimberly H. Allison

Sarah M. Dry

William C. Faquin

Karen J. Fritchie

Jennifer B. Gordetsky

Levon Katsakhyan, Pathologist-in-Training

Melinda J. Lerwill

M. Beatriz S. Lopes

Julia R. Naso, Pathologist-in-Training

Liron Pantanowitz

Carlos Parra-Herran

Rajiv M. Patel

Charles "Matt" Quick

David F. Schaeffer

Lynette M. Sholl

Olga K. Weinberg

Maria Westerhoff

ABSTRACT REVIEW BOARD

Benjamin Adam
Oyedele Adeyi
Mariam Priya Alexander
Daniela Allende
Catalina Amador
Vijayalakshmi Ananthanarayanan
Tatjana Antic
Manju Aron
Roberto Barrios
Gregory R. Bean
Govind Bhagat
Luis Zabala Blanco
Michael Bonert
Alain C. Borczuk
Tamar C. Brandler
Eric Jason Burks
Kelly J. Butnor
Sarah M. Calkins
Weibiao Cao
Wenqing (Wendy) Cao
Barbara Ann Centeno
Joanna SY Chan
Kung-Chao Chang
Hao Chen
Wei Chen
Yunn-Yi Chen
Sarah Chiang
Soo-Jin Cho
Shefali Chopra
Nicole A. Cipriani
Cecilia Clement
Claudiu Cotta
Jennifer A. Cotter
Sonika M. Dahiya
Elizabeth G. Demicco
Katie Dennis
Jasreman Dhillon
Anand S. Dighe
Bojana Djordjevic
Michelle R. Downes
Charles G. Eberhart
Andrew G. Evans
Fang Fan

Julie C. Fanburg-Smith
Gelareh Farshid
Michael Feely
Susan A. Fineberg
Dennis J. Firschau
Gregory A. Fishbein
Agnes B. Fogo
Andrew L. Folpe
Danielle Fortuna
Billie Fyfe-Kirschner
Zeina Ghorab
Giovanna A. Giannico
Anthony J. Gill
Tamar A. Giordadze
Alessio Giubellino
Carolyn Glass
Carmen R. Gomez-Fernandez
Shunyou Gong
Purva Gopal
Abha Goyal
Christopher C. Griffith
Ian S. Hagemann
Gillian Leigh Hale
Suntrea TG Hammer
Malini Harigopal
Kammi J. Henriksen
Jonas J. Heymann
Carlo Vincent Hojilla
Aaron R. Huber
Jabed Iqbal
Shilpa Jain
Vickie Y. Jo
Ivy John
Dan Jones
Ridas Juskevicius
Meghan E. Kapp
Nora Katabi
Francesca Khani
Joseph D. Khoury
Benjamin Kipp
Veronica E. Klepeis
Christian A. Kunder
Stefano La Rosa

Stephen M. Lagana
Keith K. Lai
Goo Lee
Michael Lee
Vasiliki Leventaki
Madelyn Lew
Faqian Li
Ying Li
Chieh-Yu Lin
Mikhail Lisovsky
Lesley C. Lomo
Fang-I Lu
aDeqin Ma
Varsha Manucha
Rachel Angelica Mariani
Brock Aaron Martin
David S. McClintock
Anne M. Mills
Richard N. Mitchell
Hiroshi Miyamoto
Kristen E. Muller
Priya Nagarajan
Navneet Narula
Michiya Nishino
Maura O'Neil
Scott Roland Owens
Burcin Pehlivanoglu
Deniz Peker Barclift
Avani Anil Pendse
Andre Pinto
Susan Prendeville
Carlos N. Prieto Granada
Peter Pytel
Stephen S. Raab
Emilian V. Racila
Stanley J. Radio
Santiago Ramon Y Cajal
Kaaren K Reichard
Jordan P. Reynolds
Lisa M. Rooper
Andrew Eric Rosenberg
Ozlen Saglam
Ankur R. Sangoi

Kurt B. Schaberg
Qiuying (Judy) Shi
Wonwoo Shon
Pratibha S. Shukla
Gabriel Sica
Alexa Siddon
Anthony Sisk
Kalliopi P. Siziopikou
Stephanie Lynn Skala
Maxwell L. Smith
Isaac H. Solomon
Wei Song
Simona Stolnicu
Adrian Suarez
Paul E. Swanson
Benjamin Jack Swanson
Sara Szabo
Gary H. Tozbikian
Gulisa Turashvili
Andrew T. Turk
Efsevia Vakiani
Paul VanderLaan
Hanlin L. Wang
Stephen C. Ward
Kevin M. Waters
Jaclyn C. Watkins
Shi Wei
Hannah Y. Wen
Kwun Wah Wen
Kristy Wolniak
Deyin Xing
Ya Xu
Shaofeng N. Yan
Zhaohai Yang
Yunshin Albert Yeh
Huina Zhang
Xuchen Zhang
Bihong Zhao
Lei Zhao

To cite abstracts in this publication, please use the following format: **Author A, Author B, Author C, et al. Abstract title (abs#). In "File Title." *Laboratory Investigation* 2022; 102 (suppl 1): page#**

218 Telecytology at Remote Sites with a Portable Digital Microscope & Slide Scanner: Comparison of Different Scanning Modalities

Syed Abbas¹, Terrance Lynn¹, Haiyan Liu¹, Fan Lin¹, Shaobo Zhu¹, Mark Massak¹, Sara Monaco¹
¹Geisinger Medical Center, Danville, PA

Disclosures: Syed Abbas: None; Terrance Lynn: None; Haiyan Liu: None; Fan Lin: None; Shaobo Zhu: None; Mark Massak: None; Sara Monaco: None

Background: Rapid on-site evaluation (ROSE) by remote cytopathologists using telecytology has expanded with the increase in small biopsies. In sites requiring ROSE without cytopathology staff present on-site, robotic microscopy and rapid slide scanners can be advantageous. We compared telecytology ROSE using a mini-slide scanner with various scanning modalities and compared performance with review of glass slides.

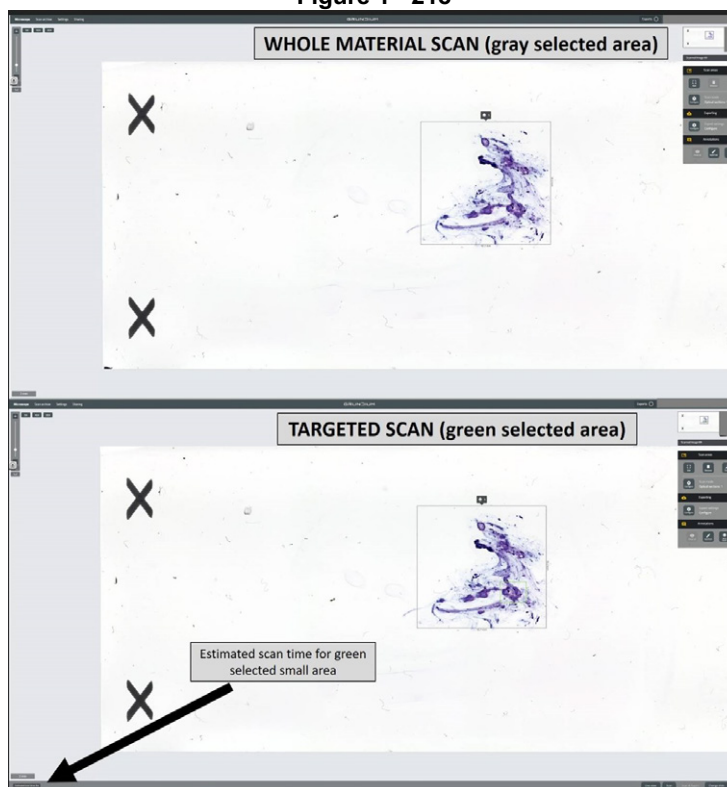
Design: The Grundium Ocus@20 portable digital microscope/slide scanner was used in a remote site in our rural healthcare system lacking on-site cytopathology staff. Telecytology ROSE was compared to glass slide reads with a 2-week washout, to examine concordance. The time for scanning the whole slide material was compared to targeted scanning of small areas of interest. [Figure 1] In addition, the ease of use for the remote pathologist was documented semiquantitatively (scale of 1 (easy)-5 (hard)). At least 2 pathologists evaluated each slide.

Results: A total of 66 reviews were completed on 30 cases by 6 pathologists. The cases included 22 (73%) fine needle aspirations (FNA) and 8 (27%) core needle biopsy (CNB) touch preparations (TPs), from a variety of locations (4(13%) lung, 4(13%) liver, 7(23%) thyroid, 7(23%) lymph node, 2(7%) bone/soft tissue, 6(20%) other). There were 19 (63.5%) neoplastic, 7 (23.5%) benign, 3 (10%) non-diagnostic, and 1 (3%) atypical. There was 1 (1.5%) major and 8 (12%) minor disagreements between telecytology and glass diagnoses. The average time to evaluate glass slides was faster (average 1.9 minutes) than targeted scan reviews (3.2 min) and whole material review (6.5 min). The average rating for ease of use was 1.6, with non-diagnostic cases being more difficult (2.8).[Table 1]

CASE INFORMATION					TELECYTOLOGY			GLASS
Case	FNA site	Type of Preparation	Number of Pathologist Reviews	Diagnosis	Avg Time to Diagnose- Whole area (min)	Avg Time to Diagnose- Targeted area (min)	Tele Ease of use (1 easy-5 hard)	Avg Time Taken to diagnose Glass (min)
1	Thyroid	FNA smears	3	Benign colloid nodule	5.8	4.1	1.6	2.6
2	Thyroid	FNA smears	3	Benign colloid nodule	6.4	5.6	2	2.3
3	Thyroid	FNA smears	3	AUS/FLUS	6.6	4.8	2.3	3.0
4	Liver	CNB TP	3	Metastatic carcinoma	8	4.2	3.3	2.6
5	Pancreas	FNA smears	3	Neuroendocrine tumor	5.7	4.4	1.6	2.6
6	Liver	FNA smears	3	Neuroendocrine tumor	9.8	5.1	1.3	2.0
7	LN- EBUS TBNA	FNA smears	2	Non diagnostic	8.9	3.7	3	1.0
8	LN- EBUS TBNA	FNA smears	2	Negative, lymphocytes	8.1	3.1	1	1.0
9	LN- EBUS TBNA	FNA smears	2	Negative, lymphocytes	8.1	3.1	1	2.0
10	LN- EBUS TBNA	FNA smears	2	Non diagnostic	8	2.7	2.5	1.0
11	Rib lesion	CNB TP	2	Lymphoma	7	2.6	1	2.0
12	Pelvic mass	CNB TP	2	Mucinous neoplasm	5.4	3.7	1.5	3.0
13	Gastric mass, EUS	FNA smears	2	Spindle cell neoplasm	6.2	3.5	1	1.0
14	Left neck	FNA smears	2	NSCLC	8.6	5.1	1	3.0
15	Lung	FNA smears	2	Chondromyxoid neoplasm	8.6	2.5	2	2.0
16	Lung	CNB TP	2	NSCLC	3.7	2.5	1	3.0
17	Thyroid/neck mass	FNA smears	2	Metastatic carcinoma	6.7	2.6	1	3.0
18	Lung	FNA smears	2	Basaloid neoplasm	7.5	2.6	1.5	2.0
19	Thyroid	FNA smears	2	Benign colloid nodule	9.5	3.7	2	2.0
20	Intra-abdominal mass	CNB TP	2	Small round blue cell tumor	8.9	3.1	3	2.0
21	Pancreas	FNA smears	2	Adenocarcinoma	7.7	2.5	1	2.0

22	LN- EBUS TBNA	FNA smears	2	Neuroendocrine carcinoma	6.1	3.6	1	2.0
23	BONE	CNB TP	2	Non diagnostic	5	2.7	3	1.5
24	LUNG	FNA smears	2	NSCLC	3.4	3.2	1	1.0
25	LN- EBUS TBNA	FNA smears	2	NSCLC	6.5	3.1	1.5	3.0
26	Thyroid	FNA smears	2	Benign colloid nodule	5.5	2.6	1	1.0
27	Liver	CNB TP	2	Metastatic carcinoma	5.7	2.0	1	1.5
28	Liver	CNB TP	2	Neuroendocrine tumor	2.7	2.0	1	1.0
29	LN- EBUS TBNA	FNA smears	2	Metastatic NSCLC	4.5	3.0	2	1.0
30	Thyroid	FNA smears	2	Benign colloid nodule	4.4	2.0	2	2.0
AVERAGE					6.5	3.2	1.6	1.9

Figure 1 - 218



Conclusions: Although glass slides are quicker to evaluate, small slide scanners offer a cost-effective way to deliver ROSE at remote sites lacking cytology support and was relatively easy for pathologists. The flexibility in using different scan modes (whole or targeted) can help in different situations, with targeted scanning being faster than whole material scanning. Scanning worked best for small CNB TPs given the smaller area of slide coverage and limited slides prepared but was more challenging in cases with multiple slides prepared, particularly EBUS FNAs and non-diagnostic cases, with smears covering the majority of the slide, given the increased time for the scan and review, and the concern of missing lesional material.

219 Are Copy Number Variations Identified in Thyroid Fine Needle Aspiration Specimens Associated with Hurthle Cell Morphology?

Rita Abi-Raad¹, Manju Prasad¹, Adebowale Adeniran¹, Guoping Cai²

¹Yale School of Medicine, New Haven, CT, ²Yale University, New Haven, CT

Disclosures: Rita Abi-Raad: None; Manju Prasad: None; Adebowale Adeniran: None; Guoping Cai: None

Background: Copy number variations (CNVs) have been reported in non-thyroid oncocyctic neoplasms, such as renal oncocytoma and chromophobe renal cell carcinoma. The association of CNVs with Hurthle cell lesions of the thyroid is still unclear. In this

study, we retrospectively reviewed the FNA cytomorphology of the cases with CNVs and correlated them with histopathologic follow-up.

Design: The pathology database was searched for thyroid FNA cases with a diagnosis of follicular lesion of undetermined significance (FLUS) and follicular neoplasm (FN)/Hurthle cell neoplasm (HCN) with molecular testing performed by ThyroSeq v3 GC between October 2017 and January 2021. Patients' demographics, cytology, ThyroSeq testing and histopathologic follow-up were retrospectively reviewed. Fischer exact test was used to analyze the relationship between variables.

Results: A total of 324 thyroid FNA cases including 228 FLUS, 46 HCN and 50 FN cases were included in the study. FLUS cases were further classified as Hurthle cell type (FLUS-HCT, 20 cases) and non-Hurthle cell type (FLUS-NHCT, 208 cases). HCN or FLUS-HCT cases showed a much higher prevalence of CNVs or CNVs with other molecular alterations (23/66=35%), compared to those classified as FN or FLUS-NHCT 14/258=5%) ($p<0.001$). A total of 105 patients (32%) had surgical follow-up. Cases with CNVs (with or without other molecular alterations) were more likely to be neoplastic (18/26; 69%), mostly with follicular pattern neoplasm (14/18, 78%) compared to cases without any molecular alteration (8/24=33% neoplastic) ($p<0.05$). In HCN/FLUS-HCT cases with CNVs ($n=14$), Hurthle cell morphology was seen in 13 (93%) cases on surgical follow up, in contrast to those without CNVs ($n=17$) where only 6 cases (35%) showed Hurthle cell morphology ($p<0.05$). Furthermore, cases with CNVs were more likely to be neoplastic (9/14, 64%) on surgical follow-up compared to the cases without CNVs (3/17, 18%) ($p<0.05$).

Conclusions: Our study demonstrated that CNVs identified in thyroid FNAs are associated with Hurthle cell morphology. The presence of CNVs with a cytological diagnosis of HCN/FLUS-HCT is suggestive of a neoplasm with Hurthle cell features, which may help triage patients who would benefit from surgical management.

220 Challenging Diagnosis in Thyroid Fine Needle Aspiration - Atypia of Undetermined Significance/Follicular Lesion of Undetermined Significance (AUS/FLUS): Clinical Follow-Up and Cyto-Histological Correlation

Andrea Agualimpia Garcia¹, Ya Xu¹

¹Baylor College of Medicine, Houston, TX

Disclosures: Andrea Agualimpia Garcia: None; Ya Xu: None

Background: The category of atypia of undetermined significance/follicular lesion of undetermined significance (AUS/FLUS) in thyroid reporting cytopathology remains as a grey zone and is challenging.

Design: We reviewed 843 thyroid fine needle aspirations (FNAs) performed in our hospital between June 2019 and August 2021. Clinical history, cytology and surgical specimens were studied on cases with the cytology diagnosis under the category of AUS/FLUS. The thyroid FNA samples were processed by direct smears with Diff-Quik and *Papanicolaou stains*, and ThinPrep Method.

Results: 186 of 843 (186/843, 22.1%) thyroid FNA cases on 145 patients had at least one diagnosis under the category of AUS/FLUS. There were 139 (139/145, 95.8 %) females and 6 (6/145, 4.1%) males with an age range of 21-75 years old. The thyroid nodules were 1.7-8.6 cm in size. There were 77 (77/145, 53.1%) patients with no follow-up FNA or resection, and 27 (27/145, 18.6%) patients followed by thyroid resection only. 41 (41/145, 28.3%) patients received repeat FNAs. Among these 41 repeat FNAs, 4 (4/41, 9.8%) cases had the most recent FNA results as non-diagnostic, 18 (18/41, 43.9%) cases as benign, 15 (15/41, 36.6%) cases as AUS/FLUS, 1 (1/41, 2.4%) case as follicular neoplasm, 3 (3/41, 7.3%) cases as suspicious for papillary thyroid carcinoma (PTC) or PTC. There were total 36 (36/145, 24.8%) patients underwent thyroid resection. In these 36 surgical specimens, nodular hyperplasia was found in 19 (19/36, 52.8%) patients (78.9% patients without repeat FNAs), follicular adenoma in 5 (5/36, 13.9%) patients, non-invasive follicular thyroid neoplasm with papillary-like nuclear features (*NIFTP*) in one (1/36, 2.7%) patient, follicular tumor of uncertain malignant potential in one (1/36, 2.7%) patient, and malignancy in 9 (9/36, 25%) patients including 7 PTCs, 1 follicular carcinoma, and 1 anaplastic carcinoma. The risk of malignancy in AUS/FLUS category confirmed by surgery was 25%.

Conclusions: The percentage of AUS/FLUS in thyroid FNAs (22.1%) in our hospital is higher than the reported 8-10%, and the risk of malignancy of these lesions (25%) is within the published range of 10-30%. Under the category of AUS/FLUS, the repeat FNAs display 43.9% of cases converted to benign, and 36.6% remain unchanged. 78.9% of AUS/FLUS cases without repeat FNAs, followed by thyroid resection, are diagnosed as nodular hyperplasia. The cyto-histological correlation has further revealed the importance of repeat FNA in patients with AUS/FLUS.

221 Deep Learning Approach for Classifying Thyroid Nodules

Mona Alabrak¹, Mohammed Megahed², Ammar Mohammed², Habiba Elfandy³, Neveen Tahoun⁴, Hoda Ismail⁵
¹National Cancer Institute Cairo University, Cairo, Egypt, ²Cairo University, Giza, Egypt, ³Dana-Farber Cancer Institute, ⁴NCI, Cairo, Shobra, Egypt, ⁵National Cancer Institute Cairo University, Giza, Egypt

Disclosures: Mona Alabrak: None; Mohammed Megahed: None; Ammar Mohammed: None; Habiba Elfandy: None; Neveen Tahoun: None; Hoda Ismail: None

Background: Thyroid nodules fine-needle aspiration cytology (FNAC) has higher sensitivity and predictive value for diagnosis than any other single diagnostic method. Among Bethesda classification, category III AUS/FLUS represents a heterogeneous population which in many cases cannot be classified as benign (Bethesda category II) or follicular neoplasm (Bethesda category IV), or others. The Bethesda category III carries a risk of malignancy 10-30% in unresected nodules. Application of ancillary tests is encouraged but are not always available on aspirates. Therefore, a deep learning model is used for thyroid nodule classification into benign (Bethesda category II) and follicular neoplasm (Bethesda category IV), including those cases diagnosed as FLUS by cytology. We aimed to explore the added value of applying artificial intelligence to increase the sensitivity of FNAC in Bethesda category III.

Design: Images were obtained from Pap-stained cytology smears of pathologically confirmed 24 thyroid cases including hyperplasia, follicular adenoma and carcinoma (12 case, each). Of those cases, 8 were diagnosed as FLUS (Bethesda category III) in FNAC. Images of regions of interest (ROI) are captured for 2008 ROIs, at 40X magnification, 1606 ROIs were used as training set and 402 ROIs as validation set.

A proposed deep learning model based on convolution neural network (CNN) has been constructed with different layers of convolutional, pooling, and fully connected layers. We applied image processing and data augmentation techniques and trained the CNN in 100 epochs with batch size 32

Results: In the validation set, our CNN model achieved an accuracy of 90.05 %, and the area under the ROC curve was 96.0 % with mean sensitivity and specificity 91.63% and 88.0 %, respectively.

Figure 1 - 221

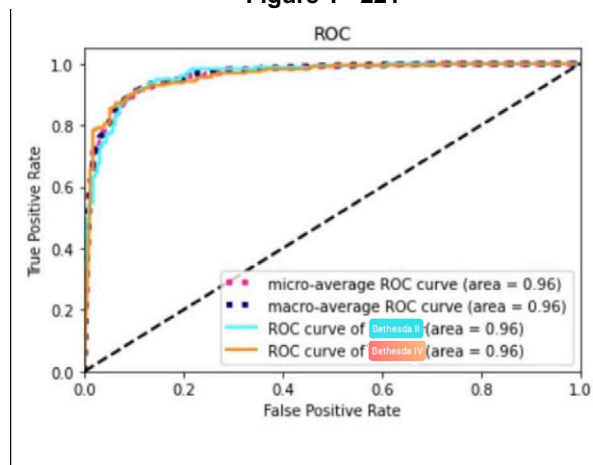
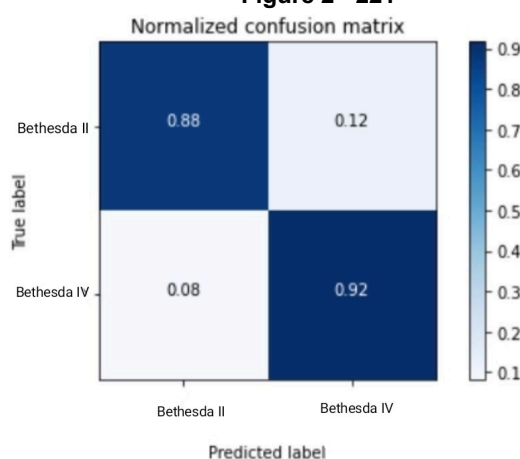


Figure 2 - 221



Conclusions: Deep learning models are promising for the classification of thyroid nodule cytology, with an expected increase in accuracy after increasing the sample size (images) in training the deep learning model.

222 Molecular Profiling of Cytology Cell Block Samples in Non-Small Cell Carcinoma of Lung: A Large Metropolitan Institutional Experience

Mohamed Alhamar¹, Oluwayomi Oyedeji², Kanika Arora², Brian Theisen³, Lisi Yuan², Ziyang Zhang², Daniel Schultz², Dhananjay Chitale³, Kyle Perry²

¹Memorial Sloan Kettering Cancer Center, New York, NY, ²Henry Ford Health System, Detroit, MI, ³Henry Ford Hospital, Detroit, MI

Disclosures: Mohamed Alhamar: None; Oluwayomi Oyedeji: None; Kanika Arora: None; Brian Theisen: None; Lisi Yuan: None; Ziyang Zhang: None; Daniel Schultz: None; Dhananjay Chitale: None; Kyle Perry: None

Background: Identifying targetable mutations is the standard of practice in the management of advanced non-small cell lung carcinoma (NSCLC). Candidates for assessment of targetable mutations often have diagnostic material limited to cytologic specimens.

We aimed to 1) Evaluate the feasibility & success of detecting genetic alterations using molecular & Florescent In-Situ Hybridization (FISH) testing based only on cell block material from patients with NSCLC 2) Compare our adenocarcinoma mutations distribution results with published data from The Cancer Genome Atlas (TCGA) of treatment naive lung adenocarcinoma.

Design: We identified 102 NSCLC cases from 2019-2020 that were tested for targeted Next Generation Sequencing (NGS) panels and *ALK* & *ROS1* FISH using only cell block material. Clinicopathologic findings including age, gender, specimen source, type of NSCLC, clinical stage, type of assay, & sequencing results were recorded.

Results: There were 54% males with median age of 70 (range 48-88). Tumor types included: 74/102 adenocarcinoma, 12/102 squamous cell carcinoma, 16/102 poorly differentiated & other carcinomas. Sources of tissues were: Lung (19/102), mediastinal lymph node (58/102), pleural fluid (20/102), & distant metastasis (5/102). Clinical stages were as follows: II=6 cases, III=15 cases, IV=81 cases.

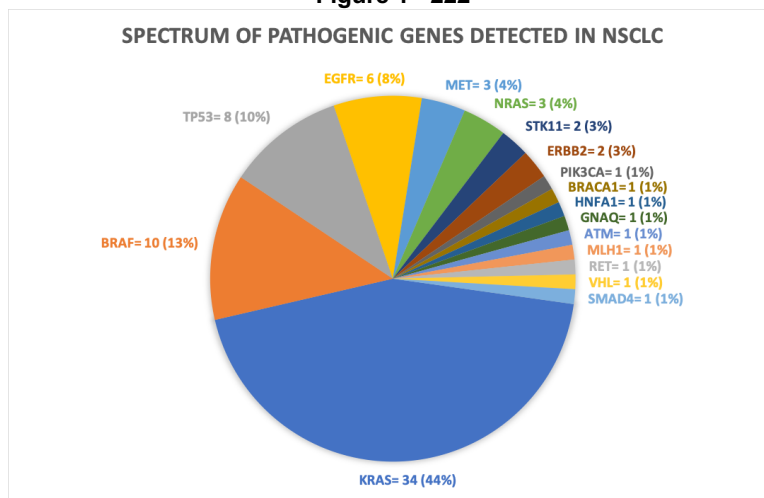
NGS was performed on 101 cases; 6 of which showed insufficient tumor quantity (QNS). 54/95 revealed pathogenic variants while no alterations detected in 34 cases & 7 cases showed variant of undetermined significance (VOUS). The average number of alterations per case was 1.1 (range 0-6) & average VOUS per case was 0.3 (range 0-5). Figure 1 depicts the spectrum of pathogenic genes detected in 54 cases. RNA Fusion panel was performed in 42 cases; 3 QNS cases & only 1 case showed *SLC34A2-ROS1* fusion. 2/35 cases were positive by *ALK* FISH & 1 case was QNS. 1/10 case was positive for *ROS1* FISH.

Table 1 compares our key adenocarcinoma detected genes with published data from TCGA of lung adenocarcinoma. Apart from *TP53* & *STK11*, our findings are relatively similar to TCGA.

Pathogenic genes detected in lung adenocarcinoma	Frequency (%)	Data from TCGA* (%)	P-value
<i>KRAS</i>	27 (40%)	76 (33%)	0.31
<i>BRAF</i>	9 (13%)	23 (10%)	0.45
<i>TP53</i>	8 (12%)	106 (46%)	< 0.00001
<i>EGFR</i>	6 (9%)	32 (14%)	0.27
<i>MET</i>	3 (4%)	16 (7%)	0.58
<i>STK11</i>	2 (3%)	39 (17%)	0.002
<i>PIK3CA</i>	1 (1%)	16 (7%)	0.13

* The Cancer Genome Atlas Research Network. Comprehensive molecular profiling of lung adenocarcinoma. Nature 511, 543–550 (2014).

Figure 1 - 222



Conclusions: 57% patients showed genomic variants detected by NGS using cell blocks only. The proportion & type of gene alterations detected is concordant with those normally detected in surgical pathology specimens of lung adenocarcinoma (except for *TP53* & *STK11* likely due to sequencing coverage limited to hotspot exons in our cohort). Molecular testing in cytology specimens is feasible & is consonant with larger sample types.

223 Utility of High-Risk HPV mRNA In Situ Hybridization in Fine-Needle Aspiration Cytology

Turky Alkathery¹, Carmen Gomez-Fernandez², Yiqin Zuo³, Nicolas Millan⁴, Youley Tjendra¹, Monica Garcia-Buitrago⁵, Merce Jorda², Jaylou Velez Torres²

¹Jackson Memorial Hospital/University of Miami Hospital, Miami, FL, ²University of Miami Miller School of Medicine, Miami, FL, ³University of Miami, Miami, FL, ⁴Jackson Memorial Hospital/ University of Miami Hospital, Miami, FL, ⁵University of Miami Miller School of Medicine/Jackson Health System, Miami, FL

Disclosures: Turkey Alkathery: None; Carmen Gomez-Fernandez: None; Yiqin Zuo: None; Nicolas Millan: None; Youley Tjendra: None; Monica Garcia-Buitrago: None; Merce Jorda: None; Jaylou Velez Torres: None

Background: Assessment of human papillomavirus (HPV) status is critical for treatment and prognosis of patients with oropharyngeal squamous cell carcinoma. Patients often present with enlarged cervical lymph nodes, and fine-needle aspiration cytology (FNAC) is frequently the initial diagnostic procedure. While p16 is the most widely used surrogate marker, the lack of specificity in cervical lymph nodes, and problems with technical interpretation can limit its utility in FNAC. High-risk (HR) HPV mRNA in situ hybridization (ISH) testing for E6/E7 proteins has emerged as a specific way to assess HPV status in FNAC cell blocks of cervical lymph nodes. Here, we evaluate the usefulness of HR HPV mRNA ISH in conventional smears and liquid based cytology (Thinprep).

Design: The pathology database was queried for FNAC samples diagnosed as metastatic squamous cell carcinoma. FNAC cases with proven HPV-related SCC (either by p16 or HR HPV ISH) in corresponding surgical specimens were selected. HR HPV mRNA ISH (HPV 16/18/31/33) was performed on conventional smears and ThinPrep. Adequate samples contained at least 100 tumor cells. The result was considered positive if there were any cytoplasmic or nuclear signals (brown dot like staining) in tumor cells. The clinical data were obtained from available medical records.

Results: We identified 29 cases, composed of 26 men and 3 women with a mean age of 58 years (range, 42-68 years). HR HPV mRNA ISH was performed on 20 smears and 9 Thinprep slides. The metastatic sites included: neck lymph nodes (28), and station seven subcarinal lymph node (1). The primary sites were in tonsil (13), base of tongue (12), nasal septum (1), nasopharynx (1), and unknown (2). All FNAC specimens were positive for HR HPV mRNA ISH. The staining pattern was sub-divided into strong and diffuse (11), moderate (4) and low (14) number of signals.

Conclusions: HR HPV mRNA ISH staining pattern was easy to interpret with diffuse, moderate or low number of signals restricted to the tumor cells. Cases with low number of signals can occur and are likely related to low transcriptionally active HPV mRNA

levels in the tumor cells. HR HPV mRNA ISH is highly sensitive for the evaluation of HPV status on FNAC samples and can be reliably performed on smears or liquid based cytology, particularly when cell blocks are unavailable or paucicellular. Our study results suggest that HR HPV mRNA ISH should be used as the initial testing modality for HPV assessment in FNAC specimens.

224 Prevalence of HR- HPV Genotypes with Abnormal Cervical Pap Smear Findings; a Single Institutional Experience with Co-Testing

Hermineh Aramin¹, Somaye Zare², Ashlee Becker¹, Farnaz Hasteh²

¹UC San Diego Medical Center, San Diego, CA, ²University of California, San Diego, La Jolla, CA

Disclosures: Hermineh Aramin: None; Somaye Zare: None; Ashlee Becker: None; Farnaz Hasteh: None

Background: New recommendation from the American Cancer Society is emphasizing on high risk human papilloma virus (HR-HPV) testing alone over HR-HPV testing in combination with cytology (co-testing) for cervical cancer screening. HPV-16/18 genotypes along with a cocktail test of 12 other HR-HPV genotypes received Food and Drug Administration approval as an option for primary screening in women who are 25 years old or older. The current study reports the number of HR-HPV results (16, 18 or other types) among patients with abnormal pap tests including LSIL, HSIL, Atypical endocervical glandular cells (AEGC)/AIS and invasive carcinomas of cervix (squamous and glandular) in our institution.

Design: From January 2019 to June 2021, 725 women with diagnoses of LSIL, HSIL, AEGC /AIS and cervical carcinoma on cervical Pap smear were included in the study using quarterly TABLOU statistics. The clinical characteristics of the patients is demonstrated in Table-1.

Results: 503 (73.4%) of patients with abnormal pap tests were HR-HPV positive and 182 (26.6%) patients were HR-HPV negative. Among women with LSIL cytology, total HR-HPV infection rate was 65.5% (331 out of 505), while in the group of women with severe cytological abnormalities, the rates were 96.1% (149 out of 155) for HSIL and 91% (10 out of 11) for SCC. Of 54 pap smears with glandular abnormalities, 40 corresponded to endometrial pathology and 14 showed endocervical abnormalities. The rate of positive HR-HPV among patients with AEGC and AIS cytology, was 85.7 % (6 out of 7) and 100 % (7 out of 7) for cervical adenocarcinoma, respectively. In HPV-positive cases the highest prevalence was reported in cervical adenocarcinoma, HSIL and SCC. Majority of HPV positive cases in LSIL and HSIL were significantly infected with non-16/18 HR-HPV genotypes (52.2 %, 54.1%, respectively).

Cytological diagnosis	LSIL	HSIL	SCC	AEGC/AIS	Cervical Adeno	Total
Positive	331(65.5%)	149 (96.1%)	10 (91%)	6 (85.7%)	7 (100%)	503 (73.4%)
Negative	174 (34.5%)	6 (3.8%)	1 (9.1%)	1(17.3%)	0 (0%)	182 (26.6%)
genotype 16	21 (4.2%)	44 (28.4%)	8 (72.7%)	1(17.3%)	3 (42.8%)	77 (11.2%)
genotype 18	5 (1%)	1 (0.6%)	0 (0%)	3 (42.8%)	4 (57.2%)	13 (1.9%)
genotype other than 16&18	264 (52.2%)	84 (54.1%)	2 (18.1%)	1(17.3%)	0 (0%)	355(51.8%)
genotype 16 and other	30 (5.9%)	15 (9.7%)	0 (0%)	0 (0%)	0 (0%)	45 (6.6%)
genotype 18 and other	10 (2.0%)	2 (1.3%)	0 (0%)	1(17.3%)	0 (0%)	13 (1.9%)
Total	505 (100%)	155 (100%)	11 (100%)	7 (100%)	7 (100%)	685 (100%)

Conclusions: Our findings support that infection with non-16/18 HR-HPV genotypes are likely to play a significant role in the pathogenesis of LSIL and HSIL. Additionally our data support that cervical cancer screening co-testing strategies that incorporate oncogenic HPV testing with cytology will be more beneficial for the detection of abnormal pap results compare to HR-HPV testing alone.

225 Telecytopathology for Rapid On-Site Evaluation (ROSE) Adequacy in Fine-Needle Aspiration of Pancreatic and Lung Lesions during COVID19 Pandemic

Hermineh Aramin¹, Anne Bartels², Vera Vavinskaya³, Jingjing Hu³, Somaye Zare², Omonigho Aisagbonhi², Ahmed Shabaik³, Farnaz Hasteh²

¹UC San Diego Medical Center, San Diego, CA, ²University of California, San Diego, La Jolla, CA, ³University of California, San Diego, San Diego, CA

Disclosures: Hermineh Aramin: None; Anne Bartels: None; Vera Vavinskaya: None; Jingjing Hu: None; Somaye Zare: None; Omonigho Aisagbonhi: None; Ahmed Shabaik: None; Farnaz Hasteh: None

Background: Telecytopathology (TCP) has a variety of different applications in clinical practice and is becoming more widely utilized especially during COVID pandemic. More recently, TCP use has been increasingly applied to the rapid on-site evaluation (ROSE) at our institution with immediate assessment by viewing cytologic smears remotely over web conferencing platform (zoom). As part of our quality control evaluation, we retrospectively investigated ROSE adequacy in two of the busiest FNA procedures at our institute (pancreas and lung) via TCP.

Design: The study includes retrospective review of 151 of pancreatic lesions and 242 lung lesions over a two-year period. The air dried Diff-Quick slides were evaluated on site for adequacy by the cytopathology fellow/ cytotechnologist and cytopathologists via TCP at the same time. The ROSE adequacy diagnosis is recorded and transcribed to the preliminary report. We reviewed the adequacy and preliminary ROSE assessment and compared it to the final diagnosis as the gold standard. The non-diagnostic rate and discrepancy rate between initial and final diagnosis were calculated.

Results: A total of 393 adequacy assessments of pancreas (151, 38%) and lung (242, 62%) were analyzed. Overall, 114 (75%) pancreatic cases and 199 (82%) lung lesions had adequate diagnosis at the time of the ROSE, while 37 (25%) of pancreatic cases and 43 (18%) of lung cases had non-adequate ROSE read specimens. Concordance between initial assessment of diagnosis and the final cytological diagnosis was identified in 94% (142 out of 151) of pancreatic cases and 93.4% (226 out of 242) of lung cases.

Of the discordant cases, the final diagnosis was upgraded to adenocarcinoma in 7/9 pancreatic lesions and either SCC, adenocarcinoma or atypia in 5/16 lung lesions. The final diagnosis was downgraded to benign category in 2/9 pancreatic lesions and 11/16 lung lesions.

Conclusions: Telecytopathology ROSE evaluation of pancreatic and lung lesions may have several advantages over in-person ROSE, including providing a suitable alternative technology, mitigating disease transmission during the COVID19 pandemic, while maximizing resources to allow more efficient use of the pathologist's time, thereby improving efficiency, eliminating downtime, and answering the increasing demand for on-site adequacy evaluation.

226 Fine Needle Aspiration of Synovial Sarcoma (SS): A 20-Year Retrospective Study of 30 Cases in a Single Institution

Sampson Boham¹, Harvey Cramer², Shaoxiong Chen³

¹Indiana University School of Medicine, Indianapolis, IN, ²Indiana University Health, Indianapolis, IN, ³Indiana University, Indianapolis, IN

Disclosures: Sampson Boham: None; Harvey Cramer: None; Shaoxiong Chen: None

Background: Synovial sarcoma (SS) is a rare mesenchymal malignancy histologically showing variable epithelial differentiation including biphasic, monophasic, and poorly differentiated subtypes. SS commonly occurs in the extremities but can occur at any anatomic location. The biological behavior of SS depends on the tumor stage, size and grade. SS diagnosis by FNA can be challenging.

Design: A computerized search of our laboratory information system was performed for the 20-year period from 1998 through 2018 to identify all cytology and surgical pathology cases in which the diagnosis of SS was rendered or considered in the differential diagnosis. All cytology, surgical pathology reports and clinical histories were retrospectively reviewed. All cytology slides were retrieved with final diagnoses and the morphological features re-evaluated.

Results: A total of 30 SS FNA cases were collected. The age of the patients ranged from 18 to 74 years with a mean age of 45. The female to male ratio was 1.3:1. The tumor sizes ranged from 0.8 to 20.0 cm with a mean of 8.17 cm. The FNA diagnoses were classified as follows: SS (17 cases, 57%), suspicious for SS (6 cases, 20%), spindle cell neoplasm (SCN) (5 cases, 17%) non-diagnostic (1 case, 3%), and other diagnoses (1 case, 3%). Histologic correlation was available for 24 FNA cases (80%). Among 17 cases diagnosed as SS by FNA, 14 cases (82%) were confirmed histologically while 3 cases had no histological follow-up. Histologic follow-up of the one non-diagnostic FNA showed SS with extensive tumor necrosis which likely accounted for the hypocellularity of that sample. All 5 FNA cases diagnosed as SCN proved to be SS on histologic follow-up. Smears and H&E-stained cell block sections showed scattered aggregates of malignant spindle cells. One lung FNA case misdiagnosed as Ewing sarcoma proved to be SS on resection. The predominant morphological pattern on the FNA slides was spindle cells with scant amphophilic cytoplasm, ovoid to spindled vesicular nuclei and inconspicuous nucleoli. All SS cases that were stained for TLE1 at the time of diagnosis showed strong diffuse nuclear positivity.

Conclusions: The above-mentioned morphological features in conjunction with the characteristic positive nuclear immunostaining for TLE1 are useful for diagnosing SS on FNA. All FNA cases diagnosed definitively as SS were confirmed histologically. If a diagnosis of SS is rendered by FNA, the diagnostic accuracy is at least 82%. The main obstacle for FNA diagnosis of SS is sample hypocellularity.

227 Assessing Rapid On-Site Evaluation (ROSE) for Adequacy of Endobronchial Ultrasound Transbronchial Needle Aspiration (EBUS-TBNA) Procedures Compared to A Direct-to-Cellblock Approach As a Response to COVID-19 Pandemic

Paul Boothe¹, Xing Zhao², Syeda Naqvi², Evita Henderson-Jackson², Nancy Mela², Barbara Centeno², Amit Tandon², Marilyn Bui²

¹H. Lee Moffitt Cancer Center & Research Institute, University of South Florida, Tampa, FL, ²H. Lee Moffitt Cancer Center & Research Institute, Tampa, FL

Disclosures: Paul Boothe: None; Xing Zhao: None; Syeda Naqvi: None; Evita Henderson-Jackson: None; Nancy Mela: None; Barbara Centeno: None; Amit Tandon: *Speaker*, Biodesix; *Speaker*, Johnson and Johnson; *Speaker*, Pinnacle; Marilyn Bui: *Consultant*, AstraZeneca, Visiopharm, ContextVision

Background: Rapid on-site evaluation (ROSE) of endobronchial ultrasound transbronchial needle aspiration (EBUS-TBNA) has been used as standard to improve diagnostic yield and to triage samples for additional testing. A method has been prompted to leveraging the expertise of cytotechnologists only or the utility of tele cytology. However, due to the COVID-19 pandemic, our institution had to discontinue ROSE for EBUS-TBNA, and instead adopted a direct-to-cellblock approach. This study aims to determine if removing ROSE affected the adequacy of samples obtained from the EBUS-TBNA cases, and if this new approach should be employed continuously for an extended period without jeopardizing the standard of care to the patient since we are still in the pandemic.

Design: We collected data of total 1903 EBUS-TBNA cases from 734 patients. 1097 cases were performed from 1/2019 to 3/2020 with ROSE on 452 patients; 806 cases were performed between 4/2020 to 12/2020 without ROSE on 282 patients, and the sample was sent directly to be processed as a cell block. Data variables collected included patient's age and gender, specimen sites and frequencies, and final cytopathological diagnosis. Calculated standardized residuals and fitted multivariate generalized linear model were performed at Moffitt Cancer Center & Research Institute Biostats Core using software SAS 9.4.

Results: On average, holding specimen site variable constant, a biopsy from a patient with ROSE is 0.936 ($=\exp^{-0.066}$) times less likely to be reported as 'Satisfactory' as compared to a biopsy taken from a patient without ROSE, and this difference is not statistically significant ($p = 0.785$).

Among all 6 categories of diagnosis, biopsies reported as 'Diagnostic for malignancy' are significantly different between ROSE and no ROSE groups with the standardized residual of 1.80 ($p = 0.036$) & only other significantly different category was 'Other'; however, a very small number of biopsies were reported in this category (3.5%).

Table 1. Multivariate generalized linear model using generalized estimating equation (GEE).

Parameter		P value Estimates	P Value	Odds Ratio	95% Confidence Limits of Odds Ratio		Type III (P value)
Intercept		2.3963	<.0001	10.982	6.893	17.496	
ROSE	Yes	-0.066	0.785	0.936	0.580	1.509	0.7857
	No	Ref	Ref	Ref	Ref	Ref	
SPECIMEN DESCRIPTION	LN, 4L	0.0462	0.8797	1.047	0.576	1.905	0.0238
	LN, 4R	0.9456	0.0041	2.57	1.35	4.91	
	LN, 11L	0.2786	0.4216	1.321	0.670	2.607	
	LN, 11R	0.4955	0.1559	1.641	0.828	3.254	
	LN, 7	0.7604	0.0098	2.139	1.201	3.810	
	LN, other	0.5107	0.3139	1.666	0.617	4.502	
	Mass	Ref	Ref	Ref	Ref	Ref	

Conclusions: The inadequacy rate of EBUS-TBNA was 6.4% higher on average in cases with ROSE when compared to a direct-to-cell block approach in this data set, however this difference was not statistically significant. This suggests that ROSE could be discontinued in favor of a direct-to-cell block approach. Although additional studies are needed, the discontinuation of ROSE for EBUS-TBNA would decrease the time and cost burden on cytopathology service while providing the same quality of care to the patient.

228 Metastatic Prostate Cancer - Assessment of Cytopathologic and Biomarker Features with Transdifferentiation and Clinical Correlates

Richard Cantley¹, Arul Chinnaiyan², Zachery Reichert², Rahul Mannan¹, Xiaoming (Mindy) Wang², Sylvia Zelenka-Wang³, Xuhong Cao², Daniel Spratt⁴, Ulka Vaishampayan², Todd Morgan², Joshi Alumkal², Liron Pantanowitz², Rohit Mehra²
¹Michigan Medicine, University of Michigan, Ann Arbor, MI, ²University of Michigan, Ann Arbor, MI, ³Michigan Center for Translational Pathology, Ann Arbor, MI, ⁴UH Cleveland Medical Center, Cleveland, OH

Disclosures: Richard Cantley: None; Arul Chinnaiyan: None; Zachery Reichert: None; Rahul Mannan: None; Xiaoming (Mindy) Wang: None; Sylvia Zelenka-Wang: None; Xuhong Cao: None; Daniel Spratt: None; Ulka Vaishampayan: None; Todd Morgan: None; Joshi Alumkal: None; Liron Pantanowitz: None; Rohit Mehra: None

Background: The diagnosis of metastatic prostatic carcinoma (MPC) by fine needle aspiration (FNA) cytology can usually be rendered by a combination of morphologic and immunohistochemical features. However, predictive and prognostic biomarkers are not routinely assessed in the workup of MPC. Additionally, MPC may present with increased proliferation or transformation to higher grade phenotypes such as small cell neuroendocrine carcinoma. This may occur de novo or under therapeutic pressures, especially second generation anti-androgen therapy and radiotherapy. Careful assessment of cytologic and biomarker features may provide useful therapeutic and prognostic information.

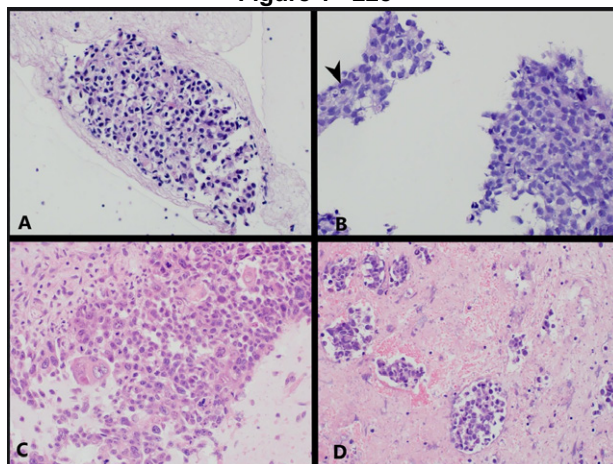
Design: We performed a retrospective review of anatomic pathology archives for cases of MPC diagnosed by FNA from 01/2014 - 01/2021. Cytology and cell block material (CBM) was re-reviewed in all cases. Patient age, previous surgical pathology findings, and prostate cancer therapies were recorded. An extensive biomarker workup was performed on CBM by immunohistochemistry. Prostate lineage markers (PLM) were performed, including NKX3.1, prostate specific antigen, and prostate specific membrane antigen. Additional markers performed included those of cell cycle dysfunction (Rb, Cyclin D1), Ki-67 proliferative index, neuroendocrine markers (synaptophysin, chromogranin), ERG, and PDL1. Based on our previous experience, cases were reclassified into one of four categories: I. Conventional MPC, II. Pro-proliferative MPC, III. Transdifferentiated MPC, and IV. High-grade neuroendocrine (small cell) MPC.

Results: 19 cases of MPC from 18 patients were identified, 16 with an established diagnosis of prostate cancer (Table 1). Primary prostate carcinomas were variable in grade but no variant morphologies (e.g. small cell) were described per reports. 13 FNA cases were conventional MPC (Fig 1A), all having retained PLMs and Ki-67 <=10%. No expression of ERG or neuroendocrine markers were seen in any conventional case. 6 cases showed progression (2 pro-proliferative, 2 transdifferentiated, 2 small cell/neuroendocrine transformation). Pro-proliferative cases (Fig 1B) exhibited mitoses (arrowhead) and apoptoses, ERG overexpression, increased Ki67 (20-60%), and retained PLMs. Transdifferentiated and high grade neuroendocrine MPCs were associated with non-classic cytomorphology (e.g. squamous cell transdifferentiation [Fig 1C] and small cell neuroendocrine transformation [Fig 1D]), elevated Ki67, and lost Rb expression (2/4). PDL1 expression was identified in 2/19 cases. 6/6 cases with progression had received prior anti-androgen therapy, compared to 5/13 with conventional features. Among patients with clinical follow-up, 5/5 with progressive features died of disease, compared to 6/11 with conventional features.

Patient	FNA	Age	History of PC	Prior ADT	FNA location	MPC CATEGORY	Vital status	PLM expression	NE expression	PD-L1 expression
1	1	65	Yes	Yes	Lymph node, left cervical	HIGH GRADE NE	DOD	+	+	-
2	2	53	Yes	Yes	Lymph node, left neck	HIGH GRADE NE	DOD	-	-	-
3	3	80	Yes	Yes	Lymph node, subcarinal	TRANSDIFFERENTIATED	Lost to follow-up	+	+	+
4	4	58	Yes	Yes	Bone, left femur	TRANSDIFFERENTIATED	DOD	+	-	-
5	5	71	Yes	Yes	Lymph node, mediastinal	PRO-PROLIFERATIVE	DOD	+	-	-
6	6	85	Yes	Yes	Lymph node, mediastinal	PRO-PROLIFERATIVE	DOD	+	-	-
7	7	68	Yes	Yes	Lymph node, mediastinal	CONVENTIONAL	Alive w/ disease	+	-	-
8	8	75	Yes	Yes	Lymph node, left supraclavicular	CONVENTIONAL	DOD	+	-	-
9	9	73	Yes	Yes	Lymph node, mediastinal	CONVENTIONAL	Alive w/ disease	+	-	-
10	10	67	Yes	No	Soft tissue, abdominal wall	CONVENTIONAL	Alive - NED	+	-	-
11	11	67	Yes	Yes	Lymph node, left cervical	CONVENTIONAL	DOD	+	-	-
12	12	65	No	No	Lymph node, left cervical	CONVENTIONAL	DOD	+	-	-
13	13	66	Yes	Yes	Lymph node, retrocaval	CONVENTIONAL	DOD	+	-	+
14	14	67	Yes	No	Lymph node, retroperitoneal	CONVENTIONAL	Alive - NED	+	-	-
15	15	90	No	No	Bone, left sacrum	CONVENTIONAL	DOD	+	-	-
16	16	67	Yes	No	Bone, right sacrum	CONVENTIONAL	Lost to follow-up	+	-	-
17	17	64	Yes	No	Bone, rib	CONVENTIONAL	Alive - NED	+	-	-
18	18	74	Yes	No	Lymph node, paratracheal	CONVENTIONAL	DOD	+	-	-
---	19	---	---	No	Lymph node, mediastinal	CONVENTIONAL	---	+	-	-

Abbreviations: FNA, fine needle aspiration; PC, prostate carcinoma; ADT, androgen deprivation therapy; MPC, metastatic prostatic carcinoma; PLM, prostate lineage markers; NE, neuroendocrine; PD-L1, programmed death-ligand 1; DOD, died of disease; NED, no evidence of disease

Figure 1 - 228



Conclusions: Morphologic and immunohistochemical assessment allow identification of aggressive and transformed phenotypes of MPC. 6/19 (32%) of cases were reclassified in our study. Identification of non-conventional cytomorphology, increased proliferation, and PD-L1 status can provide prognostic and predictive information in MPC.

229 Comparative Analysis of BRAF, EZH2 and p53 by Immunohistochemistry Versus the Mutation Detected by BRAF PCR, in Indeterminate Categories (III, IV And V of TBSRTC), in Cell Block of Thyroid FNA

Viridiana Roxana Chávez Gómez¹, Monica Serrano¹
¹Instituto Nacional de Cancerología, Tlalpan, Mexico

Disclosures: Viridiana Roxana Chávez Gómez: None; Monica Serrano: None

Background: The management of categories III, IV and V continues to be a source of controversy due to the heterogeneity of recommendations and the limited resources available in some centers. The detection of BRAF by PCR increases the diagnostic

accuracy for some thyroid carcinomas, but it is an expensive and inaccessible procedure, which forces to look for alternatives to determine the diagnosis.

OBJECTIVE: To compare the sensitivity, specificity, PPV, NPV and areas under the curve (ROC) of the cytological study plus the immunohistochemical markers BRAF, EZH2 and p53 against the cytological study plus BRAF-PCR mutation.

Design: All thyroid BAAF cell blocks with diagnoses of indeterminate categories were taken carried out between 2011 and 2019, with histopathological correlation. Immunohistochemistry studies were performed for BRAF-V600E, EZH2 and P53, in addition to the PCR determination of the BRAF mutation. The area under the curve was determined for each study.

Results: We included 25 cases, 3 (12%) with mutation detected by PCR and IHC. BRAF-IHC had a diagnostic accuracy of 68%, sensitivity of 85%, specificity of 0%, PPV of 77.27% and NPV of 0%. Compared with the detection of BRAF by PCR which had a diagnostic precision and sensitivity of 48% and 45%, respectively. The diagnostic accuracy of P53 was 72%, sensitivity of 90%, specificity of 0%, PPV of 78.26%, NPV of 0%. The test with the worst performance was EZH2, its diagnostic accuracy was 28%, sensitivity of 15%, specificity of 80%, PPV of 75% and NPV of 19.05%. The analysis of the area under the curve for the immunohistochemical markers, was on average 0.5 for the three markers, while for BRAF-PCR, it was 0.480, therefore, in this study the usefulness of these tests was not better than a random classification.

Relationship of the diagnosis by categories of SBRCT with the result of IHC, PCR and histopathology.					
Categorie	BRAF	p53	EZH2	BRAF-PCR	Histopathology
III	0	0	1	ND	Hyperplastic nodule.
	0	0	1	ND	Undifferentiated carcinoma.
	0	0	1	ND	Adenomatoid nodule.
	0	0	1	NA	Undifferentiated carcinoma.
IV	0	0	1	ND	Papillary thyroid carcinoma.
	0	0	1	ND	Follicular carcinoma.
	0	0	1	NA	Follicular carcinoma.
	0	0	1	ND	Follicular adenoma.
	0	0	1	ND	Follicular carcinoma and papillary thyroid carcinoma.
	0	0	1	NA	Undifferentiated carcinoma.
	0	0	1	ND	Medullary thyroid carcinoma.
	0	0	1	ND	Hyperplastic nodule.
	0	1	1	ND	Undifferentiated carcinoma.
	0	0	1	NA	Oncocytic carcinoma.
	0	1	1	NA	Undifferentiated carcinoma.
	0	0	1	ND	Noninvasive follicular thyroid neoplasm with papillary-like nuclear features (NI.
	0	0	1	Inválida	Medullary thyroid carcinoma.
0	0	0	Inválida	Follicular adenoma.	
V	1	0	1	V600E/Ec	Papillary thyroid carcinoma.
	0	0	0	ND	Papillary thyroid carcinoma.
	0	0	0	V600E/Ec	Papillary thyroid carcinoma.
	1	0	1	V600E/Ec	Papillary thyroid carcinoma.
	0	0	1	NA	Papillary thyroid carcinoma.
	0	0	0	NA	Papillary thyroid carcinoma.
	1	0	1	(+)	Papillary thyroid carcinoma.

Figure 1 - 229

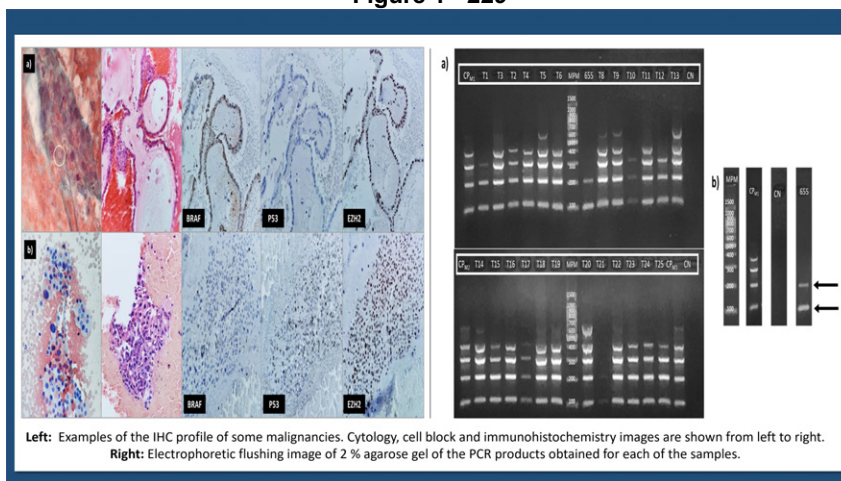
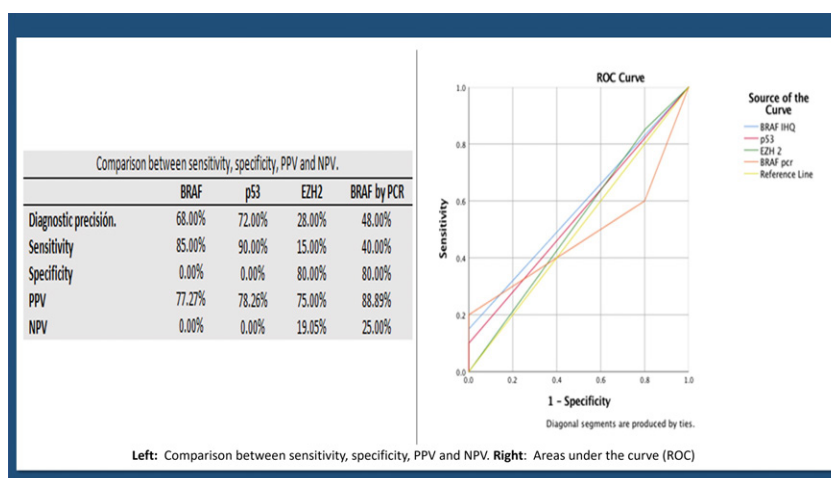


Figure 2 – 229



Conclusions: The detection of BRAF-V600E by immunohistochemistry has concordance with the detection of BRAF by PCR and can be used as a test comparable with the BRAF PCR study, so the addition of the study of immunohistochemistry could be suggested in indeterminate categories. Detection by immunochemistry of p53 should be useful when the morphologic characteristics suggest undifferentiated thyroid tumors. EZH2 did not prove useful in this study. Immunochemistry it would be a useful resource when don't have the infrastructure to do molecular studies like NGS. The sample size was small and more studies are needed.

230 Comparison of Fresh Cell Pellets and Cell Blocks for Genomic Profiling of Advanced Cancers in Pleural Effusion Specimens: Promising Preliminary Results from a Validation Study

Fei Chen¹, Christine Kim¹, Guomiao Shen¹, Xiaojun Feng¹, George Jour², Paolo Cotzia³, Tamar Brandler¹, Wei Sun¹, Matija Snuderl², Aylin Simsir⁴, Kyung Park¹

¹NYU Langone Health, New York, NY, ²New York University, New York, NY, ³NYU Langone Medical Center, New York, NY, ⁴NYU School of Medicine, New York, NY

Disclosures: Fei Chen: None; Christine Kim: None; Guomiao Shen: None; Xiaojun Feng: None; George Jour: None; Paolo Cotzia: None; Tamar Brandler: None; Wei Sun: None; Matija Snuderl: None; Aylin Simsir: None; Kyung Park: None

Background: Molecularly targeted therapies in patients with advanced cancer improve overall survival over traditional chemotherapy and require fast and accurate molecular profiling of the tumor tissues/cells. Pleural effusion (PE) is often the only

material available in the diagnosis of metastatic disease. Molecular testing is routinely done on formalin-fixed paraffin-embedded (FFPE) cell block (CB). However, CB may not contain adequate tumor content for molecular testing after multiple immunohistochemical stains performed for making a histologic diagnosis. The purpose of this validation study is to test the feasibility of enriched fresh cell pellet (FCP) for molecular testing from leftover PE specimens that would otherwise be discarded.

Design: Fresh fluids from ten (10) PE specimens after the diagnosis of metastatic adenocarcinoma was made (9 lung origin and 1 breast origin) were used for this study. Unfixed leftover fluids were refrigerated at 4 degrees for up to 7 days. Then, they were spun down to get FCP. Concurrent FFPE CBs were retrieved to make 10-15 unstained slides. DNA and RNA were extracted from FCPs and CBs using Maxwell® RSC Tissue DNA/ simply RNA Tissue Kit and DNA/RNA FFPE Kit, respectively (Promega). DNA/RNA libraries were prepared and sequenced using OncoPrint Precision Assay (OPA) on Ion Torrent Genexus Integrated Sequencer (Thermo Fisher Scientific). Data were analyzed by OPA DNA/Fusion workflow w2.6.0. There were 6 cases with clinically available molecular results (OncoPrint Focus Assay, OFA) performed for patient management; these OFA results were compared with FCP results for accuracy.

Results: All DNA/RNA extracted from FCP samples (PE volume varies from 0.5 ml to 50 ml) yielded sufficient read counts and passed sequencing quality metrics. FCP samples demonstrated all the alterations including fusion detected from CBs. One case (case1) showed an extra MAP2K1 Q56P mutation detected in the FCP specimen but not detected in CB and OFA, possibly due to relatively abundant/enriched cell content in the unused PE fluid (Table 1).

Table 1: Comparison of genomic profiling result in cell pellet and cell block using OPA platform

Case#	Cell Pellet (CP)			Cell Block (CB)			Clinical molecular results (OFA)
	DNA Read Count	RNA Read Count	Variants	DNA Read Count	RNA Read Count	Variants	
1	2,151,051	118,561	MAP2K1 Q56P*	1,945,080	123,568	None	None
2	2,192,777	152,958	EML4(20) - ALK(20)	1,797,029	172,795	EML4(20) - ALK(20)	EML4(20) - ALK(20)
3	1,851,205	138,587	None	2,041,998	226,973	None	NA**
4	1,816,494	269,962	EGFR T790M, EGFR L858R	1,717,183	238,733	EGFR T790M, EGFR L858R	EGFR T790M, EGFR L858R
5	1,857,217	322,409	None	1,781,329	307,815	None	NA**
6	1,642,958	274,305	KRAS G13D	1,889,157	293,546	KRAS G13D	NA**
7	1,592,958	337,263	EGFR P772_H773insGHP; CTNNB1 S37C; TP53 R249T*	1,697,895	218,649	EGFR P772_H773insGHP; CTNNB1 S37C; TP53 R249T*	EGFR P772_H773insGHP; CTNNB1 S37C
8	2,054,107	158,871	None	1,783,644	313,887	None	NA**
9	2,273,173	221,731	KRAS G12C	2,179,172	249,354	KRAS G12C	KRAS G12C
10	1,000,199	210,784	KRAS Q61H	1,522,416	182,055	KRAS Q61H	KRAS Q61H

*Note: TP53 is included in the OPA panel but not included in the OFA panel. MAP2K1 is in both OPA and OFA panels.

**NA: OFA not performed or pending result.

Conclusions: Our preliminary validation data shows that FCPs from refrigerated unfixed PE specimens up to 7 days after they are collected can provide a reliable source for genomic profiling in advanced cancer and be used in clinical practice with excellent accuracy.

231 Diagnostic Utility of DDIT3 Immunohistochemistry for Myxoid Liposarcoma in Fine-Needle Aspiration Cell Blocks

Li Chen¹, Jason Hornick², Vickie Jo²

¹Brigham and Women's Hospital, Boston, MA, ²Brigham and Women's Hospital, Harvard Medical School, Boston, MA

Disclosures: Li Chen: None; Jason Hornick: *Consultant*, Aadi Biosciences; *Consultant*, TRACON Pharmaceuticals; Vickie Jo: *Stock Ownership*, Merck and Co

Background: The cytologic diagnosis of myxoid liposarcoma (MLPS) can be difficult, especially high-grade MLPS which can show a predominance of round cell morphology. MLPS lacks a specific immunophenotype, and molecular genetic testing is often necessary to identify the characteristic *FUS-DDIT3* fusion. Immunohistochemistry (IHC) for DDIT3 has been recently shown to be highly sensitive and specific for MLPS on surgical specimens. The aim of this study was to evaluate the performance of DDIT3 for the diagnosis of MLPS and distinction from cytologic mimics.

Design: In total, 28 fine-needle aspiration cases with cell block material available for IHC were investigated. The cohort included: MLPS (10; 2 low-grade, 3 intermediate grade, 5 high-grade), Ewing sarcoma (13), alveolar rhabdomyosarcoma (2), extraskelatal myxoid chondrosarcoma (1), spindle cell lipoma (1), and lipoma (1). IHC for DDIT3 was performed, and nuclear staining was scored semi-quantitatively for extent (0; 1+, 1-25%; 2+, 26-75%; 3+, >75%) and intensity (weak, moderate, strong).

Results: MLPS showed nuclear staining in 9/10 cases (90%). All positive MLPS cases showed moderate (6) or strong (3) staining intensity. Extent of staining was 3+ in most MLPS cases (8/10; 80%), with 1 case showing focal 1+ staining. Notably, <20 lesional cells were present in MLPS cell blocks in 3 cases, including the case negative for DDIT3 IHC. *DDIT3* gene rearrangement was confirmed in 7 cases (5 by fluorescence in situ hybridization, 1 by karyotype analysis, and 1 by targeted next-generation sequencing) which were all positive for DDIT3 IHC; the remaining 3 FNA cases were confirmed on post-treatment resections (including the DDIT3 IHC-negative case). All other tumor types were negative for DDIT3 IHC (0/18).

Conclusions: DDIT3 IHC shows 100% specificity and 90% sensitivity for MLPS in FNA cell blocks. A potential limitation would be low cell block cellularity; however, DDIT3 was positive in 2/3 MLPS cases with sparsely cellular cell blocks. DDIT3 IHC can serve as a surrogate for molecular genetic testing in small biopsy samples and may be particularly helpful in the differential diagnosis of round cell sarcomas.

232 Utility of EZH2 Immunostaining for Atypical Bile Duct Brush Cytology

Fei Chen¹, Qian Wang², Cristina Hajdu³, Oliver Szeto¹, Aylin Simsir⁴, Tamar Brandler¹

¹NYU Langone Health, New York, NY, ²Children's Hospital of Pittsburgh of UPMC, Pittsburgh, PA, ³New York University School of Medicine, New York, NY, ⁴NYU School of Medicine, New York, NY

Disclosures: Fei Chen: None; Qian Wang: None; Cristina Hajdu: None; Oliver Szeto: None; Aylin Simsir: None; Tamar Brandler: None

Background: Bile duct brush cytology (BDBC) aids in the detection of carcinoma with specificity nearing 100% when atypical cells display sufficient malignant features for a definitive “positive” diagnosis. However, when cells appear atypical but lack apparent malignant features, additional ancillary studies are necessary for a conclusive diagnosis. Enhancer of zeste homolog 2 (EZH2), the catalytic subunit of PRC2, has shown immunohistochemical overexpression in pancreaticobiliary ductal and hepatocellular carcinomas, but not in benign ductal cells. Therefore, our study aimed to investigate the value of EZH2 immunohistochemistry (IHC) in the inconclusive “atypical” BDBC diagnostic category to determine whether it may help in arriving at a specific negative or positive diagnosis.

Design: 40 de-identified, formalin-fixed, paraffin-embedded BDBC cell blocks initially diagnosed as “atypical” from 2013-2019 with subsequently confirmed malignant or benign diagnoses were selected and reviewed. Malignant or benign confirmation was achieved through surgical histopathology, FISH testing, and/or 12-month follow-up without pancreatobiliary malignancy diagnosis. EZH2 IHC was applied to the cell blocks and analyzed for percent nuclear staining. Two cutoff values were examined based on previous literature, >0% (any nuclear staining) and >5% (over 5% of tumor cells showing nuclear staining). Cytokeratin IHC was used as a double stain to highlight the ductal epithelial cells.

Results: Among 40 atypical BDBC cases, 16 were confirmed to be malignant, and 24 were benign. 10/16 malignant and 19/24 benign cases showed any EZH2 (>0%) positive immunostaining; however, only 2/16 malignant and 3/24 benign cases showed at least 5% nuclear staining (Figure 1). There was no statistically significant difference between the two groups (Fisher's Exact Test) (p=0.295 for >0% cutoff and p=0.723 for >5% cutoff). The sensitivity, specificity, PPV, and NPV for each group are demonstrated in table 1.

Table 1: Cases of EZH2 staining in atypical cells with ultimate benign or malignant diagnoses with sensitivity, specificity, positive and negative predict values (PPV and NPV).

	Malignant (N)	Benign(N)		Malignant (N)	Benign (N)
EZH2 Positive	10	19	EZH2 Positive with 5% cut off	10	19
EZH2 Negative	6	5	EZH2 Negative	6	5
p>0.05			p>0.05		
Sensitivity:	62.50%			62.50%	
Specificity:	21.80%			21.80%	
PPV	34.50%			34.50%	
NPV	45.50%			45.50%	

Figure 1 - 232

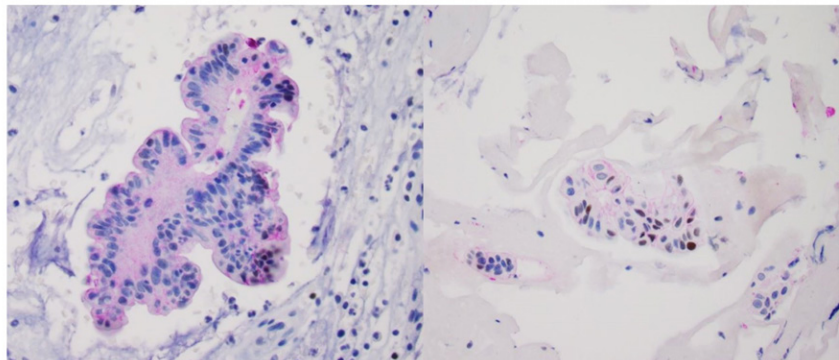


Figure 1: Weak (left) and positive (right) EZH2 (brown) immunostaining in bile duct brush cell block specimen (40x) Pink: cyokeratin double stain They both initially were diagnosed as atypical cells present and later confirmed to be inflammation.

Conclusions: EZH2 immunohistochemical staining showed significant overlap in atypical BDBC cases with benign and malignant follow up. Though EZH2 IHC has been suggested as a potential marker in the histopathologic diagnosis of pancreatobiliary malignancy, it has not been routinely used. In examining its utility in cytopathology, EZH2 did not offer any benefit in atypical cytology specimens in achieving a conclusive diagnosis of benignancy or malignancy.

233 Paucicellular Cytology Specimens: Performance Comparison between 2 Whole Slide Scanners

Amir Dehghani¹, Marc-Henri Jean¹, Mega Lahori¹, Orly Ardon¹, Oscar Lin¹, Brie Kezlarian¹
¹Memorial Sloan Kettering Cancer Center, New York, NY

Disclosures: Amir Dehghani: None; Marc-Henri Jean: None; Mega Lahori: None; Orly Ardon: None; Oscar Lin: *Consultant*, Hologic; *Consultant*, Jansen; Brie Kezlarian: None

Background: Whole slide imaging (WSI) has the potential to transform cytopathology workflows and replace glass slides. However, current scanner technology continues to struggle with tissue detection in paucicellular cytology specimens. We investigated the performance of two commercially available whole slide scanning devices with z-stacking capabilities when challenged with a cohort of paucicellular cytopathology slides.

Design: Forty paucicellular cytology specimens representing clinical cytology specimens were divided into two groups based on subjective impression of cellularity. Each slide was scanned in 5 Z-planes 2 microns apart on two scanners (“Scanner A” and “Scanner B”). A successful scan (SS) was defined as having an in-focus image in any Z-plane. A perfect scan (PS) had the most in-focus z-plane at the 0 position. A slide was not successfully scanned (NSS) if the image was not in focus (NIF) on any Z-plane, incompletely scanned (IS) or failed entirely (FE).

Results: Overall, Scanner A scanned 10 (25%) slides successfully with 7 (18%) PS. Scanner B scanned 7 (18%) slides successfully with 4 (10%) PS. In the least cellular group, Scanner A successfully scanned 4 (20%) cases with 5 (25%) NIF and 11 (55%) FE. Scanner B successfully scanned 5 (25%) slides with 1 (5%) IS and 12 (60%) NIF, 2 (10%) FE. In the group with more cells, Scanner A resulted in 6 (30%) SS, 4 (20%) NIF and 10 (50%) FE scans. Scanner B resulted in 2 (10%) SS, 10 (50%) NIF and 8 (40%) FE slides. The difference in overall scan success was not statistically significant in either group (Pearson Chi-Square =0.143, p =0.705; Pearson Chi-Square =2.5, p =0.114).

Both scanners had analogous results for 25 (63%) of slides [1 (3%) SS and 24 (63%) NSS]. Of 33 slides that failed on Scanner B, 9 (27%) scanned successfully on Scanner A. Conversely, of 30 slides that failed on Scanner A, 6 (20%) were successful on Scanner B.

Conclusions: Overall scanning success was poor in this cohort of paucicellular cytology slides. Although there was no statistically significant performance difference between these scanners, 20%-27% of failed slides scanned successfully by the second machine. These findings suggest that there may be value to use more than one scanner platform for Cytology specimens and WSI implementation requires careful validation with paucicellular specimens.

234 A Comparison Study of Papanicolaou Tests and Histologic Diagnosis in Female to Male Transgender Population

Adriana Del Barco¹, Yong Ying¹, Sung Eun Yang¹, Neda Moatamed¹
¹David Geffen School of Medicine at UCLA, Los Angeles, CA

Disclosures: Adriana Del Barco: None; Yong Ying: None; Sung Eun Yang: None; Neda Moatamed: None

Background: The need for cervical cancer screening remains in the female-to-male (FTM) transgender male population. Insufficient review and consideration of transgender patients' clinical history could lead to misinterpretation.

Design: This study was approved by our Institutional Review Board. The retrospective study was carried out by obtaining data through a computer search (Epic Beaker) which included a list of the FTM individuals who had screening Pap smears (ThinPrep and/or Sure Path) from March 2016 to July 2021. Human papilloma virus (HPV) PCR test results were included if available. The cytology results were compared with surgical pathology follow-ups.

Results: A review of 82 cervical pap smears of 73 FTM transgender male cases (age 22-63 years, 70/73 receiving testosterone therapy) revealed the following:

67/82 (82%) negative for intraepithelial lesion or malignancy (NILM), 8/82 (10%) unsatisfactory, 4/82 (0.05%) atypical squamous cell-undetermined significance (ASCUS), 2/82 (0.02%) atypical squamous cell-cannot exclude high grade squamous intraepithelial lesion (ASC-H), and 1/82 (0.01%) low grade intraepithelial lesion (LSIL).

HPV results were available for 40 patients; 10 were positive for high risk HPV. Surgical specimen follow-up was available in 11 patients. The surgical pathology follow ups included atrophy in 18 cases and one with low grade squamous intraepithelial lesion (LSIL) from an HPV positive unsatisfactory case. Among the cases with atrophy, 2 had a prior Pap diagnoses of ASC-H (one with HPV positive and the other HPV negative), one LSIL with negative HPV test, one ASCUS with HPV positive. The remaining 14 atrophic cases were interpreted as negative, with 5 of them having HPV positive result.

Cytology findings with surgical follow-up and HPV status					
Cytology diagnoses	Number of cases	Cases with surgical follow-up	HPV Not Performed	HPV Negative	hrHPV+
NILM	67	6 (benign; atrophy)	27	34	6
Unsatisfactory	8	1 (LSIL)	2	4	2
ASCUS	4	1 (LSIL)	1	3	0
ASC-H	2	2 (benign; atrophy)	1	0	1
LSIL	1	1 (benign)	0	1	0

Conclusions: In conclusion, the most common FTM transgender male cervical pap smear was NILM with atrophy followed by unsatisfactory. 2/82 of cases were interpreted as ASC-H cytologically, and subsequently diagnosed as atrophic in follow up. In order to avoid unnecessary invasive procedures, appropriate history should be provided by the clinicians and thoroughly reviewed by person screening FTM transgender male cervical pap smears.

235 Evaluation of COVID-19-Related Changes in Cytopathology Case Volume at a Large County Hospital in Texas

Mary Doan¹, Peyman Dinarvand¹

¹Baylor College of Medicine, Houston, TX

Disclosures: Mary Doan: None; Peyman Dinarvand: None

Background: COVID-19 has significantly changed the way we live and work and has caused clear disruptions in the number of cases received by pathology departments across the world. These changes have not been evaluated to determine what areas of pathology showed the greatest decreases in numbers, particularly within cytopathology. In this study, we evaluated the trends of cytopathology practice before, during and after the initial surge of COVID-19 at our county hospital (Ben Taub Hospital) in one of most populated counties in the United States.

Design: A retrospective review of our institutional database was performed to examine the numbers of cytopathology cases from June 2019 to June 2021. Cytopathology cases were stratified into the broad categories of gynecologic (GYN), non-gynecologic (non-GYN) and fine needle aspiration (FNA) cases.

Results: The number of GYN cases had the sharpest decline of approximately 90% during the acute phase of the COVID-19 pandemic in the spring of 2020 (Figure 1), starting in late February (n=1407) and March (n=829), with a trough in April 2020 (n=154). Following this initial significant decline, GYN cases began to increase in May 2020 and later; however, the GYN case volume never returned to the pre-pandemic level. Meanwhile, the number of FNA cases during same period had a decline (n=92 in February, n=73 in March, and n=54 in April), though not as dramatic as for GYN cases (Figure 2A). The volume of FNA cases never reached pre-pandemic levels, but there was nearly a complete recovery. Similarly, the quantity of non-GYN cases decreased (n=136 in February, n=113 in March, and n=96 in April), but the acceleration of the decline was much slower. The number of non-GYN cases eventually returned to pre-pandemic levels in October 2020 (Figure 2B). Volumes of cases in all three areas started to decline again in the late spring and early summer of 2021 as COVID-19 case numbers started to increase once again.

Figure 1 - 235
GYN Cases

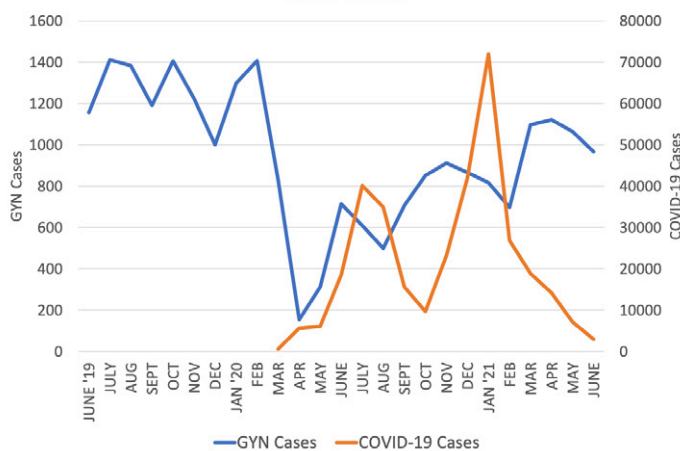


Figure 1

Figure 2 – 235

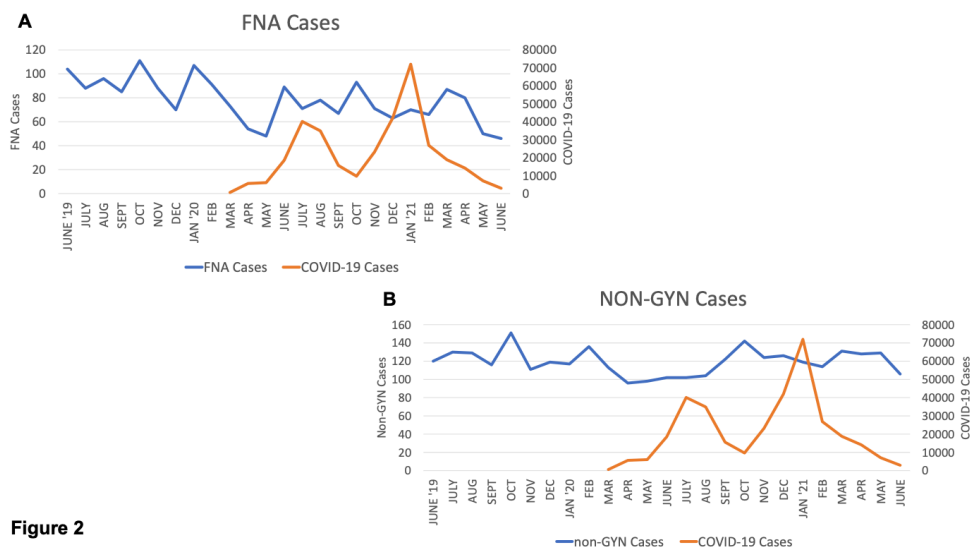


Figure 2

Conclusions: The trend in cytopathology cases at our institution demonstrated a dramatic decline for GYN cases, with a less sharp decline in FNA and non-GYN cases during the acute phase of pandemic in the spring of 2020. The large decrease in GYN cases suggests that primary screening was significantly impacted by the pandemic. Whether we should encourage patients to resume in-person visits for GYN screenings or consider changing guidelines to include the effect of COVID-19 pandemic on screening remains to be seen.

236 Validation Study of the Milan System for Reporting Salivary Gland Cytopathology: A Single Institution’s 10 Year Experience

Christopher Felicelli¹, Lucy Jager¹, Daniel Johnson¹

¹Northwestern University Feinberg School of Medicine, Chicago, IL

Disclosures: Christopher Felicelli: None; Lucy Jager: None; Daniel Johnson: None

Background: Fine-needle aspiration cytology is used extensively for initial diagnosis and management of patients with salivary gland tumors. A consensus grading schema was established in 2018 to bring forth universal reporting of salivary gland cytology specimens, The Milan System for Reporting Salivary Gland Cytopathology. The Milan System contains seven diagnostic categories that estimate the risk of malignancy and guides proper patient management. Few retrospective studies have been undertaken to review the entire Milan System in specific institutions, and we aimed to validate it at our institution with a retrospective study of 10 years.

Design: A comprehensive search of the laboratory information system for all patients who underwent salivary gland fine needle aspiration from 01/01/2011-01/01/2021 was conducted (n=670). All cases were evaluated for subsequent surgical resections during the time period (n=329). FNAs were performed by either clinicians, radiologists, or pathologists. Air-dried slides were stained with Diff-Quik, while immediately alcohol-fixed slides were stained with a Papanicolaou stain. Occasional cases had cell block preparation or a core biopsy with touch preparation performed. Cytology and surgical pathology reports were analyzed. Cytology reports from prior to the implementation of the Milan System were reviewed and assigned a category. The rate of malignancy (ROM) was assessed by comparison of the FNA diagnosis to final surgical resection diagnosis.

Results: The ROM for each category was as follows: Non-diagnostic-32%, Non-Neoplastic-20%, AUS-37.03%, Neoplasm-Benign-1.85%, SUMP- 36.36%, Suspicious for Malignancy-83.33%, and Malignant-97.73%.

Representative images of FNA "Overcall" and "Undercall" with subsequent surgical resection are shown in Figures 1 and 2.

Table 1: Demographics and Classification of the Prior 10 Years' Fine Needle Aspiration and Surgical Resection of Salivary Glands

Diagnostic category	Age (years)	Sex (M:F)	Total number	Total w/ surgical resection	Total malignant	Malignant overall	ROM
Non-diagnostic	57.82	42:40	82	25	8	9.75%	32%
Non-neoplastic	57.03	55:62	117	15	4	3.42%	20%
AUS	59.28	29:28	57	27	10	17.54%	37.03%
Neoplasm-benign	57.92	112:166	278	162	3	1.08%	1.85%
SUMP	62.28	23:35	58	44	16	27.59%	36.36%
Suspicious for malignancy	60.06	5:11	16	12	10	62.5%	83.33%
Malignant	65.46	44:18	62	44	43	69.35%	97.73%
Total	59.02	308:362	670	329	94	14.03%	28.57%

Figure 1: Overall pitfall case: (A) Papanicolaou stained FNA of a submandibular lesion showing whorled cluster of cells with slight atypia, anisonucleosis, occasional prominent nucleoli, and moderate dense cytoplasm, suspicious for malignancy (40x). (B) Surgical resection displaying lobular fibrosis, atrophy and dense lymphoplasmacytic infiltrate consistent with chronic sialadenitis (4x).

Figure 2: Undercall pitfall case: Papanicolaou stained FNA of a parotid lesion showing limited cellularity, rare clusters of small squamoid appearing cells with overlapping in a background of neutrophils and lymphocytes, called non-neoplastic (A). Surgical resection of the lesion revealed high grade mucoepidermoid carcinoma arising in an intraparotid lymph node (B).

Figure 1 - 236

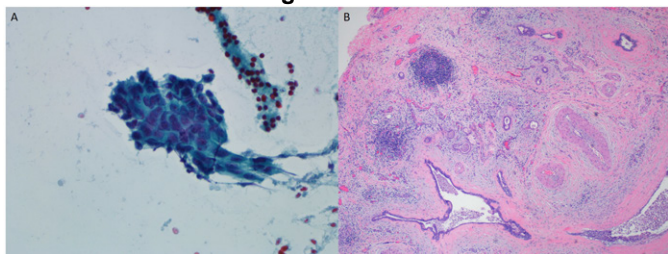
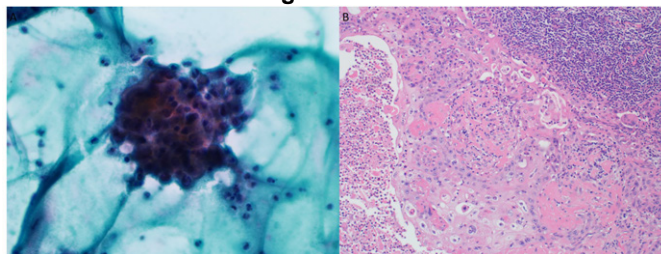


Figure 2 - 236



Conclusions: Our internal results indicate the Milan system may underestimate the ROM (>10% difference) for non-neoplastic, AUS, and suspicious for malignancy. While this data is indicative of ROM for surgically resected salivary gland lesions, the ROM for non-neoplastic may truly be lower given most lesions in this category do not undergo surgical resection. Our data correlates well with the Milan ROM for non-diagnostic, neoplasm-benign, SUMP, and malignant.

237 Retrospective Analysis of HPV Infection with Co-testing and HPV Genotyping in Cervical Cancer Screening in a Large Academic Healthcare System

Frances Feng¹, Melad Dababneh², George Birdsong³, Michelle Reid⁴, Michael Hoskins¹, Qun Wang¹
¹Emory University, Atlanta, GA, ²Emory University School of Medicine, Atlanta, GA, ³Emory University School of Medicine, Grady Memorial Hospital, Atlanta, GA, ⁴Emory University Hospital, Atlanta, GA

Disclosures: Frances Feng: None; Melad Dababneh: None; George Birdsong: None; Michelle Reid: None; Michael Hoskins: None; Qun Wang: None

Background: A key change in the 2019 ASCCP Consensus Guidelines for the management of cervical cancer screening abnormalities is from test result-based algorithms to risk-based guidelines. One of the guiding principles is HPV-based testing. HPV16 or HPV18 infections have the highest risk for CIN3 and occult cancer; therefore, HPV genotyping has greater importance in investigating squamous intraepithelial lesions, particularly for risk estimation of CIN3+. This retrospective study analyzes HPV status based on co-testing followed by HPV genotyping in HPV+ patients in a large university healthcare system.

Design: Cases were identified via computerized database searches in three affiliated hospitals (H1, H2, and H3) from January 2018 to July 2021 (H1 and H2) and October 2018 to August 2021 (H3). All patients were categorized based on co-testing results as negative for intraepithelial lesion or malignancy (NILM), atypical squamous cells of undetermined significance (ASC-US), low grade squamous intraepithelial lesion (LSIL), atypical squamous cells cannot exclude high grade squamous intraepithelial lesion

(ASC-H), high grade squamous intraepithelial lesion (HSIL), and atypical glandular cells (AGC), along with HPV status. Additionally, HPV+ patients from H3 were further subcategorized based on HPV 16 and/or 18/45 genotypes in each category. At H1 and H2, genotyping was only performed on cases with NILM cytology.

Results: A total of 63,520 Pap smears (47,737 from H1 & H2 and 15,783 from H3) are investigated. Patients with HSIL and NILM demonstrate the highest and lowest HPV+ rates (90.07%-92.83% and 4.84%-9.77%), respectively (Table 1). The highest (66.41%-86.69%) and lowest (0.5%-0.88%) co-testing rates are seen in NILM and HSIL patients, respectively, in all hospitals (Table 1, Fig.1A-1B). Similar HPV+ rates are noted across different years among different hospitals (Fig.1C-1D). HPV genotyping results show about 91% NILM/HPV+ caused by subtypes other than 16/18/45 (Fig.2A-2B). HPV16 and 18/45 infection rates increase with dysplasia severity (Fig. 2C).

Co-testing in cervical cancer screening at H1/H2 (Jan. 2018 – Jul. 2021)						
	NILM	ASCUS	LSIL	HSIL	ASC-H	AGC
HPV- cases (%)	37,340 (90.23%)	2,373 (60.24%)	426 (29.32%)	17 (7.17%)	118 (25.71%)	215 (81.13%)
HPV+ cases (%)	4,044 (9.77%)	1,566 (39.76%)	1,027 (70.68%)	220 (92.83%)	341 (74.29%)	50 (18.87%)
Total cases (47,737)	41,384	3,939	1,453	237	459	265

Co-testing and HPV genotyping in cervical cancer screening at H3 (Oct. 2018 – Aug. 2021)						
	NILM	ASCUS	LSIL	HSIL	ASC-H	AGC
HPV- cases (%)	10,084 (95.16%)	2872 (79.71%)	379 (46.11%)	14 (9.93%)	140 (44.16%)	298 (85.63%)
HPV+ cases (%)	513 (4.84%)	731 (20.29%)	443 (53.89%)	127 (90.07%)	177 (55.84%)	50 (14.37%)
HPV+ w/o genotyping	41	55	39	15	10	3
HPV16+	18	51	34	23	34	4
HPV18/45+	27	60	47	18	23	5
HPV16+HPV18/45+	1	2	4	4	4	0
HPV+ Other type	426	563	319	67	106	38
Total cases (15,783)	10,597	3603	822	141	317	348

Figure 1 - 237

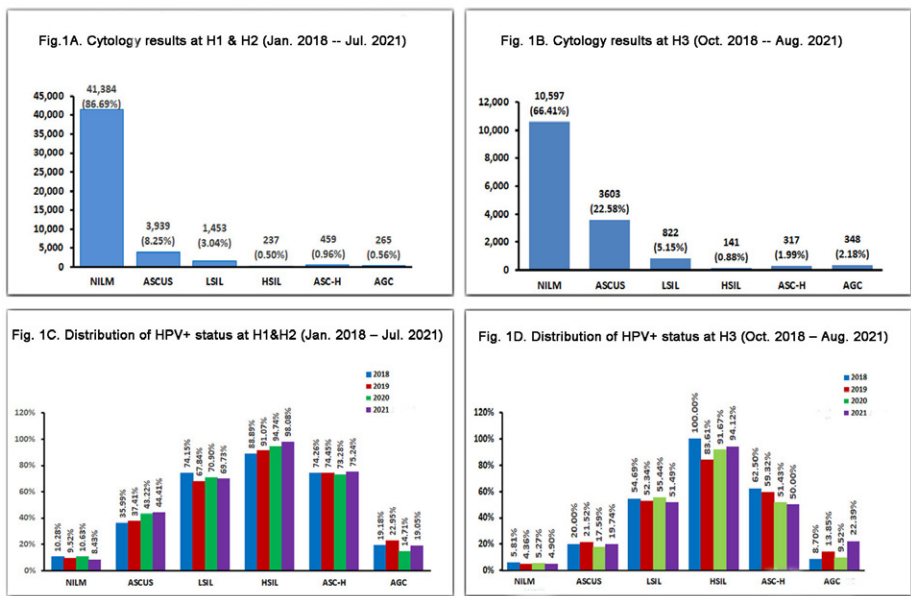
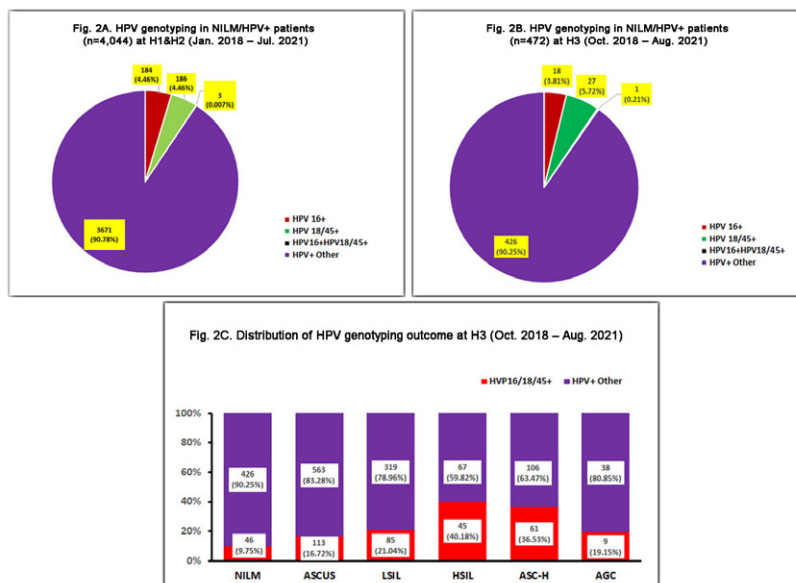


Figure 2 – 237



Conclusions: HPV infection trends are consistent within each hospital across different years. HPV16 and 18/45 infection plays a critical role in cervical squamous dysplasia and is positively associated with the severity of squamous dysplasia. Analysis of HPV-based testing in conjunction with HPV genotyping in large patient cohorts will inform risk estimation of CIN3+ and improve clinical management.

238 Subclassification of Fine Needle Aspirations for Basaloid Salivary Gland Neoplasm of Uncertain Malignant Potential is Predictive of Benign vs. Malignant Neoplasms

Sowmya Gaddam¹, Jiang Wang², Paul Lee²

¹University of Cincinnati Medical Center, Cincinnati, OH, ²University of Cincinnati, Cincinnati, OH

Disclosures: Sowmya Gaddam: None; Jiang Wang: None; Paul Lee: None

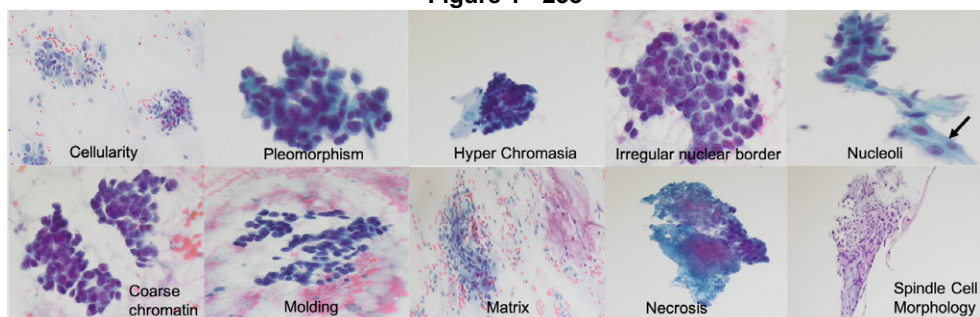
Background: Salivary gland neoplasm of uncertain malignant potential (SUMP) is a category IVB in the Milan System for Reporting Salivary Gland Cytopathology. The SUMP subclassification includes basaloid neoplasms which can represent up to 35% risk of malignancy. This study explores the possibility to further subclassify the basaloid SUMP into low-grade (benign) and high-grade (malignant) to guide surgical management. We aim to explore whether cytopathologists can predictively designate basaloid SUMP into benign vs malignant categories and to determine which specific cytomorphologic features are associated with malignancy.

Design: A consecutive cohort of 80 salivary gland FNAs with a diagnosis of “basaloid” neoplasms with clinically verified resections were identified from between 1/2011 and 7/2021. We excluded cases without follow-up resections, missing cases, and non-interpretable slides. 21 out of 80 cases qualified for the study (14 benign and 7 malignant diagnosed on resection). The available Diff-quick, alcohol fixed, thin-prep, and cell blocks were evaluated by 2 cytopathologists in a blinded-fashion. The positive and negative predictive values were calculated using a 2 x 2 chart with the known resection diagnosis. The inter-rater reliability was determined using a Cohen’s kappa calculator. 10 selected morphologic classifiers were evaluated in a dichotomized fashion with discrepancies resolved in a consensus evaluation. Fisher exact test was performed to analyze the morphologic classifiers for grading the basaloid neoplasms.

Results: The positive and negative predictive values of using high grade and low-grade determinations of basaloid neoplasms were 76.4% and 96.0% respectively. The inter-rater reliability between the two pathologists was 85% (k: 0.65). Four morphologic classifiers that were statistically significant to distinguish between the low-grade and high-grade basaloid neoplasms include pleomorphism, irregular nuclear border, nucleoli, and necrosis.

	Cellularity	Pleomorphism	Hyper Chromasia	Irregular Nuclear Border	Nucleoli	Coarse Chromatin	Molding	Matrix	Necrosis	Spindle Cell Morphology
Benign	7/14	1/14	9/14	1/14	4/14	1/14	3/14	8/14	0/14	12/14
Malignant	2/7	6/7	7/7	5/7	6/7	3/7	4/7	1/7	3/7	3/7
P	> 0.05	0.0009	> 0.05	0.005	0.02	> 0.05	> 0.05	> 0.05	0.03	> 0.05

Figure 1 - 238



Conclusions: The subclassification of low and high-grade in basaloid neoplasms of salivary gland FNAs correlates with benign vs. malignancy in follow-up resection specimens. Relatively good interobserver agreement is identified when calling low and high-grade in salivary gland FNAs. The morphologic classifiers associated with malignancy include: pleomorphism, irregular nuclear border, nucleoli, and necrosis. It is beneficial to grade SUMP basaloid neoplasms into low and high-grade categories.

239 ROSE in the Era of EUS Cores

Chiraag Gangahar¹, Tiffany Sheu¹, Liye Suo², Michael Thrall¹

¹Houston Methodist Hospital, Houston, TX, ²SUNY Upstate Medical University, Syracuse, NY

Disclosures: Chiraag Gangahar: None; Tiffany Sheu: None; Liye Suo: None; Michael Thrall: None

Background: Newly developed core needle biopsies using Franseen or fork-tip technology have dramatically altered the diagnosis of pancreas lesions. In the past, rapid on-site evaluation (ROSE) was standard, but now is much less frequent since the new needles have been shown to generate adequate specimens in most cases. ROSE is now usually reserved for tumors with unusual features. Here we describe our experience in this changed environment.

Design: We examined pathology reports and slides from endoscopically guided pancreas biopsies for the period from August 2017 to July 2019, as well as the follow-up pathologic and clinical diagnoses, if available. 108 cases had ROSE requested, out of a total of 342 (32%). Cysts were excluded.

Results: Adequacy at the time of ROSE was low (73/108; 68%). Definitive final diagnosis was rendered in only 85 cases (79%). 10 cases (9.3%) were not definitive and did not have follow-up to establish the true diagnosis. The remaining 98 cases included: 69 ductal adenocarcinomas (only 70%), 12 primary neuroendocrine tumors, 7 metastases (6 kidney and 1 breast), 3 IgG4-related pancreatitis, 3 non-IgG4 pancreatitis, 2 accessory spleen, 1 solid pseudopapillary tumor, and 1 lymphoma (Table 1). 3 of 6 ductal adenocarcinoma without definitive diagnosis had only small biopsy fragments received (<3 mm), but only 1 of the 7 non-ductal lesions without definitive diagnosis was limited to only small fragments.

Lesion Targeted	"Adequate" ROSE	Definitive Final Diagnosis Rendered	Large Biopsy Fragment Received (>3 mm)
Ductal Adenocarcinoma	54/69 (78%)	63/69 (91%)	46/69 (67%)
All Other Lesions (Including Below)	18/29 (62%)	22/29 (76%)	22/29 (76%)
Neuroendocrine Tumors	9/12 (75%)	11/12 (92%)	9/12 (75%)
Metastatic Carcinomas	5/7 (71%)	6/7 (86%)	4/7 (57%)
Pancreatitis	3/6 (50%)	3/6 (50%)	5/6 (83%)

Conclusions: ROSE is now being requested less frequently, but a higher percentage of cases are something other than ductal adenocarcinoma. This makes ROSE more challenging. Expectations for adequacy rates and definitive final diagnoses should be

adjusted downward. Even large cores (>3 mm) may not be sufficient for full work-up of non-ductal lesions. Good communication with endoscopists and careful triage is more critical than ever.

240 PD-L1 Expression in Cytological NSCLC Cell-Blocks: a Comparative Study of the Inter and Intra-Observer Variability between Conventional and Algorithm-Based Assessments

Guillermo García-Porrero¹, Allan Argueta², Maria Villalba Esparza², Ramón Soldevilla¹, Maria Luisa Bayo¹, José Echeveste¹, Laura Alvarez Gigli², Marta Abengózar Muela², Laura Garcia Tobar², Carlos de Andrea², Maria Lozano²
¹Clinica Universidad de Navarra, Pamplona, Spain, ²University of Navarra, Pamplona, Spain

Disclosures: Guillermo García-Porrero: None; Allan Argueta: None; Maria Villalba Esparza: None; Ramón Soldevilla: None; Maria Luisa Bayo: None; José Echeveste: None; Laura Alvarez Gigli: None; Marta Abengózar Muela: None; Laura Garcia Tobar: None; Carlos de Andrea: None; Maria Lozano: None

Background: The development of immunotherapy for NSCLC has made the study of PD-L1 expression by immunohistochemistry (IHC) necessary. An important percentage of these patients are diagnosed in advanced stages of the disease, and often, only cytologic material is available for analysis. In this context, cell blocks (CB) have become the most frequently used samples to conduct these tests. The use of automated strategies for image analysis could prove to be a useful tool to facilitate the interpretation of PD-L1 results and to reduce inter-observer variability.

Design: We present a case series that includes 32 CB from NSCLC, obtained using EUS and/or EBUS-guided fine needle aspiration with rapid on-site evaluation. PD-L1 detection was conducted using the Ventana PD-L1 (SP263) assay from Roche®. H&E stains and IHC for all CB were performed using the Ventana DP200 scanner from Roche®. Three pathologists analyzed all the cases using conventional microscopy, and two studied PD-L1 expression using the uPath PD-L1 image analysis algorithm from Roche®. The results of both groups were compared using Spearman correlation coefficient. Intra and inter-observer total percentage agreement scores were calculated for both cut-off points of ≥ 1% and ≥ 50%.

Results: The percentages of PD-L1 expression obtained using conventional microscopy showed good correlation to those obtained using image analysis, with a correlation coefficient ranging from 0.79-0.85 (p<0,001). Inter-algorithm correlation was found to be greater than inter-pathologist correlation (R=0,98; p<0,001 and R=0,69; p<0,001 respectively). Inter-observer and intra-observer total percentage agreement scores for both cut-off points were higher in the algorithm group.

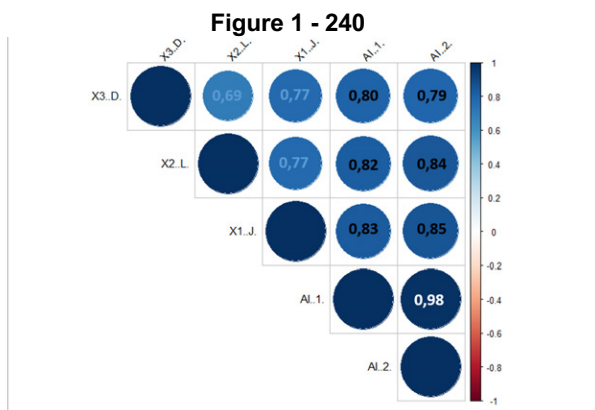


Figure 1. Inter-observer correlation. X1(conventional microscopy 1), X2 (conventional microscopy 2), X3 (conventional microscopy 3), Al.1 (uPath PD-L1 image analysis algorithm 1), Al.2 (uPath PD-L1 image analysis algorithm 2).

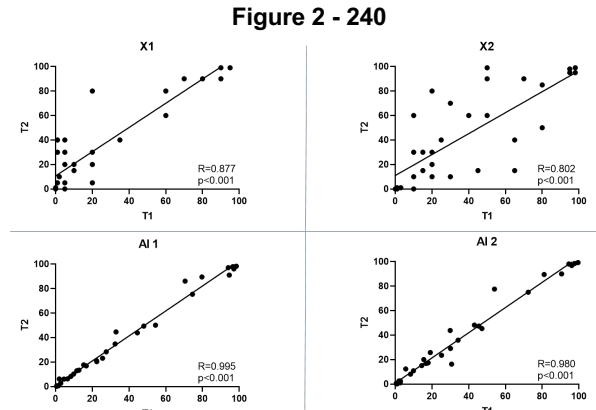


Figure 2. Intra-observer correlation. X1(conventional microscopy 1), X2 (conventional microscopy 2), Al.1 (uPath PD-L1 image analysis algorithm 1), Al.2 (uPath PD-L1 image analysis algorithm 2), T1 (first assessment), T2 (follow-up assessment).

Conclusions: The uPath PD-L1 image analysis algorithm for NSCLC from Roche® to evaluate PD-L1 in CB appears to be valid and reproducible, showing high statistical association with results obtained using conventional microscopy.

Percentages of total intra and inter-observer agreement scores for both cut-off points analyzed (>95%) were higher in the algorithm group, showing that the use of automated image analysis could significantly lower intra and inter-observer variability, allowing for a better discrimination of patients with elevated PD-L1 tumor expression from those with a lower expression.

241 Concurrent Thyroid Fine Needle Aspirations and Core Needle Biopsies: An Institutional Experience

Hamza Gokozan¹, Aysegul Eren², Abdullah Osme³, Nami Azar⁴, Jay Wasman⁴

¹New York-Presbyterian/Weill Cornell Medical Center, New York, NY, ²University Hospitals Cleveland Medical Center, Case Western Reserve University, Cleveland, OH, ³Case Western Reserve University/University Hospitals Cleveland Medical Center, Cleveland, OH, ⁴University Hospitals Cleveland Medical Center, Cleveland, OH

Disclosures: Hamza Gokozan: None; Aysegul Eren: None; Abdullah Osme: None; Nami Azar: None; Jay Wasman: None

Background: Fine needle aspiration (FNA) is the most well-established and commonly used method for the sampling of thyroid nodules. Due to limitations in FNA sampling and interpretation, core needle biopsy (CNB) has been suggested as an adjunct or alternative modality to improve diagnostic yield; therefore, we evaluated the concurrent use of FNA and CNB.

Design: Between January 2019 and October 2020, 207 consecutive patients with 254 nodules underwent concurrent radiologist-performed, ultrasound-guided FNA and CNB at University Hospitals Cleveland Medical Center. For cytology, four passes were performed with 22-25 gauge needles. Direct smears were prepared with Papanicolaou and Diff-Quik stains, and material from the needle rinses was used to prepare one ThinPrep slide for each nodule sampled. Following the FNA procedure, one or more needle cores was obtained by CNB performed with 18-20 gauge biopsy needles. H&E stained slides from each CNB were prepared using our standard surgical pathology biopsy protocol. The FNA and CNB specimens were prospectively evaluated independently by board-certified pathologists. FNA specimens were interpreted using Bethesda System criteria. CNB specimens were interpreted using similar terminology with diagnostic criteria based on the experience of the evaluating pathologists. Cases with prior indeterminate or non-diagnostic FNA results were excluded from the study.

Results: A total of 254 nodules were sampled, including 55 from men and 199 from women. The ages of the study population ranged from 21 to 90 (Median: 63). No complications were reported related to CNB or FNA. The overall results are summarized in Table 1. The combined adequacy rate was higher than those for FNA or CNB alone (240/254, 94.5%, p<0.01). Though the results did not reach statistical significance, the adequacy rate for FNA alone (222/254, 87.4%) was higher than that for CNB alone (212/254, 83.5%)(p=0.2). CNB and FNA results were concordant in 191 of the cases (191/254, 75.2%). Final surgical pathology was available in 24 cases (24/254, 9.5%). Among the 63 discordant cases, 13 underwent resection (13/63, 20.6%). The final diagnoses of eight and four of these cases were concordant with CNB and FNA, respectively. One remaining nodule that was called atypia of undetermined significance on FNA and benign follicular nodule on CNB was papillary thyroid carcinoma on resection.

FNA		CNB						Total
		Non-diagnostic or Unsatisfactory	Benign	Atypia/follicular lesion of undetermined significance	Follicular neoplasm or suspicious for follicular neoplasm	Suspicious for malignancy	Malignant	
Non-diagnostic or Unsatisfactory	14	14	1	1	0	2	32	
% in FNA category	43.75%	43.75%	3.13%	3.13%	0.00%	6.25%		
% in CNB category	33.33%	8.28%	6.25%	10.00%	0.00%	16.67%	12.60%	
% of total	5.51%	5.51%	0.39%	0.39%	0.00%	0.79%		
Benign	21	150	5	1	0	0	177	
% in FNA category	11.86%	84.75%	2.82%	0.56%	0.00%	0.00%		
% in CNB category	50.00%	88.76%	31.25%	10.00%	0.00%	0.00%	69.69%	
% of total	8.27%	59.06%	1.97%	0.39%	0.00%	0.00%		
Atypia/follicular lesion of undetermined significance	5	4	10	2	2	1	24	
% in FNA category	20.83%	16.67%	41.67%	8.33%	8.33%	4.17%		
% in CNB category	11.90%	2.37%	62.50%	20.00%	40.00%	8.33%	9.45%	
% of total	1.97%	1.57%	3.94%	0.79%	0.79%	0.39%		
Follicular neoplasm or suspicious for follicular neoplasm	0	0	0	6	0	0	6	
% in FNA category	0.00%	0.00%	0.00%	100.00%	0.00%	0.00%		
% in CNB category	0.00%	0.00%	0.00%	60.00%	0.00%	0.00%	2.36%	
% of total	0.00%	0.00%	0.00%	2.36%	0.00%	0.00%		
Suspicious for malignancy	1	0	0	0	2	2	5	
% in FNA category	20.00%	0.00%	0.00%	0.00%	40.00%	40.00%		
% in CNB category	2.38%	0.00%	0.00%	0.00%	40.00%	16.67%	1.97%	
% of total	0.39%	0.00%	0.00%	0.00%	0.79%	0.79%		
Malignant	1	1	0	0	1	7	10	
% in FNA category	10.00%	10.00%	0.00%	0.00%	10.00%	70.00%		

% in CNB category	2.38%	0.59%	0.00%	0.00%	20.00%	58.33%	3.94%
% of total	0.39%	0.39%	0.00%	0.00%	0.39%	2.76%	
Total	42	169	16	10	5	12	254
% in FNA category	16.54%	66.54%	6.30%	3.94%	1.97%	4.72%	
% in CNB category							
% of total							

Conclusions: While FNA alone had a higher adequacy rate than that of CNB alone, combining the 2 modalities resulted in a significantly higher adequacy rate than either technique alone. Our results suggest that adding CNB to FNA biopsy in the evaluation of thyroid nodules is safe and effective in reducing the number of unsatisfactory specimens as compared to using either technique alone.

242 Papanicolaou Test Findings Associated with Significant Outcomes Regardless of HPV Cotest Result

Abha Goyal¹, Mary Abdelsayed¹, Thomas Dilcher², Susan Alperstein³

¹New York-Presbyterian/Weill Cornell Medical Center, New York, NY, ²New York-Presbyterian Hospital, New York, NY, ³Weill Cornell Medicine, New York, NY

Disclosures: Abha Goyal: None; Mary Abdelsayed: None; Thomas Dilcher: None; Susan Alperstein: None

Background: The 2020 American Cancer Society guidelines strongly recommended primary HPV screening for cervical cancer prevention, to which the American Society for Colposcopy and Cervical Pathology (ASCCP) has also recently lent its support. Studies investigating the role of cytology in the detection of cervical precancer/cancer, have mainly focused on high-grade squamous intraepithelial lesion (HSIL) or worse interpretations. Here, we have examined the significance of those cytology results (in addition to ³ HSIL), that require histologic follow-up as per the current ASCCP management guidelines, regardless of the HPV test result.

Design: A database search from September 2010 to December 2019 retrieved the cervical Papanicolaou (Pap) tests with any of the following interpretations: carcinoma (CA), HSIL suspicious for invasion (SUSP), HSIL, atypical squamous cells – cannot exclude HSIL (ASC-H), low grade squamous intraepithelial lesion, HSIL cannot be excluded (LSIL-H); atypical glandular cells (AGC), AGC, favor neoplastic (AGCFN); atypical endocervical cells (AEC), AEC, favor neoplastic (AECFN); adenocarcinoma in situ (AIS) and atypical endometrial cells (AEM). Of these, those with negative HPV cotest (Hybrid Capture 2 or APTIMA platform) were included for further analysis. For this study cohort, relevant clinical history and histologic follow-up (within one year) were recorded.

Results: During the study period, a total number of 345140 Pap tests were examined. For the diagnostic categories under consideration, the number of cases, the percentage of HPV negative cases and the significant histologic follow-up findings are depicted in Table 1. Of those who were diagnosed on histology, 42 (72.4%) HSIL/AIS patients had prior abnormal cytology/histology/HPV history and 39 (66.1%) endometrial carcinoma/atypical hyperplasia patients had clinical signs/symptoms of endometrial pathology.

Pap Test Result	No. of Cases	HPV Tested	HPV Negative (%)	HPV Negative Cases with Follow-up (%)	Significant Follow-up (No. of Patients)
CA	26	22	8 (36.4)	5 (62.5)	HSIL (1), Endometrial CA (4)
HSIL	1050	795	73 (9.2)	65 (89.0)	HSIL (28)
SUSP	27	15	2 (13.3)	1 (50.0)	HSIL (1)
ASC-H	1074	888	291 (32.8)	220 (75.6)	HSIL (19), Endometrial CA (1)
LSIL-H	587	391	48 (12.3)	32 (66.7)	HSIL (8)
AEM	134	96	82 (85.4)	66 (80.4)	Endometrial CA /Atypical hyperplasia (23), Ovary/Fallopian tube tumor (2)
AGC	290	207	164 (79.2)	134 (81.7)	Endometrial CA/Atypical hyperplasia (22), Ovary/Fallopian tube tumor (4), Paget disease involving cervix (1), Metastasis (1)
AGCFN	20	14	13 (92.9)	8 (61.5)	Endometrial CA (6)
AEC	149	131	118 (90.1)	91 (77.1)	AIS (1), Endometrial CA (2)
AECFN	14	3	2 (66.7)	1 (50.0)	Gastric-type Cervical CA (1)

Conclusions: The cervical Pap test detects a small subset of significant lesions of the female genital tract (independent of the HPV test) of which a considerable proportion represents HPV-unassociated neoplasia. With the increase in HPV vaccination and the widespread adoption of risk-based approach to management of abnormal cervical cancer screening tests, the role of cytology, by itself, will diminish in the detection of HPV-associated lesions. Additional data regarding the role of cytology in the detection of HPV-independent lesions will be instrumental in the designing of future screening guidelines.

243 A Multi-institutional Validation of a Modified Scheme for Subtyping Salivary Gland Neoplasm of Uncertain Malignant Potential (SUMP)

Jen-Fan Hang¹, Jaslyn Lee², Min Nga², Kayoko Higuchi³, Yukiya Hirata⁴, Howard Wu⁵, Derek Allison⁶, Jason Gilbert⁶, Oscar Lin⁷, Mauro Saieg⁸, Arthur de Arruda⁸, Yun-An Chen⁹, Eric Huang¹⁰, Varsha Manucha¹¹

¹Taipei Veterans General Hospital, Taipei, Taiwan, ²National University Hospital, Singapore, Singapore, ³Okinawa Kyodo Hospital, Naha, Japan, ⁴University of the Ryukyus, Nishihara, Japan, ⁵Indiana University School of Medicine, Indianapolis, IN, ⁶University of Kentucky College of Medicine, Lexington, KY, ⁷Memorial Sloan Kettering Cancer Center, New York, NY, ⁸A.C.Camargo Cancer Center, Sao Paulo, Brazil, ⁹Taichung Veterans General Hospital, Taichung, Taiwan, ¹⁰University of Washington, Seattle, WA, ¹¹University of Mississippi Medical Center, Jackson, MS

Disclosures: Jen-Fan Hang: None; Jaslyn Lee: None; Min Nga: None; Kayoko Higuchi: None; Yukiya Hirata: None; Howard Wu: None; Derek Allison: None; Jason Gilbert: None; Oscar Lin: None; Mauro Saieg: None; Arthur de Arruda: None; Yun-An Chen: None; Eric Huang: None; Varsha Manucha: None

Background: The Milan System for Reporting Salivary Gland Cytopathology (MSRSGC) was introduced in 2018 and has been widely accepted by the cytopathology community internationally. Among the diagnostic categories, Salivary Gland Neoplasm of Uncertain Malignant Potential (SUMP) is the most challenging. Multiple approaches have been proposed for subtyping SUMP, and studies have shown contradictory findings regarding the risk of malignancy (ROM) for SUMP with basaloid versus oncocytic/oncocytoid features. This study aims to validate a modified scheme for subtyping SUMP in a large multi-institutional cohort.

Design: Ten institutions participated in this study, including 6 from America (5 from the US and 1 from Brazil) and 4 from Asia (2 from Taiwan, 1 from Japan, and 1 from Singapore). Consecutive salivary gland fine-needle aspirations (FNAs) during the study period were classified based on the MSRSGC. Cases diagnosed as SUMP with available cytology slides and surgical follow-up were recruited for review and subtyping based on a modified scheme as follows: basaloid SUMP (B1: absent or scant non-fibrillary matrix, B2: presence of non-fibrillary or mixed-type matrix), oncocytoid SUMP (O1: with mucinous background, O2: without mucinous background), and SUMP not otherwise specified (NOS).

Results: A total of 742 SUMP cases were identified from 9938 consecutive salivary gland FNAs. Among them, 525 (70.8%) had surgical follow-up. Cytology slides were available for 329 (62.7%) cases with the ROM of 40.1% and risk of neoplasm (RON) of 96%. After slide review, 156 (47.4%) were classified as basaloid SUMP with the ROM of 35.9% and RON of 98.1%, 101 (30.7%) as oncocytoid SUMP with a ROM of 52.5% and RON of 91.1%, and 72 (21.9%) as SUMP NOS with the ROM of 31.9% and RON of 98.6%. None of the cases were specified as clear cell predominant. The ROM of oncocytoid SUMP was significantly higher than that of basaloid SUMP (p=0.0099) and SUMP NOS (p=0.0084). No significant differences of ROM were noted between B1 and B2 (36.7% versus 35.1%, p=0.8685) and O1 and O2 (65.2% versus 48.7%, p=0.2349).

Table 1 - 243. ROM and RON of different SUMP subtypes

SUMP subtype	n	Surgical follow-up			ROM	RON
		Non-neoplastic	Benign	Malignant		
Basaloid SUMP	156	3	97	56	35.9%	98.1%
B1	79	2	48	29	36.7%	97.5%
B2	77	1	49	27	35.1%	98.7%
Oncocytoid SUMP	101	9	39	53	52.5%	91.1%
O1	23	1	7	15	65.2%	95.7%
O2	78	8	32	38	48.7%	89.7%
SUMP NOS	72	1	48	23	31.9%	98.6%
Total	329	13	184	132	40.1%	96.0%

Conclusions: SUMP comprised 7.5% of salivary FNAs in our large multi-institutional study with a ROM of 40.1% and RON of 96%. The ROM of oncocytoid SUMP was 52.5% and significantly higher than that of basaloid SUMP (35.9%, p=0.0099) and SUMP

NOS (31.9%, p=0.0084). No significant differences in ROM were noted when basaloid and oncocytoid were categorized based on different characteristics of matrix or background mucin.

244 Validation of FNA Smears for Molecular Analysis in Indeterminate Thyroid Nodules at a Single, Large Academic Medical Center

Dan Hodges¹, Daniel Johnson¹, Cord Sturgeon¹, Dina Elaraj¹, Ioannis Papagiannis¹, Ritu Nayar²

¹Northwestern University Feinberg School of Medicine, Chicago, IL, ²Northwestern University, Chicago, IL

Disclosures: Dan Hodges: None; Daniel Johnson: None; Cord Sturgeon: None; Dina Elaraj: None; Ioannis Papagiannis: None; Ritu Nayar: None

Background: FNA biopsy is critical for guiding surgical and/or clinical management of thyroid nodules. Guidelines recommend molecular analysis for indeterminate FNA diagnosis (Bethesda- AUS/FLUS, FN/SFN, SUSP). A number of molecular tests are commercially available, with limited data on equivalency of “slide-based” versus “liquid-based”. Molecular testing from FNA smears has potential benefits of avoiding repeat biopsy and providing real time morphologic correlation. Data is limited on the equivalency of molecular testing “slide-based” versus “liquid-based” aspirates. Our annual thyroid FNA volume is ~1600 with a 10.4% indeterminate rate (AUS-8.2%, Neoplasm-2%, Susp-0.2%). A dedicated FNA pass for molecular testing is collected by some of our providers, however the practice is not routine. We evaluated the feasibility of molecular testing on FNA smears to provide another option.

Design: We sent adequate cellularity (>100 cells), air-dried, Diff Quik stained FNA smears from 69 unique, deidentified, archived cases of indeterminate thyroid FNAs (AUS =53, neoplasm =16) to a proprietary commercial lab for molecular analysis. All 69 had another molecular test performed at CBLPath, Interpace or Veracyte, on a matched aspirate collected in preservative, during FNA biopsy. The results from smears were compared to corresponding prior molecular results (Table 1).

Results: 10/69 FNA smears were unsatisfactory for testing due to insufficient cellularity (14%). Of the remaining 59 cases, 28 had a prior molecular alteration identified; 41 had no alteration. Overall concordance between smear based and prior co-collected molecular analysis 78% (54/69). Similar alterations were found in 20/25 (80%) and absence of alterations correlated in 34/34 (100%). In 5 cases smear analysis did not identify alterations seen on concurrent aspirate by other testing (*EIF1AX*, *DICER1*, *EZH1*, *RET*, and *SPOP*). In one case, smear testing found a specific alteration (*NRAS Q16R*) previously called “suspicious” on Affirma test. Histologic follow up was available in 32/69 cases, including 22 (10 malignant, 12 benign) with identified alterations. Of 33 resections; 10 were malignant with alterations in 9 on original/8 on smear testing.

Original molecular testing – Company Test	Bethesda FNA Diagnostic Category	n	Number of Cases w/ Molecular Alterations Found	Number of Cases with Alterations Found by FNA Smear	Number of Cases with Alterations - Unsat	Number of Cases with Alterations Not Identified	Number of Cases With No Alteration	Total n unsat
CBLPath	AUS	28	11	8	0	3	14	3
	neoplasm	7	4	3	0	1	3	0
Thyro Seq V3 Interpace	AUS	8	3	1	2	0	5	2
	Neoplasm	5	3	2	1	0	2	1
ThyGenNEXT (aspirate in preservative) Interpace	AUS	9	5	5	0	0	3	1
	neoplasm	4	1	1	0	0	3	0
ThyGeNX (FNA smear) Veracyte	AUS	8	1	0	0	1	4	2
	neoplasm	0	0	0	0	0	0	0
Affirma								
	TOTAL:	69	28	20	3	5	35	9

Abbreviations: AUS – Atypia of Undetermined Significance; FLUS – Follicular Lesion of Undetermined Significance; FN – Follicular Neoplasm; SFN – Suspicious for Follicular Neoplasm; SUSP – Suspicious; Unsat – Unsatisfactory

Conclusions: Archived, air-dried, Diff Quik stained slides can be successfully used for thyroid molecular analysis. Adequacy was 86%; slightly below predicted (90%). After excluding insufficient cases, and those where the alteration wasn't covered on the tested panel, concordance rate approached 98%.

245 The Laboratory Dependent ASC Rate: Floating the ASC Rate

Alyaa Irhayyim¹, Rob Klein², Faisal Mukhtar³, F Zahra Aly⁴

¹UF Health Gainesville, Gainesville, FL, ²University Medical Center, Tucson, AZ, ³University of Florida, Gainesville, FL, ⁴University of Florida College of Medicine, Gainesville, FL

Disclosures: Alyaa Irhayyim: None; Rob Klein: None; Faisal Mukhtar: None; F Zahra Aly: None

Background: The Atypical Squamous Cells (ASC) reporting category of The Bethesda System For Reporting Cervical Cytology is used in cases whereby a definite diagnosis of low grade squamous intraepithelial lesion (LSIL) or high grade squamous intraepithelial lesion (HSIL) cannot be made. In such cases, the differential diagnosis includes reactive cellular changes, atrophy and immature metaplastic cells. Due to differing practitioner threshold of normal and abnormal, the ASC rate varies between pathologists and different laboratories. Monitoring of ASC/LSIL ratio is a commonly used laboratory quality assurance measure which is used to inform on over- or under-use of the category.

High risk human papillomavirus (hr-HPV) has been used in conjunction with ASC/SIL ratios as quality assurance tools to provide more granular data on the threshold of a particular pathologist lying towards reactive or neoplastic change. However, the laboratory population's overall prevalence rate of hr-HPV has not been previously examined for association with the ASC rate. The aim of the present study was to examine the overall hr-HPV prevalence rate and its relationship to the ASC rate.

Design: All cytology specimens submitted in 2019 were included in the study. The reported cytological category, associated hr-HPV test results (independent of cytological diagnosis) and cervical biopsy results were collated. The study was approved as a Quality Assurance Study.

Results: A total of 2584 cervical cytology specimens were included. A proportion of these (1909) had hr-HPV test. Hr-HPV was detected in 286 patients with the majority (82%) being non 16/18 subtype. The 20-29 age group were more likely to be infected by HPV and particularly non16/18 type. Older patients (>50 years) were less likely to be infected by HPV; however, they preferentially harbored HPV 16/18.

The ASC/LSIL ratio was nearly twice as high (3.04 versus 1.56) in those positive for non-16,18 subtypes of hr-HPV than those with HPV subtypes 16 or 18. The overall ASC/LSIL ratio for all cases was 2.66. Also, 82 of the 154 total ASCUS cases (53.25%) were in those positive for non-16,18 subtypes of HPV.

Conclusions: HPV non-16/18 is the main subtype associated with the ASC category. Instead of basing the laboratory and practitioners' quality indicator on a blanket ASC/LSIL ratio, the overall prevalence of HPV and especially of its non-16/18 subtypes should be considered in order to be more reflective of performance.

246 Performance of Afirma Genomic Sequencing Classifier and Histopathological Outcome Are Associated with Subtype of Atypia in Bethesda Category III Thyroid Nodules

Xiaobing Jin¹, Madelyn Lew¹, Brian Smola², Liron Pantanowitz¹, Xin Jing¹

¹University of Michigan, Ann Arbor, MI, ²Michigan Medicine, Ann Arbor, MI

Disclosures: Xiaobing Jin: None; Madelyn Lew: None; Brian Smola: None; Liron Pantanowitz: None; Xin Jing: None

Background: Afirma Genomic Sequencing Classifier (GSC) uses next-generation sequencing and has demonstrated improved diagnostic performance in further stratification and management of indeterminate thyroid nodules compared with its predecessor, gene expression classifier (GEC). Several studies have reported that thyroid nodules classified into various subcategories of Bethesda category III - atypia of undetermined significance (AUS) may carry different risk of malignancy. However, there is limited data regarding performance of GSC in subcategorizing AUS cases. This study accordingly aimed to investigate the association of GSC and histopathological outcome in AUS nodules with architectural atypia (AUS-A), cytological atypia (AUS-C), both architectural and cytological atypia (AUS-AC) as well as atypia with predominant Hürthle cells (AUS-HC).

Design: This retrospective study (July 2017-June 2021) included consecutive thyroid nodules that had a recurrent cytologic diagnosis of AUS with qualifiers and were tested by GSC with a diagnostic result (benign vs suspicious). All nodules were followed by either surgical interventions or at least 6 months clinical and/or ultrasound follow-up monitoring. GSC benign call rate (BCR) and malignant rate associated with suspicious GSC were calculated for the individual AUS subcategories. Statistical analysis was performed using the Fisher exact test.

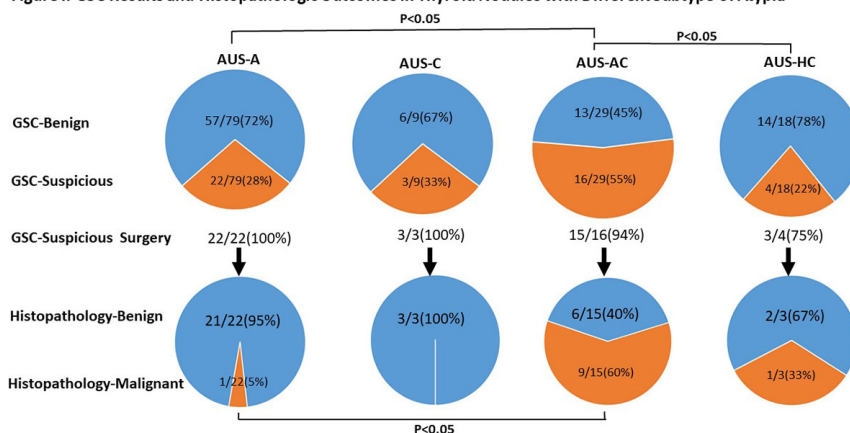
Results: (See Table 1 and Figure 1) The study included a total of 135 eligible thyroid nodules, including 79 AUS-A, 9 AUS-C, 29 AUS-AC, and 18 AUS- HC. BCR was 72% in AUS-A, 67% in AUS-C, 45% in AUS-AC and 78% in AUS-HC. BCR of AUS-A was significantly greater than that of AUS-AC ($p<0.05$). Among nodules with a suspicious GSC result, all AUS-A and AUS-C, 94% of AUS-AC and 75% of AUS-HC were surgically removed. Histology-proven malignancies were documented in 5% of AUS-A, 0% of AUS-C, 60% of AUS-AC and 33% of AUS- HC. GSC suspicious nodules in AUS-AC subcategory demonstrated a significantly higher malignant rate than that of AUS-A subcategory ($p<0.05$).

Table 1: Clinical Follow-up and Histopathological Diagnoses by Subtype of Atypia

Diagnosis	AUS-A	AUS-C	AUS-AC	AUS-HC	Total
Number of nodules	79	9	29	18	135
GSC-Benign	57	6	13	14	90
Clinically stable	45	6	10	11	72
Benign histopathology					
Nodular hyperplasia	9		2	2	13
Hashimoto thyroiditis	2				2
Follicular adenoma	1		1		2
Hürthle cell adenoma				1	1
GSC-Suspicious	22	3	16	4	45
Clinically stable			1	1	2
Benign histopathology					
Nodular hyperplasia	12	3	3	1	19
Follicular adenoma	7		3		10
Hürthle cell adenoma				1	1
NIFTP	2				2
Malignant histopathology					
Papillary thyroid carcinoma			6		6
PTC (follicular variant)			2		2
Follicular carcinoma	1				1
Hürthle cell carcinoma				1	1
Medullary carcinoma			1		1

Figure 1 - 246

Figure 1: GSC Results and Histopathologic Outcomes in Thyroid Nodules with Different Subtype of Atypia



Conclusions: These data demonstrated a significant difference in BCR of GSC and risk of malignancy associated with a suspicious GSC result among thyroid nodules classified into different subcategories of Bethesda category III (AUS). These findings may aid clinical triage and/or management of patients with Bethesda category III (AUS) thyroid nodules. To our knowledge, this may be the first study investigating the performance of GSC in subcategories of AUS nodules.

247 The "Path" to a Whipple: Impact of Telecytology Implementation on Pancreatobiliary Small Biopsies Prior to Whipple Resections

Nicole Joseph¹, Fan Lin¹, Bradley Confer¹, Joseph Blansfield², Sara Monaco¹

¹Geisinger Medical Center, Danville, PA, ²Geisinger Health, Danville, PA

Disclosures: Nicole Joseph: None; Fan Lin: None; Bradley Confer: *Consultant*, Boston Scientific Corporation; *Speaker*, Merit Endotek; Joseph Blansfield: None; Sara Monaco: None

Background: Pancreatobiliary small biopsies can be a challenge to interpret and there is a reluctance to render a malignant diagnosis unless certain given the potential for high-risk surgery. This has driven new needle technology and initiatives to maximize yield to improve patient care. Herein, we look at the implementation of rapid on-site evaluation (ROSE) by remote cytopathologists on quality metrics, including the number of diagnostic procedures and needle passes, in addition to the time to surgery.

Design: Our laboratory information system (CoPathPlus, Cerner) was used to extract Whipple procedures with pre-operative cytology specimens before (January 2019-December 2020) and after (January-September 2021) telecytology ROSE implementation.

Results: When looking at patients receiving a Whipple resection at our institution before and after telecytology implementation, there were 125 pre-operative surgical and cytology specimens from 46 total patients, including 53 (81.5%) cytology specimens from 37 patients prior to implementation and 12 (18.5%) cytology specimens from 9 patients after implementation. When comparing the groups before and after implementation, there was an increase in the utilization of ROSE by cytopathologists for pancreatobiliary specimens (0 to 88.9%), decrease in number of pre-operative biopsies (1.8 to 1.4), and decrease in the number of days between initial biopsy and Whipple resection (65.6 days to 39.0 days). For the cytology fine needle biopsies (FNB), the average number of total passes increased (2.9 to 4.1), the number of passes dedicated for cell block increased (1.5 to 2.2) and less passes were utilized for slide preparation (2.5 to 2.1). Overall, the concordance between pre-operative cytology and final surgical diagnoses increased from 67.6% to 77.8%. [Table 1]

Table 1: Comparison of Quality and Patient metrics before and after telecytology implementation in Pancreatobiliary specimens.

Metrics	Pre-ROSE Implementation	Post-ROSE Implementation
# Whipple procedures with pre-operative cytology (n,%)	37 (80.4%)	9 (19.6%)
Number of total cytology specimens	53 (81.5%)	12 (18.5%)
Avg Age (years)	66.3	60.6
Stage		
pT1N0	2 (5.4%)	0 (0%)
pT2N0	5 (13.5%)	2 (22.2%)
pT2N1	7 (18.9%)	0 (0%)
pT2N2	4 (10.8%)	1 (11.1%)
pT3N0	1 (2.7%)	0 (0%)
pT3N1	2 (5.4%)	2 (22.2%)
pT3N2	5 (13.5%)	2 (22.2%)
pT4N2	1 (2.7%)	0 (0%)
None	10 (27.0%)	2 (22.2%)
Known History of Neoadjuvant Treatment	0 (0%)	2 (22.2%)
Positive Lymph Nodes at Resection	17 (45.9%)	5 (55.6%)
Average Size of Tumor (cm)	3.6	5.0
Diagnostic Work-up Time (from 1st diagnostic episode to surgery, days)	65.6	39.0
# Pre-operative samples	1.8	1.4
ROSE used (n,%)	0 (0%)	8 (88.9%)
Adequacy by cytotech/fellow only (n,%)	37 (100%)	0 (0%)
Average # of total passes	2.9	4.1
Average # of passes used for slide preparation	2.5	2.1
Average # of passes dedicated for cell block	1.5	2.2
Concordance between cytology & surgical (n, %)	25 (67.6%)	7 (77.8%)
Discordance between cytology & surgical (n, %)	12 (32.4%)	2 (22.2%)

Conclusions: Implementation of telecytology has allowed our clinicians to utilize ROSE by cytopathologists at a rural healthcare system with multiple remote endoscopy locations. This has resulted in an improvement in various quality metrics, such as decreased number of pre-operative biopsies, decrease in the time to Whipple resection, increase in the number of passes allocated for cell block, and better concordance in diagnoses, despite an increase in needle passes. Given the limited sample size post-implementation, continuing to follow these metrics over time will help to further define the impact on our pancreatobiliary practice and patient care.

248 Cytomorphology of Poorly Differentiated Thyroid Carcinoma: Useful Features to Examine on Fine Needle Aspiration

Christine Kim¹, Fei Chen¹, Negin Shafizadeh¹, Fang Zhou², Wei Sun¹, Cheng Liu¹, Aylin Simsir², Tamar Brandler¹
¹NYU Langone Health, New York, NY, ²NYU School of Medicine, New York, NY

Disclosures: Christine Kim: None; Fei Chen: None; Negin Shafizadeh: None; Fang Zhou: *Stock Ownership*, MRNA; *Stock Ownership*, DOCS; Wei Sun: None; Cheng Liu: None; Aylin Simsir: None; Tamar Brandler: None

Background: Poorly differentiated thyroid carcinoma (PDTC) accounts for <2% of all thyroid cancers and demonstrates morphology and behavior on a spectrum between differentiated thyroid carcinomas (DTC) and anaplastic thyroid carcinomas (ATC), with high risk for recurrence and metastasis. While DTC and ATC are generally identifiable on fine needle aspiration (FNA), features of PDTC on FNA are not as well characterized. Therefore, we aimed to identify common features seen on FNA cytology samples of PDTCs with cyto-histologic and molecular correlations.

Design: We searched our database for surgically diagnosed primary or recurrent PDTC cases with preceding FNA cytology. Cytology slides were reviewed by a cytopathologist to assess cytomorphologic characteristics including cellularity, chromatin quality, nuclear/cytoplasmic ratio, trabecular pattern, sheets, irregular nuclear borders, prominent nucleoli, overlapping/crowded cells, nuclear pseudo-inclusions, grooves, necrosis, mitoses, and endothelial wrapping.

Results: There were 12 cytology cases. Female:male ratio was 7:5, age: 40-83 years, (median 63, mean 64). Cytology diagnoses included Atypia of undetermined significance (AUS), Bethesda III (1, 8%), Suspicious for follicular neoplasm (SFN), Bethesda IV (3, 25%); Suspicious for papillary thyroid carcinoma (PTC), Bethesda V (2, 17%), and PDTC, Bethesda VI (6, 50%). The majority of cases showed increased cellularity (11, 92%), enlarged neoplastic cells (11, 92%), and sheets (11, 92%). Mitoses were present in 2 cases (15%) and possible necrosis in 1 (8%). 6/7 cases with molecular testing showed mutations, four (67%) of which included *TERT* or *TP53*. The remainder were *TERT* (1, 14%); *BRAF V600E*, *PIK3CA*, *DNMT3A*, *VHL* (1, 14%); and *BRAF K601E*, *TERT*, *EIF1AX* (1, 14%); *TERT*, *NRAS* (1, 14%); *TP53* (1, 14%); and *PTEN* (1, 14%) (Tables 1-2).

Table 1. Cytomorphologic features of poorly differentiated thyroid carcinoma

Characteristics	Cases; (percentage %)
Cellularity	Cellular: 11 (92%), Scant: 1 (8%)
Trabecular pattern	2 (17%)
Microfollicular pattern	6 (50%)
Sheets/clusters	11 (92%)
Isolated cells	9 (75%)
Monomorphic	7 (58%)
High N:C ratio	7 (58%)
Enlarged cells	11 (92%)
Chromatin quality	Fine: 9 (75%), Coarse: 3 (25%)
Irregular nuclear borders	5 (42%)
Prominent nucleoli	3 (25%)
Overlapping/crowded cells	9 (75%)
Nuclear pseudo-inclusions	1 (8%), 2 possible (17%)
Nuclear grooves	5 (42%)
Necrosis	Possible 1 (8%)
Mitoses	2 (17%)
Endothelial wrapping	0 (0%)

Table 2. Cytology and histologic correlation with molecular alterations.

Case	Bethesda category	Molecular alteration	Surgical resection diagnosis
1	V, Suspicious for papillary thyroid carcinoma	<i>TERT</i> <i>BRAF K601E</i> <i>EIF1AX</i>	Poorly differentiated thyroid carcinoma, pT3aN0a
2	V, Suspicious for papillary thyroid carcinoma	<i>TERT</i> <i>NRAS</i>	Poorly differentiated thyroid carcinoma, Background papillary thyroid microcarcinomas, pT3aNX
3	VI, Poorly differentiated thyroid carcinoma	Not performed	Poorly differentiated thyroid carcinoma, pT3aN0a
4	III, Atypia of undetermined significance	<i>TP53</i>	Poorly differentiated thyroid carcinoma with diffuse necrosis, foci with giant cell and partial squamoid differentiated suspicious for evolving anaplastic transformation, pT3bN0a
5	IV, Suspicious for follicular neoplasm with Hurthle cell features	<i>PTEN</i>	Poorly differentiated thyroid carcinoma
6	IV, Suspicious for follicular neoplasm	Negative	Background papillary thyroid carcinomas, pT1aN0 Poorly differentiated thyroid carcinoma with diffuse necrosis pT4aN1a
7	VI, Consistent with poorly differentiated thyroid carcinoma	Not performed	Poorly differentiated thyroid carcinoma, pT2NXM1
8	IV, Follicular neoplasm	<i>TERT</i>	Poorly differentiated thyroid carcinoma, pT3NXM1
9	VI, Poorly differentiated carcinoma	Not performed	Not available Reportedly with metastatic thyroid carcinoma to lymph nodes and femur, with areas of solid growth consistent with poorly differentiated thyroid carcinoma
10	VI, Poorly differentiated thyroid carcinoma	<i>BRAF V600E</i> <i>PIK3CA</i> <i>DNMT3A</i> <i>VHL</i>	Not available History of papillary thyroid carcinoma status post total thyroidectomy with right neck mass
11	VI, Poorly differentiated thyroid carcinoma	Not performed	Not available Reportedly poorly differentiated thyroid carcinoma at outside hospital, pT3N1bM1 with bone and lung metastasis
12	VI, Most consistent with poorly differentiated thyroid carcinoma	Not performed	Not available Reportedly with metastatic thyroid cancer to lung

Figure 1 - 248

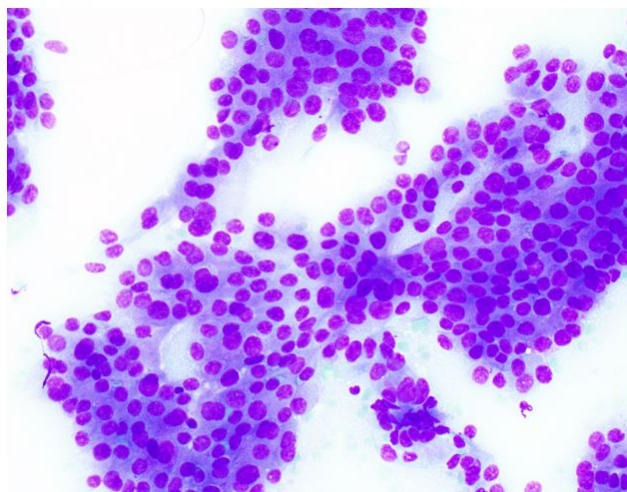


Figure 1. Enlarged follicular cells in sheets with N:C ratio >0.5 from case 3, which was called PDTC on cytology and surgical resection (Diff-Quick stain, 40x)

Figure 2 - 248

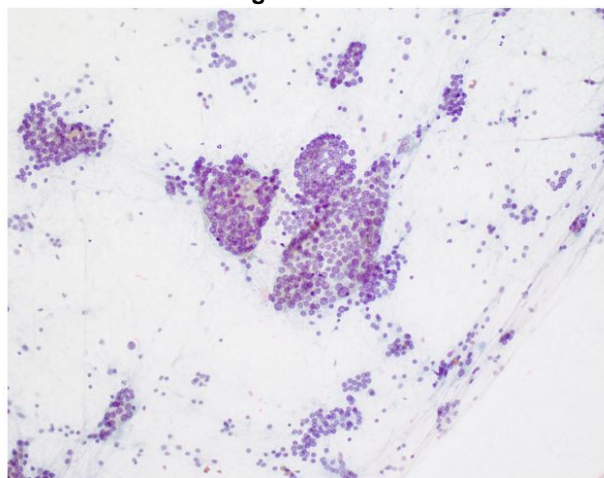


Figure 2. Follicular cells in sheets, few microfollcles, as well as scattered isolated cells from case 8, which was diagnosed as follicular neoplasm on cytology and PDTC on surgical resection. (Ultrafast Papanicolaou stain, 20x).

Conclusions: The cytomorphologic characteristics most commonly identified included increased cellularity, presence of sheets, and enlarged nuclei. Only few cases demonstrated characteristics of the Turin criteria for histologic diagnosis of PDTC, suggesting that the histologic criteria for PDTC may not be reliably used in FNA cytology. Due to overlapping features with DTC, including microfollicular pattern or PTC nuclear features, 3 cases were undercalled as SFN; 3 were called either AUS or suspicious for PTC. Additional data including molecular profiling can aid in achieving the proper diagnosis and management, as PDTC tended to display higher risk mutations involving *TERT* and *TP53*.

249 To Stack or Not to Stack: Does Z-Stacking Improve Morphologic Evaluation of Urine Cytology Whole Slide Images (WSI) for High-grade Urothelial Carcinoma (HGUC)?

David Kim¹, Robert Burkhardt¹, Susan Alperstein², Hamza Gokozan¹, Abha Goyal¹, Jonas Heymann², Ami Patel¹, Momin Siddiqui²

¹New York-Presbyterian/Weill Cornell Medical Center, New York, NY, ²Weill Cornell Medicine, New York, NY

Disclosures: David Kim: None; Robert Burkhardt: None; Susan Alperstein: None; Hamza Gokozan: None; Abha Goyal: None; Jonas Heymann: None; Ami Patel: None; Momin Siddiqui: None

Background: Although the advent of whole slide images (WSI) has transformed the practice of pathology with increasing clinical and research benefits, adoption has been slower in cytology. Difficulties in performing multifocal plane scanning (Z-stack) on 3-dimensional (3D) cell clusters have been a hurdle. ThinPrep® preparations may alleviate the issue as the process produces a monolayer of cells, reducing clusters. To date, no study has evaluated the utility and necessity of Z-stack WSI in urine cytology specimens. This study investigates the utility of Z-stacked images for morphologic assessment and the experience of evaluating urine ThinPrep® WSI.

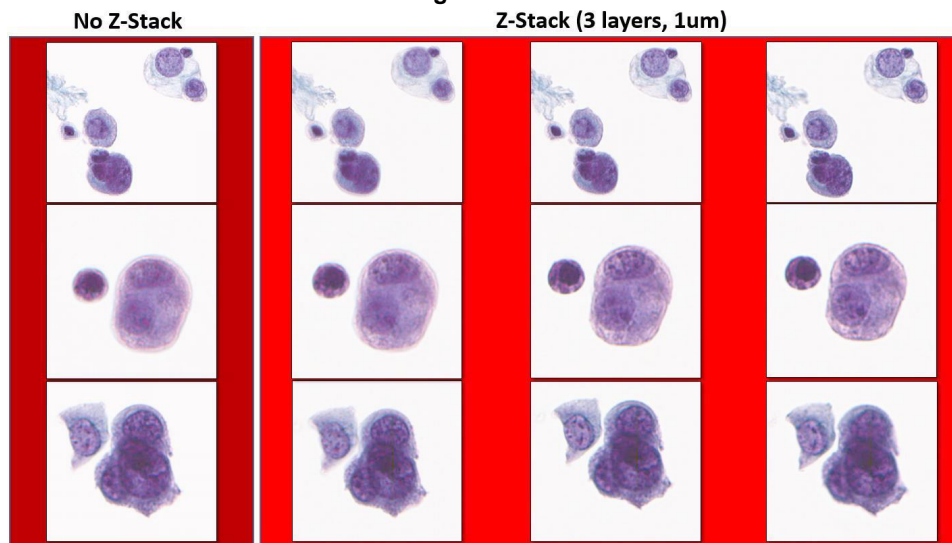
Design: Thirty urine ThinPrep® cases with biopsy-confirmed diagnoses of HGUC (n = 22) and negative for high-grade urothelial carcinoma (NHGUC) (n=8) were selected. Slides were scanned at 40x magnification on the Leica Aperio AT2 without Z-stack and with Z-stack at 3 layers of 1µm each (Fig 1). Six cytopathologists and 1 cytotechnologist evaluated the cases in two rounds without knowing whether the cases were Z-stacked. The first round was without Z-stack, then after a two-week wash-out period, a second round of the same cases with Z-stack were evaluated. Concordance with the original pathology reports, inter-observer concordance, and intra-observer concordance between the two rounds were calculated using a weighted Cohen’s Kappa (CK). A survey was given after each round to evaluate the experience.

Results: For slides without Z-stack, CK with the original report ranged from 0.606-1 (p<0.05), reflecting substantial to perfect concordance. For slides with Z-stack, CK with the original report ranged from 0.533-1 (p<0.05) also indicating substantial to perfect concordance. For both rounds, interobserver CK was moderate to perfect. CK between rounds were 0.697-1 (p <0.05), indicating substantial to perfect concordance (Table 1). The average scan time and file size for slides without Z-stack are 6.27 minutes and 827 megabytes whereas for Z-stack slides they are 14.06 minutes and 2.65 gigabytes. The post-evaluation surveys demonstrated a range in comfort and utility with slightly more favorable opinions for Z-stacked cases.

Reviewer	No Z-stack (Round 1)		Z-stack (Round 2)		Intraobserver Kappa No Z-stack and Z-stack
	Kappa to OP	Interobserver Kappa	Kappa to OP	Interobserver Kappa	
A	0.958	0.509-0.958	1	0.533 - 1	0.958
B	0.606	0.439-0.72	0.645	.490-0.645	0.697
C	1	0.615-0.958	1	0.533 - 1	1
D	0.615	0.417-0.615	0.533	0.533 - 0.606	0.726
E	0.675	0.591-0.711	0.606	0.595 - 0.606	0.815
F	0.842	0.417-0.883	0.766	0.412-0.766	0.798
G	0.879	0.622-0.92	1	0.533 - 1	0.879

OP = Concordance with the original pathology report, Interobserver Kappa = concordance between reviewers, Intraobserver Kappa = Concordance between rounds of no Z-stack and Z-stack

Figure 1 - 249



Conclusions: Z-stack images provide minimal diagnostic benefit for urine ThinPrep® WSI. In addition, Z-stacked Urine WSI do not justify the prolonged scan times and larger storage needs compared to those without Z-stack. Concordance is high with or without Z-stack in the evaluation and diagnosis of HGUC in a mix with NHGUC. However, participants were more comfortable with Z-stack slides. While more rigorous studies and further optimization in user experience are needed for primary digital sign-out, Z-stack for Urine ThinPrep® may be unnecessary.

250 Efficient Labeling of High Quality Cytology SurePath Images for Machine Learning

Silva Kristo¹, Agnes Colanta², Rema Rao¹, Simon Sung¹

¹Albert Einstein College of Medicine, Montefiore Medical Center, Bronx, NY, ²Montefiore Medical Center, Bronx, NY

Disclosures: Silva Kristo: None; Agnes Colanta: None; Rema Rao: None; Simon Sung: None

Background: Current approach in supervised machine learning (ML) in pathology is limited by annotation of region of interest on tissue sections. Furthermore, traditional approach to annotation of histology images are not suitable for cytopathology preparations. We propose a highly efficient labeling process (heLP) for cytology ML application using SurePath Pap smear slides and demonstrate potential application for screening Pap smears using open-source convolutional neural network (CNN) trained using heLP image data set.

Design: We collected a total of 50 Pap smear cases, including 20 high grade (HG), 20 low grade (LG) and 10 normal slides. All HG and LG cases were correlated with biopsy results. All slides were scanned using Philips image scanner at 40x without z-stack. The whole slide image (WSI) files saved as TIFF were extracted in 500 x 500 pixel tiles with coordinates using modified OpenSlide program and saved as PNG files. HG and LG images were selected and saved in designated folder by 4 experienced cytopathologists (figure 1). Normal images were selected from cases signed out as such by cytotechnologists. Tiled images were used without masking abnormal cells. The selected images were distributed in 8:2 ratios randomly for training and validation set, respectively. We used fixed feature extractors and trained added classifiers on the training set using pre-trained ResNet152. Fitted CNNs were further evaluated and compared on independent test set of 10 HG, 10 LG, and 10 normal slides. All work was implemented in Python language on Pytorch platform.

Results: We collected 6056 images (1181 HG, 1000 LG, 3875 normal) and randomly distributed as described above. The time spent by each cytopathologist in selecting images was about 1-2 hours. The highest validation accuracy achieved was 90.5%. The sensitivity, specificity, positive predictive value, and negative predictive value for detecting low grade and high grade cells are, 74.7%, 98.4%, 96.0%, and 92.0%, respectively. On testing slides, the fitted CNN showed 100% sensitivity for detecting HG lesions (figure 2).

Figure 1 - 250

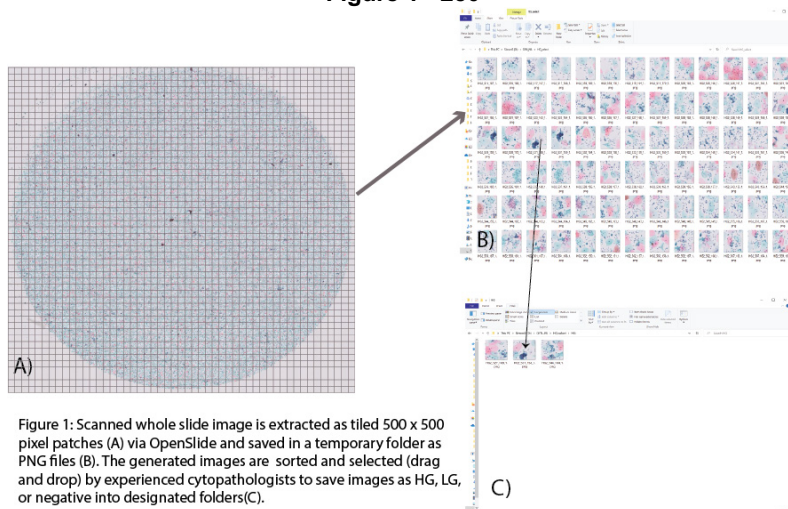


Figure 1: Scanned whole slide image is extracted as tiled 500 x 500 pixel patches (A) via OpenSlide and saved in a temporary folder as PNG files (B). The generated images are sorted and selected (drag and drop) by experienced cytopathologists to save images as HG, LG, or negative into designated folders(C).

Figure 2 – 250

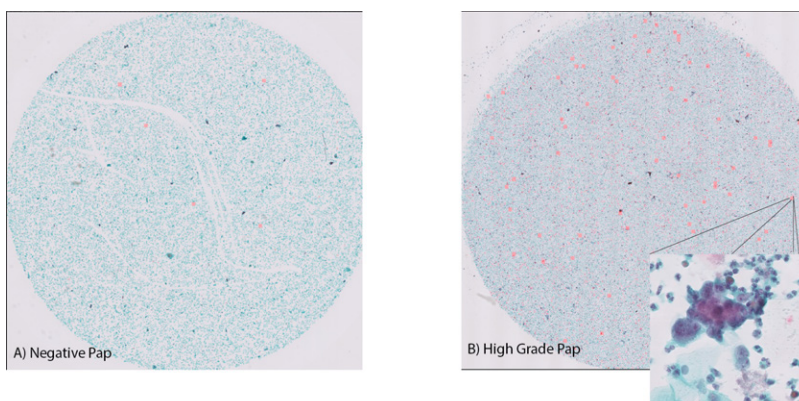


Figure 2: Examples of negative pap SurePath screened by fitted ResNet152 (A) and high grade SurePath slide (B). The red squares are areas highlighted by the trained algorithm as potential high grade lesions. Inset (B) shows high power view of the detected lesion.

Conclusions: In our proof of concept study, we demonstrate a highly efficient method in labeling images for ML. The proposed method reduces time required for annotation and allows selection of high quality images for training CNN. Our pilot study is limited by number of cases/images used, however, testing the trained algorithm shows a promising potential for application of ML trained with heLP as a screening method in cytopathology.

251 Next Generation Sequencing (NGS) testing on Endobrochial Ultrasound – Guided Fine Needle Aspiration (EBUS-FNA) in Pap-Stained Smears: Results in Patients with Lung Adenocarcinoma

Tania Labiano¹, Maria Lozano², Monica Bronte³, Yessica Rodriguez³, Teresa Dot Gomara³, Jesús Elizalde³, Elena Almudevar³, Ana Echevoyen³, Sergio Curi³, Idoia Morilla³, David Guerrero³

¹Complejo Hospitalario de Navarra, Cizur Menor, Spain, ²University of Navarra, Pamplona, Spain, ³Complejo Hospitalario de Navarra, Pamplona, Spain

Disclosures: Tania Labiano: None; Maria Lozano: None; Monica Bronte: None; Yessica Rodriguez: None; Teresa Dot Gomara: None; Jesús Elizalde: None; Elena Almudevar: None; Ana Echevoyen: None; Sergio Curi: None; Idoia Morilla: None; David Guerrero: None

Background: Cytological samples obtained by EBUS-FNA are a good source of quality material for NGS profiling in the routine diagnostic workup of patients with advanced lung adenocarcinoma (ADC). Rapid On-Site Evaluation (ROSE) allows pathologist to evaluate specimen adequacy and select the most appropriate material obtained for further molecular studies. A multidisciplinary molecular tumour board should evaluate for every patient with NSCLC diagnosis

Design: We included consecutive 44 lung ADC cases diagnosed by EBUS-FNA from May 2020 to February 2021. ROSE and sample management were performed by cytopathologists in order to preliminary processing and subsequently select slides NGS. DNA and RNA extraction were performed with specific kits from Papanicolaou stained smears. Oncomine Focus Assay, 52-genes panel (Thermo Fisher Scientific) was used to study mutations, copy number variations and gene fusions. After automated library preparation on the Ion Chef™ equipment, the libraries are sequenced on the S5™ sequencer. The findings were discussed at a multidisciplinary molecular tumor board.

Results: Forty-four patients were included (29 M/15F), mean age 63.6 years (range 37-83). In 3 cases the results were not valid and in two cases only DNA studies could not be performed. Mean measured DNA and RNA concentration was 16.6 ng/μl (range 1.57-36) and 24.3 ng/μl (2.2-97) respectively. Five patients have no genomic aberrations (12.1%). In 36 patients there were 51 molecular alterations in total: 10 in *KRAS*, 8 in *EGFR*, 6 in *MET*, 4 in *RET*, 2 in *ALK*, 2 in *MAPK2*, 2 in *BRAF* and others (*mTOR*, *PIK3CA*, *MYC*, *HRAS*, etc.). Co-occurring molecular alteration rate was 33.4% (12 out of 36). Five patients received anti-EGFR TK (Osimertinib, Gefitinib and Erlotinib) and 1 patient received Alectinib (anti-ALK) with maintained partial responses. Seven patients received immunotherapy with good response. Three patients were rebiopsied after cancer progression (6.8%).

Conclusions: Cytological samples obtained by EBUS-FNA are a source of good DNA quality for routine NGS. Co-occurring molecular alterations are frequent. Routine NGS testing in EBUS-FNA samples allows a comprehensive diagnosis (initial or after recurrence), increase targeted therapeutic options and better survival in lung ADC patients.

252 Epithelioid Hemangioendothelioma: a Challenging Diagnosis on Rapid On-Site Evaluation

Mega Lahori¹, Narasimhan Agaram¹, Amir Dehghani¹, Carlie Sigel¹

¹Memorial Sloan Kettering Cancer Center, New York, NY

Disclosures: Mega Lahori: None; Narasimhan Agaram: None; Amir Dehghani: None; Carlie Sigel: None

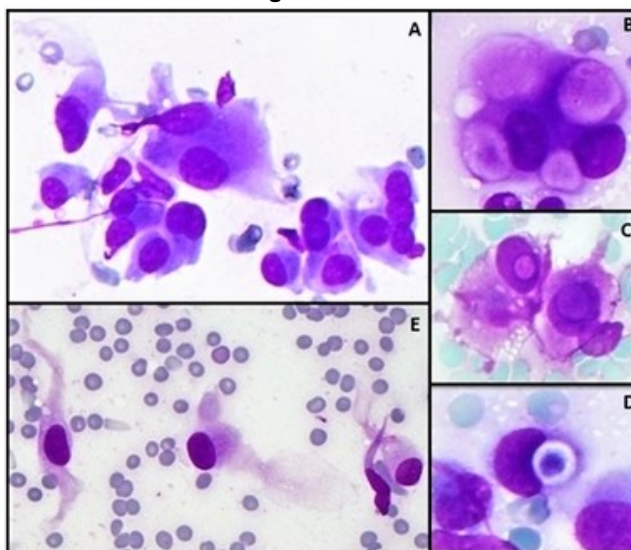
Background: Epithelioid hemangioendothelioma (EHE) is a vascular tumor of intermediate malignant potential, which presents as infiltrative lesions involving multiple organs. It can be difficult to recognize on rapid on-site evaluation. We have reviewed our institutional experience with the cytologic diagnosis of this neoplasm and hereby describe the cytomorphological features that can aid in rapid on-site evaluation (ROSE).

Design: Twenty-six cytology specimens from 19 patients, obtained between 2012-2020, with biopsy confirmation of EHE were identified from our institutional database. All cytology slides were reviewed, and selected cytologic features were recorded.

Results: The cohort included specimens obtained from liver (n=15), lung (n=6), or other (n=5) sites. ROSE was performed in 92.3% cases; 29% cases deemed satisfactory for final diagnosis were reported as inadequate during ROSE. Tumor cellularity in most cases was scant to moderate. Tumor cells were arranged as single discohesive cells and small clusters. Fibrotic or fibromyxoid stromal fragments were admixed with tumor cells. Most tumor cells had epithelioid to plasmacytoid morphology with pale voluminous delicate cytoplasm and ovoid or bean-shaped eccentric nuclei. The nuclear size was 2-3 times the size of the hepatocyte nucleus. Cells with long, delicate cytoplasmic processes, lobulated nuclei and bi/multi-nucleation were frequently seen

in all cases. Other distinctive features included intranuclear pseudoinclusions (84.6%), intracytoplasmic lumina (69.2%), blister cells (single perinuclear rigid vacuole) (50%), intact or fragmented RBCs within intracytoplasmic lumina (15.4%), nucleoli (65.3%) and nuclear grooves (69.2%). Mitoses or necrosis were absent. Of 11 tested cases, *WWTR1-CAMTA1* and *YAP1-TFE3* fusions were detected in 9 and 2 cases, respectively.

Figure 1 - 252



Epithelioid hemangioendothelioma cytology smears. A, Loosely cohesive cluster of tumor cells with abundant pale cytoplasm, cytoplasmic tails, large ovoid and bean-shaped eccentric nuclei and interspersed binucleation. B, Giant tumor cell with multiple intracytoplasmic lumina. C, Intranuclear pseudoinclusions. D, Blister cell with intracytoplasmic lumen containing an erythrocyte. E, Tumor cells with the characteristic long, tapering cytoplasmic processes. (Diff-Quik stain, x 400)

Conclusions: EHE has distinctive cytologic features (discohesive cells or small clusters with admixed stroma, large ovoid to lobulated eccentric nuclei, abundant pale cytoplasm with long, tapering processes, along with infrequent intracytoplasmic lumina, intranuclear pseudoinclusions, blister cells and RBCs in intracytoplasmic lumina) which are often under-recognized during ROSE due to the relative paucity of tumor cells or morphologic similarity with hepatocytes or histiocytes.

253 TRPS1 Expression in Metastatic Breast Carcinoma from Pleural Fluid

Zaibo Li¹, Bryce Parkinson¹, Anil Parwani², Rulong Shen¹

¹The Ohio State University Wexner Medical Center, Columbus, OH, ²The Ohio State University, Columbus, OH

Disclosures: Zaibo Li: None; Bryce Parkinson: None; Anil Parwani: None; Rulong Shen: None

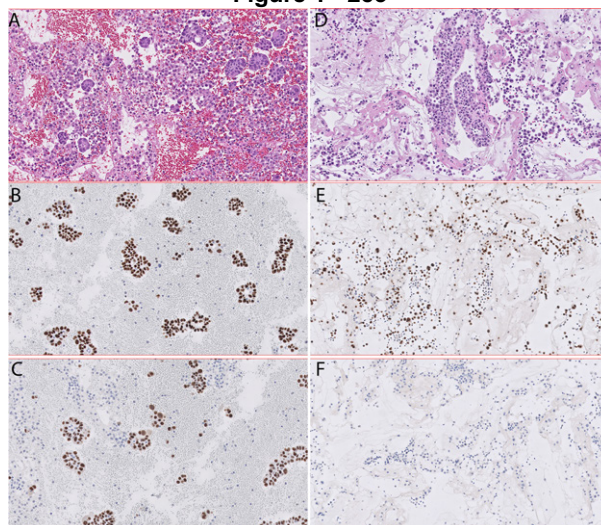
Background: TRPS1 has been recently demonstrated as a highly sensitive and specific marker for breast carcinomas, however, it has not been established in cytology specimens. We aimed to evaluate the utility of TRPS1 to diagnose breast cancer on cytology specimens (pleural fluids).

Design: Forty-nine metastatic breast carcinoma cases diagnosed on pleural fluid specimens were included in the study. TRPS1 immunohistochemistry was performed on cell block sections and evaluated with both intensity and percentage of tumor cells with positive staining. Results were correlated with other markers including estrogen receptor (ER) and GATA3. Representative images of TRPS1 expression were illustrated in figure 1. (A-C) One pleural fluid case with metastatic breast carcinoma (A), which is positive for TRPS1 (B) and GATA3 (C). (D-F) One pleural fluid case with metastatic breast carcinoma (D), which is positive for TRPS1 (E), while negative for GATA3 (F).

Results: The results showed TRPS1 was highly expressed in breast carcinomas (95.9%, 47/49). In contrast, GATA3 showed less positive rate (81.6%) comparing to TRPS1. Two cases were negative for TRPS1 and both of them were negative for ER and GATA3. (Table 1) Both TRPS1 and GATA3 showed 100% positivity in ER-positive metastatic breast carcinoma cases.

		Total		ER+		ER-		ER unknown	
GATA3	+	40	81.6%	19	100.0%	13	81.3%	8	61.5%
	-	8	16.3%	0	0.0%	3	18.8%	5	38.5%
TRPS1	+	47	95.9%	19	100.0%	14	87.5%	13	100.0%
	-	2	4.1%	0	0.0%	2	12.5%	0	0.0%
	<10%	3	6.1%	0	0.0%	4	25.0%	0	0.0%
Total		49	100.0%	19	38.8%	16	32.7%	13	26.5%

Figure 1 - 253



Conclusions: TRPS1 is a highly sensitive new diagnostic marker for metastatic breast carcinoma in cytology specimens.

254 Clinicopathologic Correlation of Metastatic Prostatic Carcinoma

Xiaoqi Lin¹, Qiuying (Judy) Shi², Ximing Yang³

¹Northwestern University, Chicago, IL, ²Emory University, Atlanta, GA, ³Feinberg School of Medicine/Northwestern University, Chicago, IL

Disclosures: Xiaoqi Lin: None; Qiuying (Judy) Shi: None; Ximing Yang: None

Background: Prostatic carcinoma (PC) is mostly indolent. It may be challenging to diagnose metastatic PC, because (1) it may be the initial diagnosis in patients without history of PC; (2) patients may have history of multiple malignancies; (3) its cytomorphology and immunoprofile may overlap with carcinoma of other organs. This study focuses on clinicopathologic correlation of metastatic PCs, which has not been well studied before.

Design: 146 metastatic PCs without or with neuroendocrine differentiation (NED) were retrieved from our cytology database from 2011 to 2020. Triplicate tissue microarrays (TMA) of 54 surgically excised PCs were constructed to represent limited cytology tissue biopsy for immunohistochemical stains (IHC) with appropriate positive and negative controls. Tumors with >5% cells staining positive were considered immunoreactive.

Results: See Table1.

IHC studies show that PCs can be immunoreactive to CDX2(26%), TTF1(4%), GATA3(4%), PAX8(2%), CK7(17%), CK20(15%), NKX3.1(98%), PSA(82%), PSAP(72%) and PSMA(86%). PCs with NED may be positive for p63, and may be negative for NKX3.1, PSA, PSAP and PSMA.

Table 1 - 254. Clinicopathologic correlation of metastatic PCs without and with NED

	PC (%)	PC+NED (%)	Total (%)
No	134 (92)	12 (8)	146
No History of PC	13 (10)	0 (0)	13 (9)
Grade Group	4.0 ± 1.1	3.6 ± 1.8	4.0 ± 1.2
≥2 Primaries	9 (7)	1 (8)	10 (7)
Metastatic Location			
Lymph node	66 (49)	2 (17)	68 (47)
Bone	38 (28)	2 (17)	40 (27)
Liver	14 (10)	7 (58)	21 (14)
Lung	9 (7)	0 (0)	9 (6)
Soft tissue	7 (5)	1 (8)	8 (5)
Pancreas	1 (1)	0 (0)	1 (1)

Conclusions: PCs can be immunoreactive to CDX2, TTF1, GATA3, PAX8 and p63 as well as cytokeratins CK7 and CK20, which may result in misinterpretation as metastatic carcinoma from non-prostate organs (gastrointestinal tract, lung, urothelial origin, pancreas, etc.) and inappropriate treatment. NKX3.1 is the most specific and sensitive immunomarker for PCs; however, metastatic PC with NED are likely negative for NKX3.1, PSA, PSAP, and PSMA. Metastatic PCs mostly present as high-grade patterns, and 8% show NED. 9% metastatic PCs do not have history of PC, and 7% have history of two or more primaries. The most common metastatic location of PCs is lymph node (47%), followed by bone (27%), liver (14%), etc.; whereas, PCs with NED more commonly metastasize to liver as compared to PCs without NED (58% vs. 10%). During interpretation of biopsies, if any cytologic or histologic features that could be seen in PC are identified in male patients, IHC stains for NKX3.1, PSA, PSAP and PSMA should be performed to confirm/exclude prostatic origin, even if immunoreactive to CDX2, GATA3, TTF1, PAX8, CK7 or CK20. For metastatic carcinoma with NED negative for NKX3.1, PSA, PSAP and PSMA in patients with history of PC, comparison with prostate specimens (morphology and IHC stains) and clinical correlation should be performed. In addition, NED may be seen after treatment.

255 HPV-Negative Cancer and High-Grade Lesions: Is Cervicovaginal Cytology Dispensable?

Lawrence Lin¹, Maryam Noori Koloori², Aylin Simsir³, Tamar Brandler²

¹NYU Langone Medical Center, New York, NY, ²NYU Langone Health, New York, NY, ³NYU School of Medicine, New York, NY

Disclosures: Lawrence Lin: None; Maryam Noori Koloori: None; Aylin Simsir: None; Tamar Brandler: None

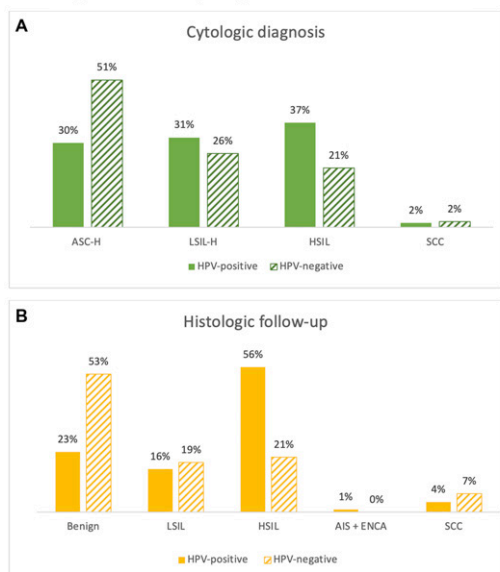
Background: The American Cancer Society recently recommended HPV testing alone for cervical cancer screening, leaving cytology (Pap) with or without HPV as secondary options. However, significant lesions may be missed with HPV testing alone. We aimed to evaluate HPV-negative cancer and high-grade squamous intraepithelial lesions (HSIL) diagnosed on Pap compared with HPV-positive lesions.

Design: This was a retrospective cohort of patients with Pap diagnosis of suspicious for HSIL, HSIL or squamous cell carcinoma (SCC) from 10/2013-06/2020. The suspicious for HSIL category included atypical squamous cells, cannot exclude HSIL (ASC-H) and low-grade squamous intraepithelial lesion, cannot exclude HSIL (LSIL-H). Pap diagnosis and histologic follow-up were compared, stratified by HPV status.

Results: 311 Paps with HPV testing were included. 249 (80%) were HPV-positive, while 62 (20%) were HPV-negative. The most common Pap diagnosis for HPV-positive squamous lesions was HSIL (37%), while the majority of HPV-negative lesions were inconclusive for HSIL (ASC-H: 53% and LSIL-H: 26%) (Figure 1A). Histologic follow-up was present in 254 cases (82%) with HPV-positive cases showing significantly more histologic HSIL or cancer than HPV-negative cases (60% vs 28%; p= 0.0002). Although the majority of HPV-negative lesions had benign histology (51%), a substantial proportion of cases showed HSIL (9/42; 21%) or cancer (3/42; 7%) on histologic follow-up (Figure 1B), which represents 5% of cases. In the HPV-negative histologically confirmed HSIL and cancer lesions, 50% of the cases had an initial cytology diagnosis of ASC-H or LSIL-H, while the other half were HSIL or SCC (Figure 2).

Figure 1 - 255

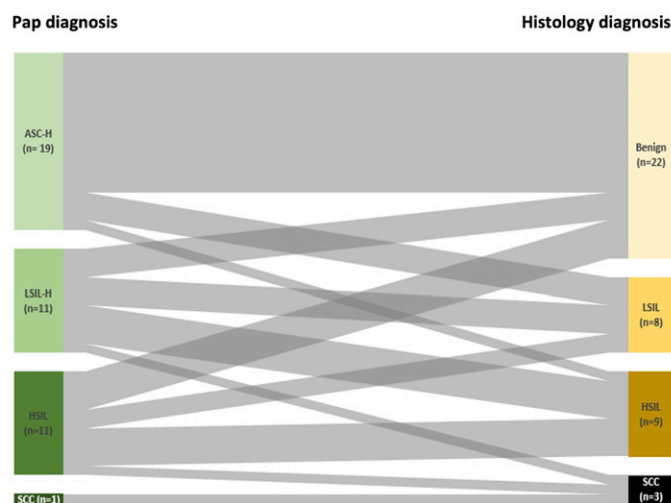
Figure 1: Distribution of Pap diagnosis (A) and histologic follow-up (B) in HPV-positive and HPV-negative cases of ASC-H, LSIL-H, HSIL and SCC.



LSIL: low-grade squamous intraepithelial lesion; HSIL: high-grade squamous intraepithelial lesion; ASC-H: atypical squamous cells, cannot exclude HSIL; LSIL-H: LSIL, cannot exclude HSIL; SCC: squamous cell carcinoma; AIS: adenocarcinoma in situ; ENCA: endocervical adenocarcinoma;

Figure 2 - 255

Figure 2: Alluvial plot showing the cyto-histologic correlation of HPV-negative lesions



LSIL: low-grade squamous intraepithelial lesion; HSIL: high-grade squamous intraepithelial lesion; ASC-H: atypical squamous cells, cannot exclude HSIL; LSIL-H: LSIL, cannot exclude HSIL; SCC: squamous cell carcinoma

Conclusions: The percentage of HSIL/cancer cases in HPV-negative patients is significant (5%). Our findings highlight the importance of Pap testing in addition to HPV analysis in cervical cancer screening.

256 Paps with Combined Squamous and Glandular Abnormalities versus Glandular Abnormalities Alone: Correlation with HPV Status and Histologic Outcomes

Lawrence Lin¹, Maryam Noori Koloori², Tamar Brandler², Aylin Simsir³

¹NYU Langone Medical Center, New York, NY, ²NYU Langone Health, New York, NY, ³NYU School of Medicine, New York, NY

Disclosures: Lawrence Lin: None; Maryam Noori Koloori: None; Tamar Brandler: None; Aylin Simsir: None

Background: Coexisting squamous and glandular cell abnormalities in cervicovaginal cytology specimens (Paps) are uncommon and may indicate either endocervical gland involvement by a squamous lesion or association of squamous and glandular lesions. There is limited literature on cytologic-histologic correlation of combined squamous/glandular lesions; therefore, we aimed to evaluate the histologic follow-up and HPV status of Paps with combined squamous/glandular abnormalities in comparison to those with atypical glandular cells (AGC) only.

Design: This was a retrospective study, which included patients with Pap diagnoses of AGC with (AGC+Sq) or without (AGC-alone) associated squamous cell abnormalities from 10/2013-06/2020. HPV status and histologic outcome was compared between AGC+Sq and AGC-alone cases. AGC+Sq was further stratified into AGC endometrial, AGC endocervical and AGC not otherwise specified (NOS).

Results: 205 Paps from 196 patients were included. 151 patients were AGC-alone, while 54 were AGC+Sq. AGC-alone was predominantly represented by AGC NOS (48%), while AGC+Sq were mainly AGC, endocervical (57%) (Figure 1A). Associated squamous cell abnormalities included: 2 LSIL, 7 HSIL, 26 ASCUS, 18 ASC-H and 1 LSIL-H. HPV testing was available in 162 cases (79%): 57% of AGC+Sq were HPV-positive, 86% of AGC-alone were HPV-negative (Figure 1B). Histologic follow-up was available in 165 cases (80%), showing that the majority of AGC+Sq cases were squamous lesions (50%, including 5 cases with concurrent glandular lesion) followed by benign diagnoses (41%), whereas AGC-alone cases were predominantly benign (70%) or adenocarcinoma (22%) (Figure 1C). HPV status did not seem to impact histologic outcomes in the AGC-alone group (p=1.00). However, in the AGC+Sq group, HPV-positive cases showed a significantly higher rate of HSIL and cancer as compared to HPV-negative cases (65% vs 21%; p=0.019; Figure 2A), particularly in the AGC endocervical subgroup (Figure 2B).

Figure 1 - 256

Figure 1: Cytologic (A), HPV testing (B) and histologic follow-up (C) in the AGC-alone (glandular interpretation alone) and AGC+Sq groups (combined squamous and glandular interpretation).

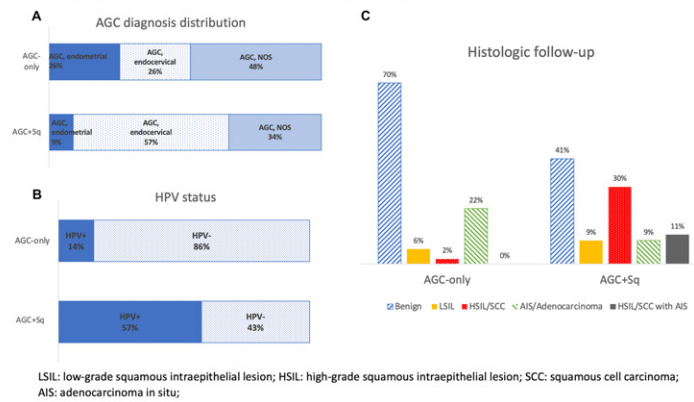
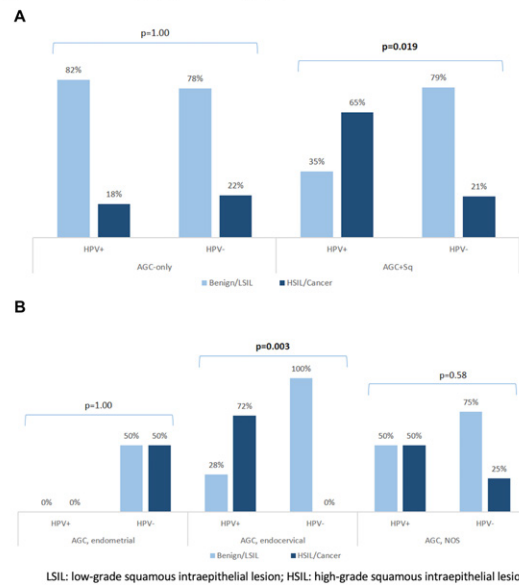


Figure 2 – 256

Figure 2: HPV status in relation to HSIL and cancer diagnoses: in AGC-alone (glandular interpretation alone) and AGC+Sq (combined squamous and glandular interpretation) groups (A); in combined squamous and glandular group per AGC subtype (B).



Conclusions: Paps with combined squamous and glandular interpretation are predominantly represented by squamous lesions on histology. HPV testing is helpful in the evaluation of combined lesions as the majority of HPV-positive cases display HSIL or cancer on follow-up, particularly in the AGC endocervical subgroup. In contrast, HPV testing has little utility in Paps with glandular-only diagnoses, as the majority of these lesions are HPV-negative and correspond to benign findings or endometrial adenocarcinoma.

257 Immunohistochemical Evaluation of NR4A3, SOX10, and DOG1 in Cytology and Surgical Specimens of Acinic Cell Carcinoma and Normal Salivary Gland Tissue

Terrance Lynn¹, Fan Lin¹, Sara Monaco¹, Haiyan Liu¹
¹Geisinger Medical Center, Danville, PA

Disclosures: Terrance Lynn: None; Fan Lin: None; Sara Monaco: None; Haiyan Liu: None

Background: DOG-1 and SOX10 (SRY-related HMG-box 10) are well-known markers for salivary acinar and intercalated duct differentiation. Recently, a recurrent genomic rearrangement t(4;9)(q13;q31) was discovered in acinic cell carcinoma (AciCC),

resulting in nuclear overexpression of NR4A3 (Nuclear Receptor Subfamily 4, Group A Member 3). The latter can be detected by immunohistochemistry (IHC). Our study aims to evaluate the expression of NR4A3, DOG-1 and SOX10 by IHC on 14 surgical AcicC and normal salivary gland tissue, and 13 cytology cell blocks of AcicC, to assess their utility in daily practice, especially cytology samples.

Design: Fourteen surgical cases of AcicC and normal salivary gland tissue, as well as 13 cases of cytology FNA of AcicC were retrieved. IHC evaluation of NR4A3 (sc-393902, Santa Cruz Biotechnology Inc.), DOG1 (SP31, Cell Marque) and SOX10 (Cat. No, 383A-75, Cell Marque) on surgical tissue sections and cytology cell blocks were performed. The staining results were assessed using the scale: negative (<5% cells), 1+ (5-25%), 2+ (26-50%), 3+ (51-75%), and 4+ (>75%). Scores of 3+ or 4+ were considered diffuse and 1+ or 2+ were considered focal. The staining pattern (nuclear, luminal, basal lateral, cytoplasmic, or partial membranous) and intensity (strong, moderate, or weak) were recorded.

Results: The results are summarized in Table 1. Strong/diffuse nuclear expression for NR4A3 was identified in 100% (surgical: 14/14; cytology: 13/13) of AcicC (Fig.1a), but none of the normal salivary acinar cells (Fig.1b). In contrast, DOG1 and PAX8 expressed in both AcicC and normal acinar cells (Fig.1d). Membranous or cytoplasmic expression of DOG-1 was identified in 100% of surgical (14/14) and 85% of cytology (11/13) AcicC. Among the 11 DOG1+ cytology AcicC, 45% (5/11) showed focal partial membranous/weak cytoplasmic staining (Fig.1c). Nuclear expression of SOX10 identified in 79% (11/14) of surgical and 85% (11/13) of cytology AcicC.

Table 1 - 257. Comparison the Expression of NR4A3, SOX10, and DOG 1 in AcicC and Normal Salivary Gland Tissue

Acinic Cell Carcinoma (Surgical)				
		NR4A3 IHC Positive	SOX10 IHC Positive	DOG1 IHC Positive
Total Number of Cases:	14	14 (100%)	11 (79%)	13 (93%)
Staining Characteristics				
Pattern	Nuclear	14	11	0
	Luminal	0	0	6 (1 only)
	Basal Lateral	0	0	0
	Cytoplasmic	0	0	7 (2 only)
Amount of Tumor Staining	4+ (>75%)	13	8	3
	3+ (50-75%)	1	2	8
	2+ (25-50%)	0	1	2
	1+ (5-25%)	0	0	0
Intensity of stain:	Strong	14	14	1
	Moderate	0	0	2
	Weak	0	0	10
Normal Salivary Gland Tissue				
		NR4A3 IHC Positive	SOX10 IHC Positive	DOG1 IHC Positive
Total Number of Cases:	14	0 (0%)	14 (100%)	14 (100%)
Staining Characteristics				
Pattern	Nuclear	0	14	0
	Luminal	0	0	0
	Basal Lateral	0	0	14
	Cytoplasmic	0	0	0
Amount of Tumor Staining	4+ (>75%)	0	6	6
	3+ (50-75%)	0	4	2
	2+ (25-50%)	0	4	6
	1+ (5-25%)	0	0	0
Intensity of stain:	Strong	0	7	3
	Moderate	0	7	3
	Weak	0	0	8
Acinic Cell Carcinoma (Cytology)				
		NR4A3 IHC Positive	SOX10 IHC Positive	DOG1 IHC Positive
Total Number of Cases:	13	13 (100%)	11 (85%)	11 (85%)
Staining Characteristics				
Pattern	Nuclear	13	11	0
	Luminal	0	0	0
	Partial membranous	0	0	11 (Moderate)
	Cytoplasmic	0	0	11 (weak)
Amount of Tumor Staining	Diffuse (3 +or 4+)	11	5	7
	Focal (1+ or 2+)	2	6	4

Figure 1 - 257

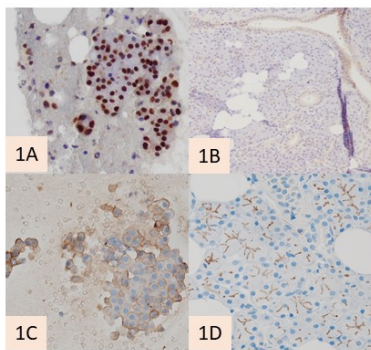


Figure 1. Nuclear Expression of NR4A3 on cytology specimen (1A) and no staining of normal salivary gland tissue on surgical specimen (1B). Partial membranous/weak cytoplasmic staining of DOG-1 expression in AcicC on cytology (1C) and normal salivary acinar tissue (1D).

Conclusions: Our data demonstrates that nuclear expression of NR4A3 by IHC is highly sensitive (100%) and specific for AcicC in both cytologic and surgical specimens. While DOG1 and PAX8 expressed in both AcicC and normal acinar cells, with less sensitivity in cytology samples (85% for both). The interpretation of DOG1 in cytology samples may be challenging due to its partial membranous/weak cytoplasmic staining pattern and its expression in normal acinar cells. Large series of study is necessary to validate our findings.

258 TRPS1 is a Highly Sensitive and Specific Marker for Diagnosing Triple-negative Breast Carcinomas on Cytologic Samples

Terrance Lynn¹, Jianhui Shi¹, Haiyan Liu¹, Sara Monaco¹, Jeff Prichard², Fan Lin¹
¹Geisinger Medical Center, Danville, PA, ²Geisinger Health, Danville, PA

Disclosures: Terrance Lynn: None; Jianhui Shi: None; Haiyan Liu: None; Sara Monaco: None; Jeff Prichard: None; Fan Lin: None

Background: Recent studies demonstrated that trichorhinophalangeal syndrome type 1 (TRPS1) was a highly sensitive marker for diagnosing breast carcinomas, including triple-negative breast carcinomas (TNBCs) on surgical specimens, with a diagnostic sensitivity of 86%, which is superior to GATA3 with a reported sensitivity of 21-51% (Modern Pathology 34:710-719, 2021). A diagnosis of metastatic TNBC is frequently encountered on cytologic samples; however, the utility of TRPS1 expression in TNBC on cytologic samples has not been reported. In this study, we focused on the evaluation of TRPS1 expression in TNBCs on cytologic samples, with a comparison to the performance of GATA3 and evaluation in a large spectrum of extramammary tumors.

Design: Immunohistochemical analysis of TRPS1 (PA5-84874; 1:200 dilution; Thermo Fisher) was performed on 35 TNBC cases on surgical specimens, 29 consecutive TNBC cases on cytologic specimens with available cell blocks (8 fluid, 13 fine needle aspiration, and 8 core biopsy samples), 981 tumors on tissue microarray sections, including mesothelioma (N=18), lung carcinoma (CA) (N=91); head and neck tumors (N=120); hepatobiliary (N=110); gynecological CA (N=126); melanoma (N=32); skin neuroendocrine CA (N=27), genitourinary tumors (N=371); and gastrointestinal CA (N=86). Percentage of nuclear expression for TRPS1 and GATA3 on both surgical and cytologic samples was interpreted as negative (<1% of tumor cells with nuclear staining), 1+ (1-25%), 2+ (26-50%), 3+ (51-75%), and 4+ (>75%) to compare the diagnostic sensitivity.

Results: Of the surgical specimens, 35 of 35 (100%) TNBC cases were positive for TRPS1, all with diffuse positivity, whereas 27 of 35 (77%) were positive for GATA3, with diffuse and strong positivity in 7 cases (20%). Of the cytologic samples, 27 of 29 (93%) TNBC cases were positive for TRPS1, with diffuse positivity in 20 cases (74%), whereas 12 of 29 (41%) were positive for GATA3, with diffuse positivity only in 2 cases. The positive staining results for non-breast tumors are summarized in Table 1.

Table 1. Summary positive staining results for TRPS1 using semiquantitative scale (0-4)

	Negative	Positive				Total positive cases (N,%)
		Low Positive		Diffuse Positive		
Diagnosis	0	1+	2+	3+	4+	
Ovarian serous CA	37	4	0	0	0	4, 9.8%
Bladder small cell CA	25	0	1	2	0	3, 10.7%
Skin melanoma	29	0	0	2	1	3, 9.4%
Benign mixed tumor	12	3	5	0	0	8, 40%

Note: CA - carcinoma

Figure 1 - 258

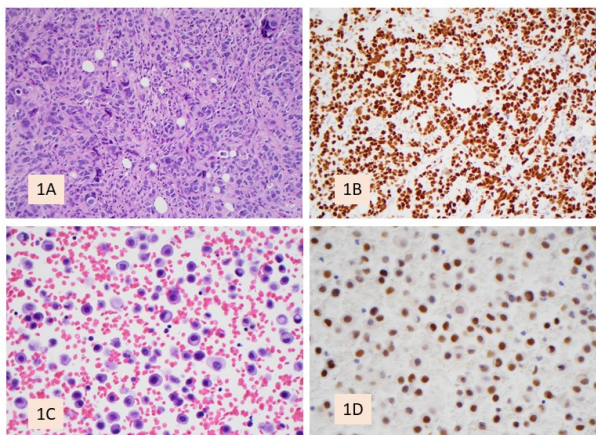


Figure 1 (1A to 1D) showing an example of triple negative breast carcinoma (TNBC) on surgical specimen (1A) with diffuse nuclear staining for TRPS1 (1B) and an example of TNBC on pleural fluid (1C) with diffuse nuclear positivity for TRPS1 (1D). GATA3 is completely negative on both cases (not shown here).

Conclusions: Our data confirmed that TRPS1 is a highly sensitive and specific marker for diagnosing TNBC on surgical specimens as reported in the literature. In addition, these data demonstrated that TRPS1 is a much more sensitive marker than GATA3 in detecting metastatic TNBC on cytologic samples. Therefore, including TRPS1 in the diagnostic IHC panel is recommended when a metastatic TNBC is suspected.

259 Whole Slide Image-based Analysis of SurePath Pap Testing: An Initial Institutional Experience

Padmini Manrai¹, Minhua Wang², Angelique Levi¹, Rita Abi-Raad², Sudhir Perincheri¹, Adebowale Adeniran², Guoping Cai¹
¹Yale University, New Haven, CT, ²Yale School of Medicine, New Haven, CT

Disclosures: Padmini Manrai: None; Minhua Wang: None; Angelique Levi: None; Rita Abi-Raad: None; Sudhir Perincheri: None; Adebowale Adeniran: None; Guoping Cai: None

Background: Pap testing is the primary screening method for cervical cancer and is a labor-intensive process that involves initial screening by cytotechnologists and further evaluation by pathologists. Artificial intelligence (AI) systems based on deep learning is an emerging technique that expands the field of pathology practice. In this study we explored the potential role of CellVigene software, a whole slide image (WSI)-based analysis using multiple quantifiable parameters targeting membrane, nuclear and cytoplasmic features, in assisting cytomorphologic evaluation of Pap testing.

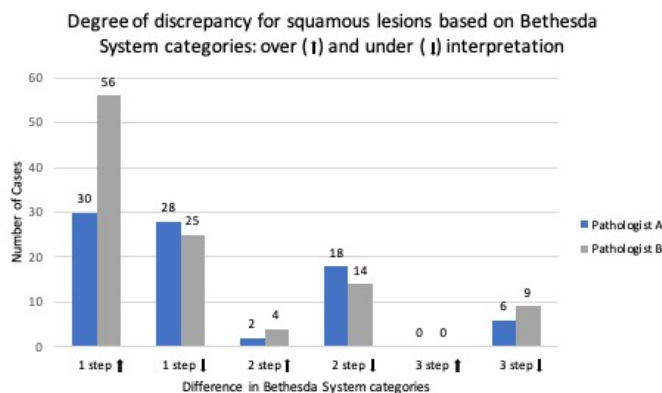
Design: The study cohort included SurePath Pap tests from 348 patients representing the spectrum of the 2014 Bethesda System for Reporting Cervical Cytology: negative for intraepithelial lesion or malignancy (NILM, 227 cases), atypical squamous cells of undetermined significance and cannot exclude high grade lesion (ASCUS, 32 cases; ASC-H, 23 cases), low and high grade squamous intraepithelial lesion (LSIL, 13 cases; HSIL, 21 cases), and atypical glandular cells (AGC, 32 cases). WSIs from high-definition scanned slides were analyzed to identify cells of interest and categorize them into HSIL, LSIL, ASCUS and crowded cell

groups. Two pathologists rendered final interpretations based on their independent review of the software selected images and these were compared with initial diagnoses made on glass slides.

Results: The overall concordance between final interpretation and original diagnosis was 69% (pathologist A) and 61% (pathologist B). By diagnostic category, NILM had the highest concordance (86% pathologist A; 76% pathologist B) while low concordance was seen with ASCUS, ASC-H/HSIL and AGC (Table 1). For cases with abnormal squamous findings, discrepant results between the WSI-based and initial diagnoses were further classified as one, two, or three step discrepancies, the majority of which were one step (69% pathologist A and 75% pathologist B) (Figure 1).

Diagnosis	NILM	ASCUS	LSIL	ASC-H/HSIL	AGC
Pathologist A	196/227	10/32	9/13	13/44	13/32
	86%	31%	69%	30%	41%
Pathologist B	172/227	10/32	8/13	17/44	7/32
	76%	31%	62%	39%	22%

Figure 1 - 259



Conclusions: This was our first experience with WSI-based AI-assisted analysis for Pap smear evaluation. The results indicated that WSI-based interpretation correlated relatively well with traditional glass slide-based diagnosis; however, significant discrepancies were seen in higher grade squamous and glandular cases, which impacts clinical management. The causes for such discrepancies needs to be further analyzed and correlated with histopathologic follow-up. There is room for improvement as we incorporate WSI-based imaging technology in practice.

260 Accuracy of Grading Primary and Secondary Malignant Salivary Gland Tumors on Cytology – A Single Institute 8 -year Retrospective Review

Varsha Manucha¹, Anne Kane¹

¹University of Mississippi Medical Center, Jackson, MS

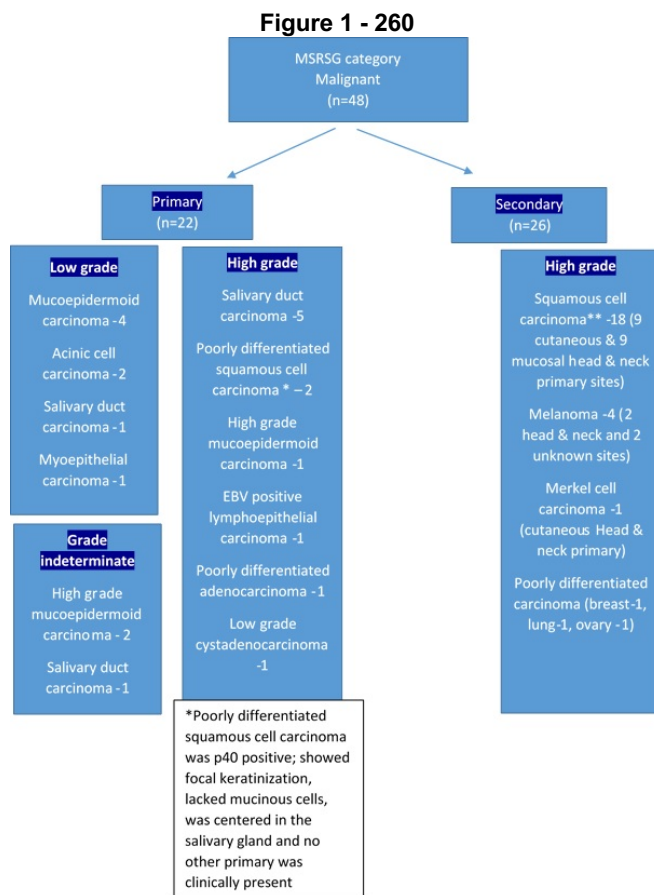
Disclosures: Varsha Manucha: None; Anne Kane: None

Background: Malignant salivary gland tumors (MSGT) include a broad spectrum of primary SGT, metastatic tumors, and rarely lymphomas and sarcomas. Since specific diagnosis is largely dependent on adequate cellular material, ancillary studies, and clinical history, the Milan system of reporting salivary gland cytology (MSRSGC) recommends grading MSGT into high (HG) or low grade (LG) when possible, given the impact of tumor grade on clinical management.

Design: Salivary gland tumors diagnosed as malignant on cytology (2012-2020) were retrieved. Only the non-lymphomatous tumors with histologic material were selected. The grade of the tumors, demographic data, and site of FNA was obtained from cytology reports. SGTs without a grade were reviewed and a grade was assigned when possible. The goal of this study is to review the accuracy of grading primary and secondary MSGT on cytology with subsequent histology.

Results: There were 48 malignant tumors on cytology, of which, 22 (45.8%) were primary SG (parotid, 16 and submandibular 6; average age 62.5 years), and 26 (54%) were metastatic (parotid, 20 and submandibular, 6; average age 66 years). In the group of

primary MSGT, 1 salivary duct carcinoma and 1 cystadenocarcinoma were inaccurately graded as LG and HG respectively and 2 HG mucoepidermoid carcinomas and 1 salivary duct carcinoma were graded as indeterminate. In the group of metastatic, all were graded HG (figure 1). Squamous cell carcinoma (SqCC), followed by melanoma constituted the majority of secondary MSGT. There was 1 case of Merkel cell carcinoma and 1 each from the ovary, breast, and lung. At the time of FNA clinical history of primary malignancy was known in 34% of cases.



Conclusions: MSGT can be graded with an accuracy rate of 89% on cytology. HG tumors are more commonly (54%) secondary, suggesting that a possibility of metastasis should be excluded when encountering HG cytology even in the absence of clinical history.

261 Fine Needle Aspiration of Lesions Involving Bone: Diagnostic Performance and Comparison to Concurrent Core Biopsies

Iryna Mazur¹, Alisa Nobee¹, Ahmed Lazim¹, Aileen Grace Arriola¹
¹Temple University Hospital, Philadelphia, PA

Disclosures: Iryna Mazur: None; Alisa Nobee: None; Ahmed Lazim: None; Aileen Grace Arriola: None

Background: Fine needle aspiration (FNA) of lesions involving bone are uncommon as compared to usual sites like thyroid or lung. In this retrospective study, we compare the diagnostic performance of FNAs of bone lesions as compared to concurrent core biopsies (CCBx).

Design: Bone FNA and touch prep (TP) cases (1/1/10-7/16/21) were retrieved and the following data collected: site, diagnosis, ROSE adequacy, and radiologic and clinical impression of the targeted lesion. Cytology diagnoses were divided into nondiagnostic (Nondx), negative for malignancy (NFM), atypical, suspicious for malignancy (SFM), and positive for malignancy/neoplasm (PFM/N). Association of categorical values was assessed with Fisher’s exact test using JMP Pro 16.0.

Results: 141 cases were identified (FNA=107, TP=32; both=2), with 81.6% (n=115) containing CCBx. Hip (48%,n=68) and vertebrae (32%,n=45) were most common sites. There was a high clinical suspicion for tumor in 78%; benign/indeterminate/infectious impressions were more common in the Nondx/NFM/atypical categories. Table 1 summarizes the cytology diagnoses and associations. Overall, 88 (62%) of FNA/TP deferred final diagnosis to CCBx mostly due to ancillary tests. Most were malignant (39%,PFM/N+SFM) due to metastatic carcinoma (69%) from lung or breast (56%); 20% (n=11/55) were deferred to the CCBx for definitive diagnostic work-up. There were 10 mesenchymal lesions sampled (such as chondrosarcoma, rhabdomyosarcoma, fibrous dysplasia, chondromyxoid fibroma), with only 30% called PFM/N and rest categorized as NFM/atypical. Nondx cases (15.6%) all showed inadequate cellularity on ROSE. There were 15/115 (13%) discordant diagnoses between FNA and CCBx: 8/15 false negative FNA (CCBx: plasma cell neoplasm in 3, carcinoma in 4, and Paget disease in 1), 4/15 due to sampling (nondx on FNA, malignant on CCBx), and 3/15 atypical on FNA with negative CCBx.

Table 1 - 261. Cytologic diagnostic categories of lesions involving the bone and comparison to various clinical and pathologic features.

	Nondx (n=22, 15.6%)	NFM (n=43, 30.5%)	Atypical (n=21, 14.8%)	SFM (n=6, 4.2%)	PFM/N (n=49, 34.8%)	p-value
Procedure						
FNA	20 (91%)	34 (79%)	12 (57%)	4 (66%)	37 (75%)	0.0488
TP	2 (9%)	8 (19%)	9 (43%)	1 (17%)	12 (25%)	
both	0 (0%)	1 (2%)	0 (0%)	1 (17%)	0 (0%)	
Definitive Dx deferred to CCBx						
No	5 (23%)	22 (51%)	3 (14%)	0 (0%)	23 (47%)	0.0027
Yes	17 (77%)	21 (49%)	18 (86%)	6 (100%)	26 (53%)	
Discordant Dx vs CCBx						
No	13 (76%)	24 (75%)	17 (85%)	6 (100%)	40 (100%)	0.0029
Yes	4 (24%)	8 (25%)	3 (15%)	0 (0%)	0 (0%)	
Stains performed						
No	20 (91%)	37 (86%)	17 (81%)	6 (100%)	29 (59%)	0.0064
Yes	2 (9%)	6 (14%)	4 (19%)	0 (0%)	20 (41%)	
ROSE Adequacy						
Adequate	0 (0%)	19 (58%)	11 (58%)	5 (83%)	43 (96%)	<0.0001
Not adequate	20 (100%)	14 (42%)	8 (42%)	1 (17%)	2 (4%)	
Clinical impression						
Benign	2 (12%)	2 (5%)	0 (0%)	0 (0%)	1 (2%)	<0.0001
Indeterminate	1 (6%)	6 (16%)	1 (5%)	2 (33%)	0 (0%)	
Infectious	2 (12%)	10 (27%)	1 (5%)	0 (0%)	0 (0%)	
tumor/metastasis	12 (70%)	19 (52%)	18 (90%)	4 (67%)	46 (98%)	

Conclusions: At our institution, the most common indication for FNA of bone lesions is metastatic carcinoma. Most cases can be adequately categorized on cytology alone, with CCBx necessary for definitive characterization for IHC/molecular testing and for diagnosis of mesenchymal-type lesions. Discordances accounted for a small percent overall, with CCBx containing the diagnostic material. Hence, lesions involving the bone should be sampled by both FNA and CCBx to maximize diagnostic accuracy.

262 Risk of Anal Intraepithelial Neoplasia in High-risk Populations According to Human Papillomavirus Genotypes

Austin McHenry¹, Marwan Azar², Angeliqe Levi¹, Guoping Cai¹, Rita Abi-Raad³

¹Yale University, New Haven, CT, ²Yale New Haven Hospital, Yale School of Medicine, Branford, CT, ³Yale School of Medicine, New Haven, CT

Disclosures: Austin McHenry: None; Marwan Azar: None; Angeliqe Levi: None; Guoping Cai: None; Rita Abi-Raad: None

Background: Anal cytology screening (ACS) is recommended for detection of anal intraepithelial neoplasia (AIN), but guidelines regarding its use for high-risk populations such as persons with HIV infection or high-risk sexual behavior are limited. The role of ACS in combination with certain high-risk human papillomavirus (hrHPV) genotypes remain largely unclear. In this study, we reviewed our experience with ACS in conjunction with HPV genotype and histologic outcomes.

Design: The departmental database was searched for all ACS performed between January 2016 and July 2021. ACS were categorized as benign or abnormal (ASCUS and above). Biopsies were categorized as ≤AIN1 (benign or AIN1) or ≥AIN2 (AIN2-3 or SCC). HIV status and concurrent hrHPV genotype result, including HPV16/18 or HPV-non 16/18 (31, 33, 35, 39, 45, 51, 52, 56, 58, 59, 66, 68) were recorded if available.

Results: Of 1,482 ACS cases, 52 cases (from 13 female and 39 male patients with a median age of 48) had adequate hrHPV result and surgical follow-up available, including 49 with abnormal ACS. Of those, 19 patients had a surgical follow-up with a diagnosis of \geq AIN2 yielding an incidence of 38.7% (19/49). The incidence of \geq AIN2 was significantly higher in female patients (8/11; 73%) compared to male patients (11/38; 29%). The incidence was even higher in HIV-positive female patients (6/8; 75%), especially in the presence of positive hrHPV (6/7; 86%) (Table 1).

There were 19 male patients with abnormal ACS and HPV genotype result, including 18 HIV-positive and 1 HIV-negative patients. Genotypes in HIV-positive males consisted of HPV16 (n=1), HPV18 (n=5) and HPV-non-16/18 (n=12) while one HIV-negative patient was positive for HPV-non-16/18. Of all males with abnormal ACS and available genotype, 8 had \geq AIN2 on surgical follow up, an incidence of \geq AIN2 at 42% (8/19). The incidence of \geq AIN2 was 100% (6/6) with HPV16/18 and 15% (2/13) with HPV-non-16/18. In HIV-positive males, the incidence of \geq AIN2 was 44% (8/18) overall, 100% (6/6) with HPV16/18 and 17% (2/12) with HPV-non-16/18. Only one female with abnormal ACS had HPV genotype result available.

Table 1 - 262: ACS and surgical follow-up stratified by HIV and sex

	PAP: \geq ASCUS (n=49)	Bx: \leq AIN1	Bx: \geq AIN2
hrHPV-positive (n=40)			
HIV+F	7	1 (14%)	6 (86%)
HIV-F	3	1 (33%)	2 (67%)
HIV+M	29	19 (66%)	10 (34%)
HIV-M	1	1 (100%)	0 (0%)
hrHPV-negative (n=9)			
HIV+F	1	1 (100%)	0 (0%)
HIV-F	0	0 (0%)	0 (0%)
HIV+M	8	7 (88%)	1 (12%)
HIV-M	0	0 (0%)	0 (0%)

Abbreviations: AIN, anal intraepithelial neoplasia; ASCUS, atypical squamous cells of undetermined significance; Bx, biopsy; HIV, human immunodeficiency virus; F, female; M, male; hrHPV, high-risk human papilloma virus; PAP, Papanicolaou test.

Conclusions: HIV-positive females with abnormal ACS and positive hrHPV carry the highest risk of \geq AIN2 compared to other risk groups, including HIV-positive males. In males overall and HIV-positive males in particular, the incidence of \geq AIN2 is highest in abnormal ACS with HPV16/18 genotypes but remains significant with HPV-non-16/18. These data may prove helpful in designing screening guidelines.

263 Cytomorphologic Observations on the Sclerosing Variant of Well-Differentiated Pancreatic Neuroendocrine Tumors: Towards Making Specific Diagnoses Early

David McKenzie¹, Chanjuan Shi², Avani Pendse³

¹Duke University Health System, Durham, NC, ²Duke University Medical Center, Raleigh, NC, ³Duke University Medical Center, Durham, NC

Disclosures: David McKenzie: None; Chanjuan Shi: None; Avani Pendse: None

Background: The recently described sclerosing variant of pancreatic neuroendocrine tumor (spNET) shows prominent stromal fibrosis, decreased cellularity and serotonin expression in tumor cells. Although prognostic data are currently ambivalent, spNETs <2 cm were shown to be associated with metastatic disease, making earlier diagnosis crucial for positive patient outcomes. The aim of our study is to evaluate cytology specimens of spNET to determine its characteristic features to facilitate an earlier diagnosis.

Design: Twenty-five cases of spNET, 23 fine needle aspiration (FNA) and 2 touch preparations (TP) of core biopsies and ten FNA cases of typical pancreatic neuroendocrine tumor (tpNET) were reviewed for the following parameters by two pathologists (DM and AP): adequate or insufficient diagnostic material, smear/TP cellularity, presence of fibrosis on smears and cell block, and pattern of fibrosis. We also recorded the radiographic findings in the pancreas.

Results: SpNET specimens were more often non-diagnostic, with only 56% (14 of 25) of cases at least suspicious for neuroendocrine tumor compared to 100% (10 of 10) of tpNET. The tpNET smears were more commonly hypercellular (70%, 7 of

10) than spNET (8%, 2 of 25). At least focal fibrosis was observed in both spNET (40%, 10 of 25) and tpNET (80%, 8 of 10). Notably, 3 spNET cases showed small groups of crushed tumor cells trapped in large fibrotic fragments (Figure 1). Fibrosis was separate or was loosely associated with larger groups of tumor cells in rest of the spNET and in tpNET cases (Figure 2). In addition, of the 19 cases of spNET with available imaging, 9 (47%) demonstrated dilation of the pancreatic duct and 8 (42%) showed at least partial pancreatic atrophy. In contrast, 1 of 10 (10%) tpNET cases demonstrated pancreatic duct dilation and 2 of 10 (20%) showed pancreatic atrophy.

Figure 1 - 263

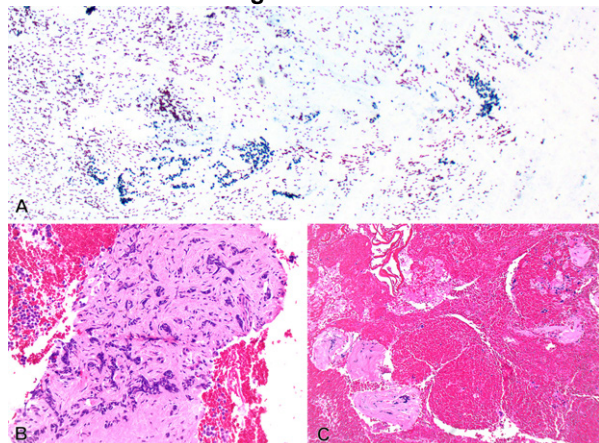
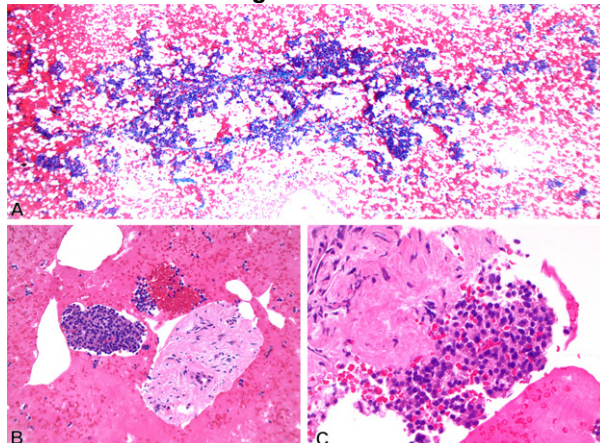


Figure 2 - 263



Conclusions: Cytology samples from spNET were more often non-diagnostic and relatively hypocellular compared to their tpNET counterparts. Small groups of crushed tumor cells embedded in larger fibrotic fragments, commonly seen in surgical resections from spNET, were only seen in a minority of cases. These findings suggest that the presence of fibrosis makes obtaining a diagnostic sample from this variant difficult. In a hypocellular NET cytology specimen with characteristic fibrotic fragments, especially in the presence of relevant radiographic findings, the possibility of sclerotic variant can be included in the diagnosis.

264 Risk of Malignancy in Serous Fluid Cytopathology Based on the International System with a Spotlight on Atypical Category

Sepideh Besharati¹, Abel Gonzalez¹, Patricia Wasserman¹, Adela Cimic¹

¹Columbia University Medical Center, New York, NY

Disclosures: Sepideh Besharati: None; Abel Gonzalez: None; Patricia Wasserman: None; Adela Cimic: None

Background: Serous fluids are common specimens in cytopathology laboratories. The International System for Serous Fluids (TIS) has been created in an attempt to standardize reporting and clarify categories to improve clinico-cytologic communication. The 5 categories are I. Nondiagnostic (ND), II. Negative for malignancy (NFM), III. Atypia of undetermined significance (AUS), IV. Suspicious for malignancy (SFM), V. Malignant (MAL).

Design: A total of 851 pleural effusions (PE) (N=565) and ascites fluids (AF) (N=286) were submitted in our laboratory from 1/1/2018 to 1/1/2019 and they were re-classified in accordance with TIS (figure 1). Collected data included clinical history, use of immunostains, and follow-up specimens (same specimen type or same location biopsy), if available. (Table 1). We calculated the risk of malignancy (ROM) based on 2.5-year follow-up data collected through our laboratory information system and electronic medical record.

Results: In our cohort, we had 11% of AUS cases (10.6% for PE and 11.5% for AF) and only 2.5% of SFM cases (2.3% for PE and 3.1% for AF). For PE a total 39 cases have a follow-up in the AUS category (of which 13 are malignant); in the SFM category 10 cases have follow-up (of which 6 are malignant). For AF in the AUS category, the follow-up is obtained in 26 (of which 6 cases are malignant). For SFM category, 6 cases have follow-up (of which 4 are malignant). Proportionally, the highest percentage of cases with inadequate volume (<75ml) is seen in the AUS category, 30% and 23% for PE and AF respectively.

Table 1 – 264: Frequency and risk of malignancy in different TIS serous fluid categories

Category/ specimen type	Number (%)		Clinical history of malignancy		Volume <75ml		Use of immunostains		ROM (%)	
	PE	AF	PE	AF	PE	AF	PE	AF	PE	AF
ND	21 (3.7%)	3(1.0)	103(34.5)	1(0.6)	16(17.0)	2(2.9)	0(0.0)	0(0.0)	n/a	n/a
NFM	315(55.7)	191(66.7)	4(1.34)	68(44.4)	57(60.6)	47(69.1)	60(24.3)	31(40.7)	5.5	4
AUS	60(10.6)	33(11.5)	25(8.3)	29(18.95)	14(14.8)	10(14.7)	25(10.1)	18(23.6)	33	23
SFM	13(2.3)	9(3.1)	13(4.3)	7(4.5)	3(3.1)	2(2.9)	9(3.6)	3(3.9)	60	66
MAL	156(27.6)	50(17.4)	153(51.3)	48(31.3)	4(4.2)	7(10.2)	152(61.7)	24(31.5)	100	100
Total	565(100)	286(100)	298(100)	153(100)	94(100)	68(100)	246(100)	76(100)		

Figure 1 - 264

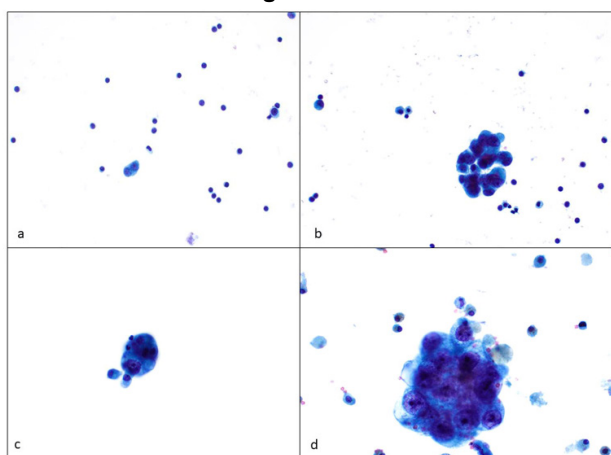


Figure 1. Serous fluid classification based on International System for Serous Fluids

- a. Negative for malignancy-a couple of reactive mesothelial cells in the background of occasional lymphocytes
- b. Atypia of undetermined significance-likely reactive mesothelial cells
- c. Suspicious for malignancy-small number of suspicious cells present only on monolayer preparation
- d. Malignant-metastatic adenocarcinoma in a patient with ovarian mass

Conclusions: The TIS is a new system with limited published data on usage of atypical/ undetermined categories. In our cohort, we limit the interpretation of AUS to 10-11% of the submitted cases. ROM in the published literature for AUS ranges from 13-100% with a mean of 66%. We found that the AUS has a ROM of 33% for PE and 23% for AF. Interestingly, the reported ROM for the SFM category is 0-100% with a mean of 82%. Our study shows that ROM for the SFM category is 60-66% for PE and AF respectively (table 1). In order to improve clinical care in our practice, only a limited number of specimens are assigned into the atypical category. The liberal use of immunocytochemical stains aids with a more definitive classification. The implementation of TIS will improve the clinical approach to atypical categories based on the calculated ROM.

265 Utility of NOR-1 Immunohistochemistry in Fine Needle Aspiration Cytology Diagnosis of Acinic Cell Carcinoma

Karleen Meiklejohn¹, Minhua Wang², Morgan Hrones¹, Rita Abi-Raad², Guoping Cai³, Adebowale Adeniran², Manju Prasad², Syed Gilani²

¹Yale School of Medicine, Yale New Haven Hospital, New Haven, CT, ²Yale School of Medicine, New Haven, CT, ³Yale University, New Haven, CT

Disclosures: Karleen Meiklejohn: None; Minhua Wang: None; Morgan Hrones: None; Rita Abi-Raad: None; Guoping Cai: None; Adebowale Adeniran: None; Manju Prasad: None; Syed Gilani: None

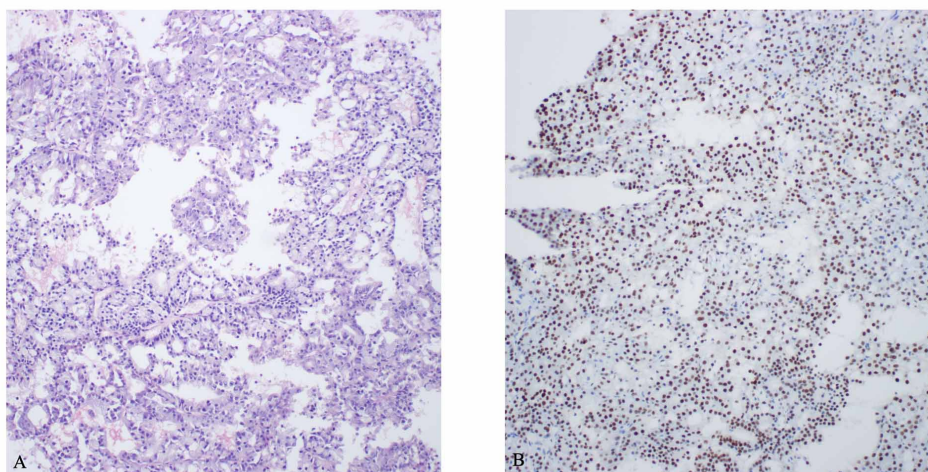
Background: Fine needle aspiration (FNA) is a useful tool for pre-operative evaluation of salivary gland lesions. Although the Milan System has been developed to streamline a uniform reporting of these lesions, it remains challenging to make a specific diagnosis on FNA, especially where there is morphologic overlap among the lesions included in the differential diagnosis. Acinic cell carcinoma (AcCC) is composed of neoplastic salivary gland acini, and as such can be difficult to distinguish from normal tissue

and other neoplastic mimickers in FNA specimens. This study examined the utility of NOR-1, a new immunohistochemical marker, in distinguishing AcCC from its potential mimickers.

Design: This study was undertaken after acquiring approval from the institutional review board. We retrospectively reviewed our database for confirmed cases of AcCC with available cytology cases along with cell block (CB) material. Additional cases with non-AcCC salivary neoplasm diagnosis were selected for comparison. Immunohistochemistry with anti-NOR-1 (NR4A3) antibody (SC-393902, 1:50) was performed on the cell block sections. Stained slides were then reviewed for nuclear staining and classified as positive (weak, moderate, or strong) or negative (no staining).

Results: Twenty-four cases were included in this study including 6 AcCC cases (3 from metastatic sites, 2 from parotid gland and 1 from cheek) and 18 non-AcCC cases (5 salivary duct carcinomas, 3 mucoepidermoid carcinomas, 1 epithelial-myoepithelial carcinoma, 4 pleomorphic adenomas, 3 Warthin's tumors and 2 basal cell adenomas). Of the 6 AcCC cases, four showed diffuse moderate-to-strong staining, one showed focal moderate staining and one showed focal weak staining for NOR-1. All cases with non-AcCC diagnoses were negative. Of note, normal salivary gland acini present in the cell block of a non-AcCC case showed no nuclear staining.

Figure 1 - 265



A: Neoplastic cells forming microcystic type structure (Cell block x100), B: nuclear positivity for NOR-1 (NR4A3) in tumor cells (Immunostain x 100)

Conclusions: NOR-1 (NR4A3) immunohistochemistry has potential to be a useful tool in triage of salivary gland cytology cases, if a cell block is available for immunostaining. Additionally, this marker may be useful in distinguishing neoplastic acini from benign acini. More studies are needed to further validate these findings, as well as evaluate the significance of staining intensity and tumor proportion positivity.

266 The Value of Endobronchial Ultrasound Guided-Fine Needle Aspiration in Research Biobanking

Monica Miyakawa-Liu¹, Laura Lundi¹, Sukhmani Padda², Danielle Leuenberger³, Arthur Sung¹, Meghan Ramsey¹, Viswam Nair⁴, Harmeet Bedi¹, Michael Ozawa⁵

¹Stanford Health Care, Palo Alto, CA, ²Cedars-Sinai, Los Angeles, CA, ³Stanford Medicine/Stanford University, Palo Alto, CA, ⁴Fred Hutchinson Cancer Research Center, Seattle, WA, ⁵Stanford University, Stanford, CA

Disclosures: Monica Miyakawa-Liu: None; Laura Lundi: None; Sukhmani Padda: *Advisory Board Member, AstraZeneca; Consultant, JazzPharma; Consultant, G1 Therapeutics; Advisory Board Member, Janseen Pharmaceuticals; Advisory Board Member, Blueprint Medicines; Speaker, Nanobiotix*; Danielle Leuenberger: None; Arthur Sung: None; Meghan Ramsey: None; Viswam Nair: None; Harmeet Bedi: None; Michael Ozawa: None

Background: Endobronchial Ultrasound Guided-Fine Needle Aspiration (EBUS FNA) is a low risk procedure which is routinely used to obtain tumor samples for histologic and molecular diagnostics of thoracic malignancies. With the ongoing demand for tissue for research, identifying ways to increase the availability of these samples while prioritizing patient safety is imperative.

Design: A pilot project including 10 patients was conducted at Stanford University to determine the utility of biobanking for research studies, with a primary assessment of tumor cellularity. Patients with suspected or diagnosed thoracic malignancy and technically facile locations for tissue acquisition by EBUS FNA, as assessed by an interventional pulmonologist, were consented. After the standard clinical procedure, an additional 2-3 aspirates were performed. Rapid on-site evaluation (ROSE) was conducted. A cell block was created from the clinical and research aspirates, and cellularity and percentages of tumor were compared. Cellularity was calculated as number of intact cells per 20x power field, averaged over 3 fields. Tumor percentage was calculated as number of neoplastic cells over the total number of cells available on the same power field.

Results: Of the patients included in the study, 8 had a diagnosis of NSCLC (7 Adenocarcinoma, 1 Adenosquamous) and 2 had SCLC. All patients eligible for molecular testing successfully completed this on their clinical sample (n= 8, 100%). Research passes were performed on lymph nodes in 7 cases (stations 7 (2), 4R (2), 11R (2) and 11L (2)), the lung in 2 cases, and a recurrent mediastinal mass in 1 case. One sample was noted to be extensively necrotic. Of the 9 non-necrotic samples, the clinical samples median total cellularity was 40 (Q1: 35, Q3: 60, IQR: 25) and the median % tumor was 41.1 (Q1: 17.5, Q3: 77.5, IQR: 60). Of the research passes, the median total cellularity was 40 (Q1: 25, Q3: 65, IQR: 40) and the median % tumor was 30 (Q1: 17.5, Q3: 65, IQR: 47.4). There were no complications related to the study

Figure 1 - 266

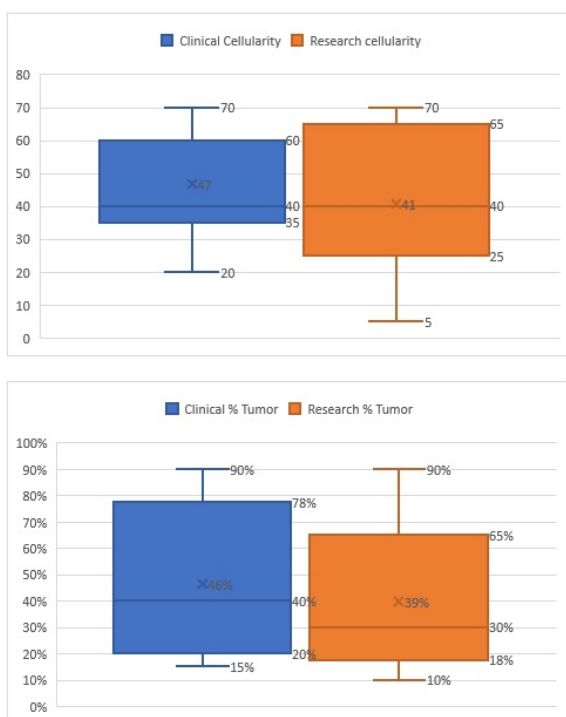
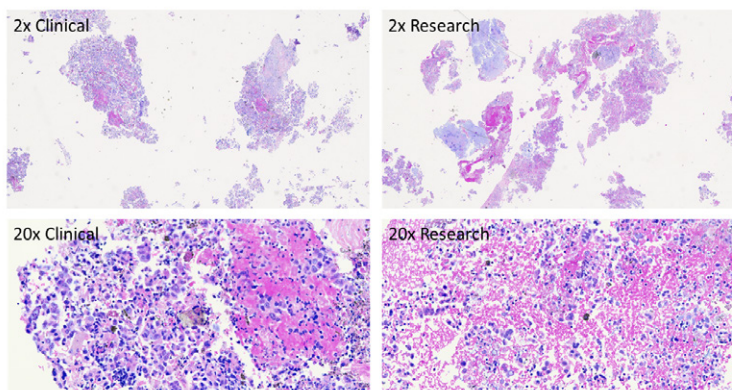


Figure 2 - 266



Conclusions: The viable cellularity and percentage tumor of the samples from additional research passes during the EBUS procedure, without added safety concerns, suggests this is a worthwhile method to obtain a variety of tumor samples for future research testing.

267 The Value of Cytology in Diagnosing Blastomycosis

Fernando Alekos Ocampo Gonzalez¹, Joanna Solarewicz¹, Xinhai Zhang², Paolo Gattuso¹, Lin Cheng¹
¹Rush University Medical Center, Chicago, IL, ²Rush University, Chicago, IL

Disclosures: Fernando Alekos Ocampo Gonzalez: None; Joanna Solarewicz: None; Xinhai Zhang: None; Paolo Gattuso: None; Lin Cheng: None

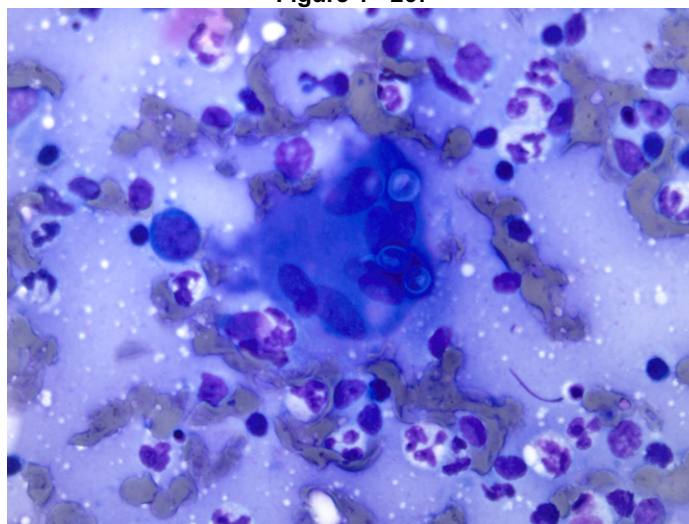
Background: Blastomycosis is a deep fungal infection caused by organisms in the *Blastomyces* genus, typically *B. dermatitidis*, endemic to the Mississippi and Ohio River valley and midwestern USA. *Blastomyces* can be identified by fungal

culture, antigen testing or histology . Here we performed a cohort study of blastomycosis cases, to compare their cytological findings with histological results, and to evaluate the role of cytology in diagnosis.

Design: The pathology database at Rush University Medical Center was searched for cases of Blastomycosis with either cytology-only or concurrent cytology-surgical pathology samples, from 1998-2021. The pathological materials and medical records of the identified cases were reviewed.

Results: 30 cases with cytology were found (26 touch preps for frozen sections, 4 fine needle aspirations). There were 18 males and 12 females, with age ranging from 13-76 years. All patients were residents of Illinois with no relevant travel history. Sites included lung (12 cases), extremities (10 lower, 1 upper), lymph node (5 cases), and thoracic wall (2 cases). 5 patients had disseminated disease. 23/30 cases showed Blastomyces on cytology, with 10/23 showing yeast forms within multinucleated giant cells (MNGCs). Microbiology results were available for 22/30 patients, with 18 cases showing either positive culture or antigen test. 29/30 cases had concurrent surgical pathology specimens; 27/29 showed Blastomyces on permanent sections by GMS stain. The overall concordance on Blastomycosis diagnosis between cytology and surgical pathology was 20/27 (74.1%). Surprisingly, 2 positive FNAs had negative concurrent surgical samples. Comparing with permanent sections, only 5/26 (19.2%) cases were diagnosed on H&E stained frozen section slides. However, Blastomyces yeast forms were identified on the Diff-Quik stained touch prep slides in 19/26 (73.1%) cases.

Figure 1 - 267



Conclusions: The most common site of Blastomycosis is lung, followed by extremities. Cytology is a reliable method for the diagnosis of Blastomycosis regardless of infection site. Cytology in conjunction with surgical pathology and microbiology can increase the sensitivity and specificity of Blastomycosis diagnosis. Yeast forms are better appreciated on Diff-Quik stained cytology materials (19/26, 73.1%) than the H&E stained frozen section slides (5/26, 19.2%). Almost half of the positive cytology cases showed yeast form within MNGCs. Spotting these cells can help identify the organisms faster on immediate assessment.

268 Challenges of HPV Testing in Head and Neck Aspirates and the Utility of Liquid Based Testing Platforms

Kaitlyn Ooms¹, Dawn Underwood¹, Erica Kaplan¹, Emily McMeekin¹, Brenda Sweeney², William Faquin³, Christopher Griffith⁴

¹Cleveland Clinic, Cleveland, OH, ²Massachusetts General Hospital, Boston, MA, ³Massachusetts General Hospital, Harvard Medical School, Boston, MA, ⁴Cleveland Clinic Foundation, Cleveland, OH

Disclosures: Kaitlyn Ooms: None; Dawn Underwood: None; Erica Kaplan: None; Emily McMeekin: None; Brenda Sweeney: None; William Faquin: None; Christopher Griffith: None

Background: The incidence of high risk HPV (HR HPV) associated oropharyngeal squamous cell carcinoma (OPSCC) is increasing and determination of HPV status on cytologic samples is critically important for clinical management decisions.

Unfortunately, aspirates represent a challenging specimen for HPV testing and various institutions have found different solutions to this challenge. Here we present our institutional experience in p16 staining of Cellient cell blocks and testing of liquid based samples in our internal Roche cobas validation and send-out BD Onclarity testing.

Design: Electronic database search of CoPath™ was performed to identify FNA specimens of metastatic squamous cell carcinoma in which p16/HPV testing was attempted or a comment noted that testing was not feasible on the sample. Aspirates were collected in CytoLyt® media and cell blocks were made after spinning the solution down and placing into PreservCyt® media with the Cellient cell block system. Results of p16 on cell block samples was correlated to p16 IHC and/or HR HPV RNA in situ hybridization on histologic specimens of the same metastatic site or primary tumor or rarely with results of the Onclarity assay described below. In-house validation testing was performed from the PreservCyt solution using the Roche cobas assay and correlated with p16/HPV RNA CISH on histology. Send-out HR HPV testing on PreservCyt® fluid was determined by BD Onclarity assay that had been previously validated for this sample type. Onclarity results are reported for clinical action and only select cases have follow-up confirmation of HPV status.

Results: 161 aspirates were found meeting inclusion criteria between 2015 and 2021. 98 of these cases were determined to be HPV positive on histology or Onclarity (41 negative, 22 undetermined). p16 IHC on cell block was attempted on 106 cases (see table). Roche cobas was performed on 39 cases. Onclarity was performed on 34 cases with results presented in the table. p16 IHC on Cellient® cell blocks has high rates of inadequate material (14.2%), indeterminate results (14.2%) and only accurately indicates an HPV association in a minority (22.2%) of aspirates from HPV positive tumors. In contrast, both liquid based methods (Roche cobas and BD Onclarity) using CytoLyt® material provided higher sensitivities (>90%) and specificity (100%) with few indeterminate cases.

p16 IHC on Cellient cell block results (n=106)					
p16 Interpretation	N (%)				
Insufficient/inadequate/unsatisfactory	15 (14.2)	(n=62)		HPV Status	
Equivocal/indeterminate/inconclusive	15 (14.2)			+	-
Negative	58 (54.7)	p16	+	17	0
Positive	18 (17.0)		-	35	10
Roche cobas results (n=38)					
HR HPV Interpretation	N (%)				
Invalid	2 (5.3)	(n=28)		HPV Status	
Negative	19 (50.0)			+	-
Positive	17 (45.7)	p16	+	16	0
			-	1	11
BD Onclarity results (n=34)					
HR HPV Interpretation	N (%)				
Indeterminate	1 (2.9)	(n=14)		HPV Status	
Negative	13 (54.2)			+	-
Positive	17 (50.0)	Onclarity	+	11	0
			-	0	3
Comparison of three testing modalities					
		p16 on CB	Roche cobas	Onclarity	
Sensitivity		32.7%	94.1%	100%	
Specificity		100%	100%	100%	
NPV		22.2%	91.7%	100%	
PPV		100%	100%	100%	
Accuracy		43.5%	96.4%	100%	

Conclusions: Our findings indicate that liquid based methods for HPV determination is superior to p16 immunostaining on Cellient® cell blocks.

269 Bronchoalveolar Lavage (BAL) Cell Count in COVID-19 (+) and COVID-19 (-) Patients, Including a Comparison of COVID-19 Recovered versus Deceased Patients

Mindy Pang¹, Po Chu Fung², Neda Moatamed², Sung Eun Yang²

¹UCLA Pathology and Laboratory Medicine, Los Angeles, CA, ²David Geffen School of Medicine at UCLA, Los Angeles, CA

Disclosures: Mindy Pang: None; Po Chu Fung: None; Neda Moatamed: None; Sung Eun Yang: None

Background: COVID-19 is a contagious disease caused by SARS-CoV-2. Clinically, this disease can range from having mild to more severe symptoms including death due to disease. Our aim in this study is to determine if there are any significant differences

in the BAL cell count differentials between COVID-19 (+) and COVID-19 (-) patients, including a comparison of patients who recovered from the disease and those who died due to disease.

Design: A retrospective computer search (EPIC Beaker) was performed on BALs from 1/20/20 to 6/6/21. Patients were included if they had a (+) COVID-19 test and BAL performed. For a comparison group we included BAL specimens from COVID-19 (-) lung transplant patients. 59 patients met this criteria: 10 COVID-19 (-) and 49 COVID-19 (+) (24 COVID-19 recovered and 25 COVID-19 deceased). The control group had 5 male and 5 female patients, mean age of 37. The COVID-19 (+) group had 37 male and 12 female patients with mean age of 60. For each BAL specimen, 3 cytospin slides were prepared (2 PAP and 1 MGG) and analyzed for differential cell count performed by a cytotechnologist. BAL specimens were also sent to microbiology and other infectious agents were noted if applicable. A p-value with t-test unequal variances was performed to compare any significant differences in the cell count between groups.

Results: Mean cell count percentages in the COVID-19 (+) and COVID-19 (-) is as seen in Table 1. In comparing the BAL cell counts of COVID-19 (+) versus COVID-19 (-) groups, there was a significant difference between the mean neutrophil cell count (p-value 0.04). No significant difference was found in the mean percentages of macrophages, lymphocytes, or eosinophils. In the COVID-19 recovered versus deceased groups, there was no significant difference found between the groups. Of the 10 COVID (-) patients, 1 patient was positive for *Candida spp.* infection on microbiology studies. Of the 49 COVID (+) patients, 11 cases were positive for one or more fungal organisms [*Candida spp* (8); *Aspergillus species* (3); and *Saprochaete Capitata* (1)].

	BAL cell count (mean %)					
	# of cases	macrophages	lymphocytes	neutrophils	eosinophils	fungal infection (# of patients)
COVID-19 (-)	10	62	13.2	17.8	6.8	1
COVID-19 (+), all	49	55.8	9.1	33.6	1.5	11
COVID-19 (+) recovered	24	52	7.3	38.7	2	2
COVID-19 (+) deceased	25	59.5	10.7	28.8	1.1	9

Conclusions: A significant difference was seen in the neutrophil cell count between COVID-19 (+) and COVID-19 (-) patients, which is as expected given the infection. There was no significant difference in the COVID-19 (+) recovered vs COVID-19 (+) deceased groups. The range of symptoms seen in COVID-19 (+) patients cannot be explained by differences in the inflammatory cell count of patients in our study.

270 The Role of Insulinoma Associated Protein 1 in the Evaluation of Effusions Suspected for Small Cell Carcinoma and Its Sensitivity in Comparison With Other Neuroendocrine Markers

Arshna Qureshi¹, Claire Michael², Aparna Harbhajanka¹

¹Case Western Reserve University/University Hospitals Cleveland Medical Center, Cleveland, OH, ²University Hospitals Cleveland Medical Center, Cleveland, OH

Disclosures: Arshna Qureshi: None; Claire Michael: None; Aparna Harbhajanka: None

Background: Effusion cytology (EC) is critical in diagnosis of advanced small cell lung carcinomas (SCLC) due to ease of access. Nonetheless, EC for SCLC can be challenging especially with primary diagnosis due to limited cellularity. Immunohistochemistry (IHC) is an important adjunct to confirm SCLC in difficult cases with extensive crush artifacts and to rule out other differentials, e.g. lymphoma and other small blue cell tumors. However, IHC markers may react differently in EC samples than in fine needle aspiration samples. Thus, a highly sensitive marker is needed for use in EC. In this direction, a new neuroendocrine (NE) marker, insulinoma associated protein 1 (INSM1) has shown high sensitivity and specificity on tissue based specimens. However, there is sparse literature on the role of INSM1 in EC for suspected SCLC. Thus, the goal of our study is to assess the sensitivity of INSM-1 in EC and compare it with other NE markers.

Design: Clinicopathologic features were evaluated in 33 SCLC cases diagnosed in our institution from 2011 to 2021. In addition, IHC stains for chromogranin (CG), synaptophysin (SYN), CD56, INSM-1 and thyroid transcription factor (TTF-1) were done on available cases.

Results: A total of 33 cases (Table 1) with a mean age of 71.6 years were reported as diagnostic (30 cases) or suspicious (3 cases) of SCLC. 50% cases were diagnosed primarily on EC. The tumor cellularity was moderate in 50%, low in 29% and high in 21% cases. Tumor cells were mostly present as small clusters and single cells (62%), 29% cases had predominantly single cells, and 8% cases showed mainly large clusters. All cases revealed nuclear molding and hyperchromasia with numerous lymphocytes

in the background (Fig1-2). Notably, INSM1 showed a sensitivity of 95%, which was higher than CD56 (80%), TTF-1 (82%), and CG (90%), while slightly lower than SYN (100%). Interestingly, in 3 cases where SYN and CG were focally positive, INSM1 had up to 80% positivity. Moreover, SYN showed background staining in 50% cases, which made the assessment difficult. In contrast, INSM1 showed reliable and strong nuclear staining.

S. No.	Age	sex	Cytologic diagnosis (suspicious Vs definitive)	1° vs 2° diagnosis	Cellularity (Low/mod/high)	Clusters (Cl)/single cells (SC)	INSM-1	TTF-1	Synaptophysin	Chromogranin	CD-56	Survival after effusion in days (outcome)
1	66	F	Definitive	1°	N/A	N/A	Positive	Scattered positivity	Positive	Negative	Positive	5 (alive)
2	93	F	Definitive	1°	Moderate	CL+SC	Positive	Positive	Patchy positive	Patchy positive	Patchy positive	24(died)
3	92	M	Definitive	1°	Moderate	CL+SC	Positive	Positive	Positive	Positive	N/A	8 (alive)
4	81	M	Definitive	1°	High	CL+SC	Positive	Positive	Positive	Positive	Negative	306(died)
5	65	M	Definitive	2°	Low	SC	Positive	Positive	Positive	Negative	Positive	341(died)
6	65	F	Definitive	1°	Moderate	CL+SC	Positive	Positive	Positive	Positive	Positive	8(alive)
7	89	F	Definitive	1°	Moderate	CL+SC	Positive	Negative	Positive	Focal positive	Positive	22(died)
8	72	F	Definitive	2°	N/A	N/A	N/A	Positive	Positive	Positive	Positive	N/A
9	39	M	Definitive	1°	N/A	N/A	N/A	N/A	N/A	N/A	N/A	128(died)
10	72	F	Definitive	1°	Moderate	CL+SC	Positive	N/A	Positive	Positive	Positive	176(alive)
11	54	F	Definitive	2°	High	CL+SC	Positive	Positive	Positive	Positive	Negative	30(died)
12	76	F	Definitive	1°	Moderate	CL+SC	Negative	Positive	Positive	Positive	Positive	10(died)
13	62	M	Suspicious	2°	Low	RARE SC	N/A	Negative	Positive	Positive	Positive	45(died)
14	56	F	Definitive	1°	Moderate	CL+SC	Positive	Positive	Positive	Positive	Positive	260(died)
15	68	M	Definitive	1°	N/A	N/A	N/A	Positive	Positive	Positive	N/A	50(died)
16	76	M	Definitive	2°	N/A	N/A	N/A	Positive	Positive	N/A	Positive	17(died)
17	73	F	Definitive	2°	N/A	N/A	N/A	N/A	N/A	N/A	N/A	19(alive)
18	67	F	Definitive	2°	Moderate	CL+SC	Positive	Positive	Positive	Positive	Positive	34(died)
19	86	F	Definitive	1°	High	CL+SC	N/A	Positive	Positive	Positive	N/A	5(died)
20	75	F	Definitive	2°	Moderate	CL+SC	Positive	Negative	Positive	Positive	Negative	N/A
21	73	F	Suspicious	1°	Low	SC	Positive	Positive	Positive	Positive	Positive	390(alive)
22	76	M	Definitive	1°	Moderate	CL+SC	Positive	Positive	Positive	Positive	N/A	330(alive)
23	66	M	Suspicious	1°	Low	RARE SC	Positive	Negative	Positive	Negative	N/A	82(died)
24	59	F	Definitive	2°	Moderate	CL+SC	Positive	Positive	Positive	Positive	Positive	8(died)
25	76	F	Definitive	1°	High	CL+SC	Positive	Positive	Positive	Positive	Positive	N/A
26	77	F	Definitive	2°	Low	CL+SC	Positive	Negative	Positive	Positive	N/A	42(died)
27	96	M	Definitive	1°	Low	SC	Positive	Positive	Positive	Positive	N/A	10(alive)
28	62	F	Definitive	2°	Moderate	N/A	N/A	N/A	Positive	Positive	N/A	19(died)
29	62	F	Definitive	2°	High	CL+SC	Positive	Positive	Positive	Positive	Positive	N/A
30	61	M	Definitive	1°	N/A	N/A	N/A	Positive	Positive	Positive	Positive	441(alive)
31	82	F	Definitive	2°	Moderate	SC +RARE SMALL CL	Positive	Positive	Positive	Positive	Positive	21(died)
32	73	M	Definitive	1°	Low	SC + RARE SMALL CL	Positive	Positive	Positive	Positive	Positive	338(alive)
33	88	F	Definitive	1°	MODERATE	N/A	Positive	Positive	Positive	Positive	N/A	2(alive)

Figure 1 - 270

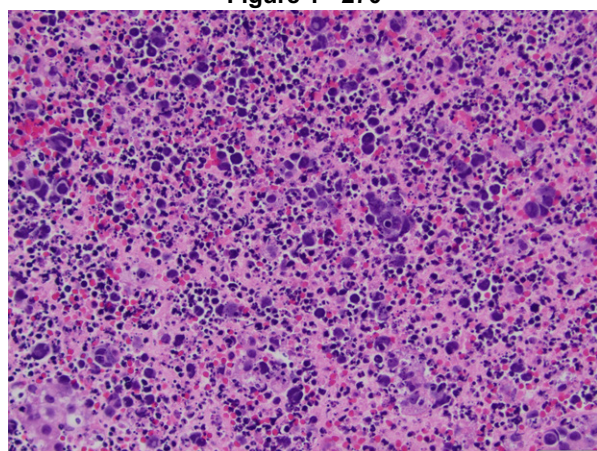
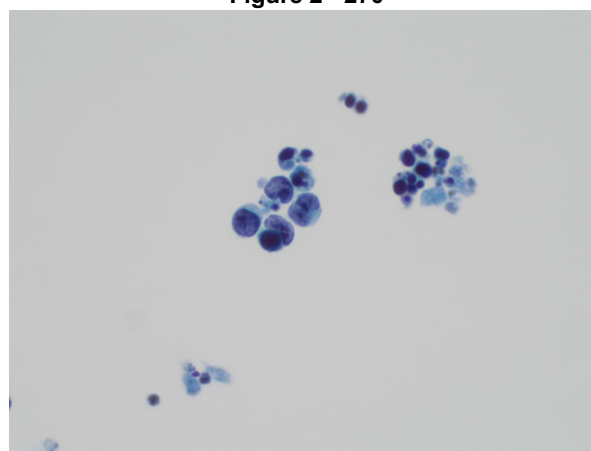


Figure 2 - 270



Conclusions: SCLC patients rarely present primarily with pleural effusion. The cytomorphology of SCLC is characteristic. Therefore, knowing the cytomorphological spectrum of SCLC in EC may help in accurate diagnosis and appropriate management.

Furthermore, INSM1 with its crisp nuclear staining and high sensitivity proves to be a useful additional marker in the limited sample of effusion specimen.

271 Cytologic Findings in Intraductal Papillary Neoplasm of Bile Duct (IPNB): An Analysis of 18 Cases

Michelle Reid¹, Raul Gonzalez², Jiaqi Shi³, Barbara Centeno⁴, Alyssa Krasinskas⁵, Olca Basturk⁶, N. Volkan Adsay⁷
¹Emory University Hospital, Atlanta, GA, ²Beth Israel Deaconess Medical Center, Harvard Medical School, Boston, MA, ³University of Michigan, Ann Arbor, MI, ⁴H. Lee Moffitt Cancer Center & Research Institute, Tampa, FL, ⁵Emory University, Atlanta, GA, ⁶Memorial Sloan Kettering Cancer Center, New York, NY, ⁷Koç University Hospital, Istanbul, Turkey

Disclosures: Michelle Reid: None; Raul Gonzalez: None; Jiaqi Shi: None; Barbara Centeno: None; Alyssa Krasinskas: None; Olca Basturk: None; N. Volkan Adsay: None

Background: IPNB is a rare tumoral intraepithelial neoplasm that often presents as an obstructive mass and is typically diagnosed radiologically as "ordinary" cancer despite its incomparably better behavior than cholangiocarcinoma. Histologic subtypes include gastric, pancreatobiliary, intestinal and oncocytic (IOPN). Although definitive diagnosis is increasingly being made on cytologic samples, the literature regarding the cytologic features in IPNB is extremely limited.

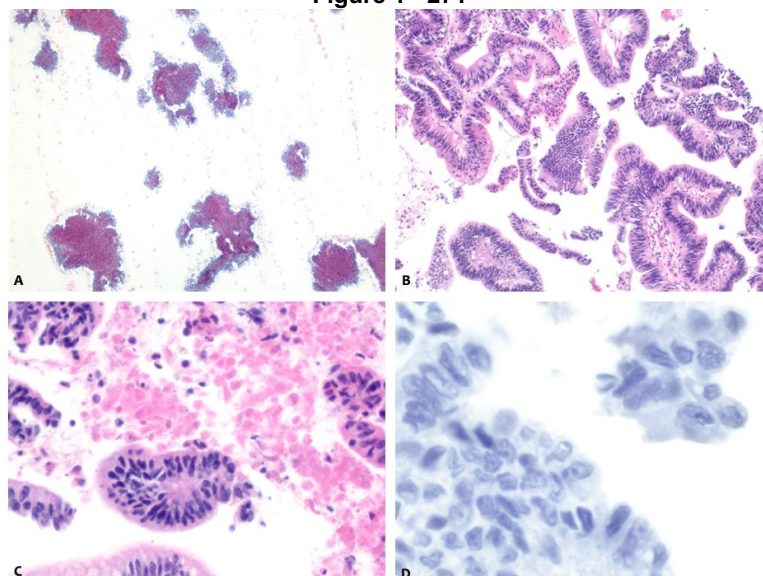
Design: Eighteen IPNBs collected from 16 patients across 5 institutions were analyzed.

Results: Seven females and 9 males, median age 64 years (range 33 - 91) had documented radiologic evidence of intrahepatic (HD) or common bile duct (CBD) dilatation/mass in 12 (75%) or liver mass, NOS in 4 (25%). Age, gender and location were unknown in 1. ERCP findings included a polypoid/papillary intraductal mass in 8 (50%), stricture in 1 (6%) and were unknown in 7 (44%). Sampling included bile duct brushing (n=8), FNA (n=9) and touchprep (n=1). Original diagnoses were: atypical cells (n=4), IPNB (n=8), IOPN (n=4, 2 from a patient with multifocal disease), and adenocarcinoma (n=2). Hypercellularity, papillae with fibrovascular cores (FVCs), and drunken honeycomb/complex branching sheets were seen in the majority but high-grade features were variable (33-89%). Cytoplasmic (50%) and extracellular mucin (33%) were less common. Nuclear palisading was striking in 5 (28%), 4 of which were intestinal IPNBs. [Figure 1] Oncocytic cells predominated in the 4 IOPNs. [Figure 2] [Table] Resection (n=11) revealed IPNB, median size 3.5cm (range 1.1-5.1), with an invasive component in 6 (55%), of median size 1.9cm (range 0.15 - 2.1), including 3 T1N0Mx and 3 T2N0/N1Mx tumors.

Table 1 – 271: Cytologic Findings in 17 Samples from 15 Patients

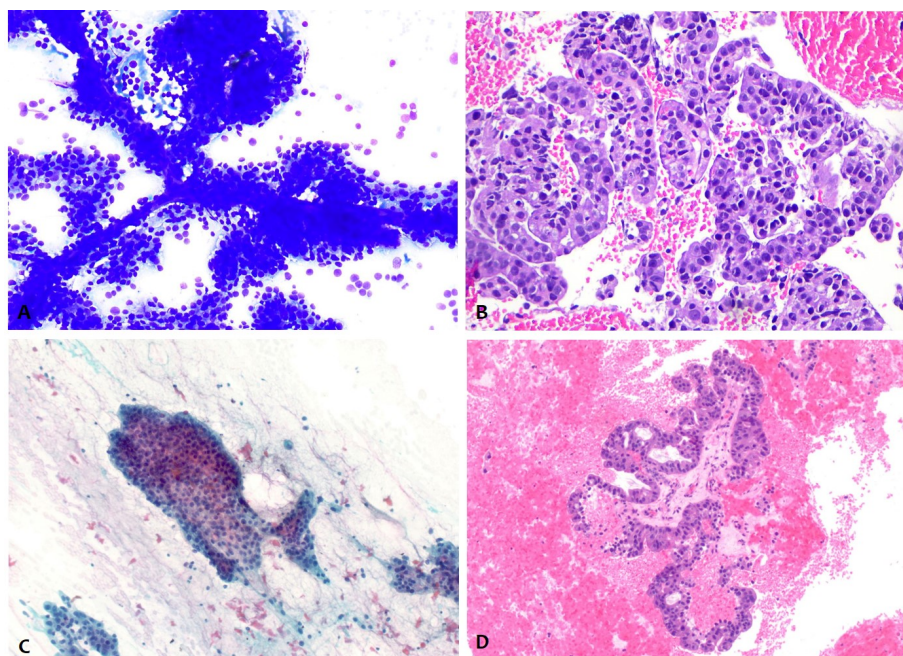
Low Power Architectural Features								
Hypercellular sample	Flat sheets	Branching/ Complex sheets	Drunken Honeycomb sheets	Papillae on smear/ ThinPrep	Fibrovascular cores	Papillae on cell block	Thick Extracellular mucin	Necrotic debris
15 (83%)	10 (56%)	11 (61%)	17 (94%)	13 (72%)	11 (61%)	14 (78%)	6 (33%)	7 (39%)
High Power Cytologic Features								
Anisonucleosis	Single cells	Single cell necrosis	Abnormal Mitoses	Prominent Nucleoli	Hyperchromasia	Hypochromasia	Irregular Nuclei	Cytoplasmic mucin
11 (61%)	16 (89%)	6 (33%)	6 (33%)	12 (67%)	15 (83%)	11 (61%)	15 (83%)	9 (50%)

Figure 1 - 271



FNA of an intestinal type intraductal papillary neoplasm of bile duct with hypercellular smear composed of complex branching sheets (A) and papillae on cell block (B). Papillae are lined by tall columnar cells with pseudostratified nuclei (B). Note foci of comedo necrosis (C) and marked nuclear atypia on high power view of negative MUC1 immunostain.

Figure 2 – 271



FNA of pancreatobiliary type IPNB showing (A) branching papillae and corresponding cell block (B) with complex papillae lined by high N/C ratio cells with prominent nucleoli and focal cytoplasmic mucin. FNA of IOPN with honeycomb sheet, background mucin (C) and corresponding cell block (D) with broad papillae lined by pseudostratified oncocyctic cells.

Conclusions: IPNB has subtle but distinctive cytologic characteristics that are helpful in diagnosis and distinction from cholangiocarcinoma for which it may be mistaken, but from which it should be differentiated due to its less aggressive behavior/treatment when non-invasive. Tumor is often unsuspected on imaging however ERCP often shows a polypoid/papillary intraductal mass which should raise the IPNB differential. Accurate diagnosis is possible on cytology as evidenced in 67% of cases. Cytologic findings include branching papillae with FVCs, complex branching/drunken honeycomb sheets, and high-grade features including single high nuclear/cytoplasmic ratio cells, scant cytoplasmic mucin, irregular nuclei and prominent nucleoli. Abundant extracellular mucin is rarely seen in IPNB.

272 Comparison of TRPS1 and GATA-3 Immunoperoxidase Staining Using Cytologic Smears In Entities Reportedly Positive for GATA-3

Prih Rohra¹, Cady Ding¹, Esther Yoon¹, Qiong Gan¹

¹The University of Texas MD Anderson Cancer Center, Houston, TX

Disclosures: Prih Rohra: None; Cady Ding: None; Esther Yoon: None; Qiong Gan: None

Background: Diagnosis of metastatic breast carcinoma (BC) is frequently encountered in cytology practice and may be challenging as the tumor cells can morphologically resemble carcinoma of other primary origins. It is also not uncommon that direct smears are the only sample type that can be used for immunostaining study in cytology. Trichorhinophalangeal syndrome type 1 (TRPS1), a novel GATA transcriptional factor, is reported to be a highly sensitive and specific marker for BC comparing to GATA-3, including triple negative BC (TNBC), in histologic samples. However, its sensitivity and specificity in detecting metastatic BC as well as other GATA-3-positive tumor in direct cytologic smears has not been well studied.

Design: 1. Immunoperoxidase stainings of TRPS1 and GATA-3 on cytologic direct smears have been validated in our clinic immunohistochemical laboratory following standard guidelines. Then we identified cytology cases containing at least 2 direct smears: a) 20 GATA-3-positive metastatic BC, 10 GATA-3-negative and clinically believed metastatic TNBC based on history and extensive work-up; b) 5 FNA cases of epithelioid entities that are reported to be GATA-3-positive and highly related to cytology service including bladder carcinoma, paraganglioma, mesothelioma, neuroblastoma, parathyroid adenoma, salivary ductal carcinoma/secretory carcinoma. 2. Immunoperoxidase staining of TRPS1 and GATA-3 were performed on the chosen smears following the standard protocol used in our clinical laboratory. The staining results were reviewed by two cytopathologists.

Results: 1. TRPS1 is positive in all 20 GATA-3-positive metastatic BC and in 7/10 GATA-3-negative metastatic TNBC. Representative pictures were shown in Figure 1. 2. TRPS1 is negative in all 5 cases of entities that have been reported to be variably positive for GATA3, including bladder carcinoma, parathyroid adenoma, mesothelioma, salivary ductal carcinoma/secretory carcinoma, neuroblastoma. GATA-3 is variably positive ranging from 60-100% of these cases (Table 1).

	TRPS1 (+/total)	GATA3 (+/total)
non-TNBC (GATA3+)	20/20	20/20
TNBC (GATA3-)	7/10	0/10
Urothelial carcinoma	0/5	5/5
Paraganglioma	0/5	5/5
Parathyroid adenoma	0/5	5/5
Mesothelioma	0/5	3/5
Neuroblastoma	0/5	5/5
salivary duct carcinoma	0/5	4/5

Figure 1 - 272

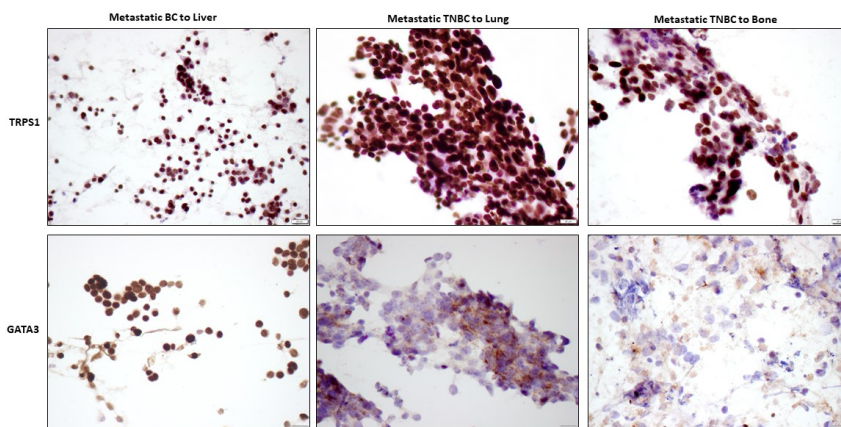


Figure 1. Comparison of TRPS1 and GATA-3 staining in metastatic breast carcinoma (ER positive) versus triple-negative breast carcinoma.

Conclusions: 1. TRPS1 is as sensitive as GATA-3 in GATA-3-positive metastatic BC, and is more sensitive than GATA-3 in TNBC on cytologic smears. 2. When cytologic smears are the only available material, TRPS1 and GATA-3 could be used together to differentiate breast primary from other primaries that have been reported to be variably positive for GATA-3 including bladder carcinoma, mesothelioma, parathyroid adenoma and paraganglioma.

273 Tissue Fragment Assessment in Small Volume Biopsies by Computer Vision

Rebecca Rojansky¹, Steven Long², Dita Gratzinger³

¹Stanford Hospital and Clinics, Stanford, CA, ²University of California, San Francisco, San Francisco, CA, ³Stanford University Medical Center, Stanford, CA

Disclosures: Rebecca Rojansky: None; Steven Long: None; Dita Gratzinger: None

Background: Small volume biopsies (SVB) are increasingly used for diagnosis of hematolymphoid malignancies. In some cases SVB may even be sufficient to diagnose transformation, a task which is particularly challenging in the setting of small and/or fragmented specimens as it often requires broader architectural assessment. Adequacy criteria for SVBs specifically for the purpose of ruling out transformation have not been previously characterized. We developed an unbiased automated tissue finder tool to determine the geometric characteristics of diagnostic vs. non diagnostic SVB in the context of ruling out transformation in follicular lymphoma.

Design: A total of 152 biopsy workups for patients with a history of follicular lymphoma from two academic institutions were analyzed (1/1/2012-12/31/2016). Included specimens were SVB, defined as fine needle aspiration (FNA) with cell block and/or core biopsy, performed for the purpose of ruling out transformation. Data obtained from electronic medical records at each institution were entered into a shared REDCap database with IRB approval. TIFF Images were acquired either on a microscope-mounted camera at 5X magnification or were extracted from whole slide images and downsampled 15 fold.

Results: The software correctly distinguishes tissue fragments from background (Figure 1a) and replicates manual measurements (Figure 1b). A definitive diagnosis was reached in a majority of biopsies (79%). Characteristics of diagnostic and non-diagnostic biopsies overlap, including number of tissue fragments, fragment size, and total amount of tissue (Figure 2a). Of these metrics, greatest intact fragment length is most correlated with definitive diagnosis (Table 1). Lower gauge needles and radiographic over ultrasound guidance trend toward larger tissue fragments (Figure 2b,c).

Table 1. Pearson correlation of tissue metrics versus definitive diagnosis

	Correlation Coefficient
Fragments	0.03
Fragment Length	0.05
Fragment Area	0.00
Total Area	0.01
Flow Done	0.07

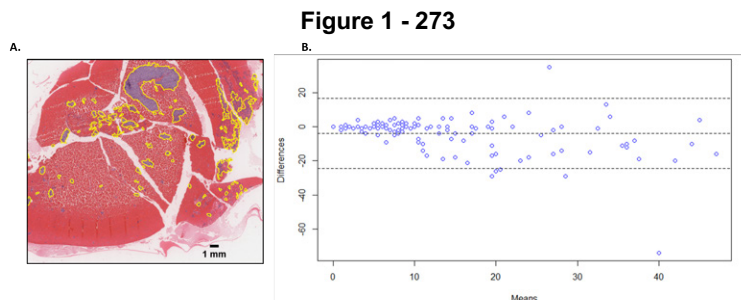


Figure 1. Digital fragment identification. A) Computer vision software identifies tissue fragments and distinguishes them from admixed blood and fibrin. Identified fragments are outlined in yellow. B) Bland Altman comparison of fragment quantitation by digital versus manual assessment. Hashed lines indicate the region within 1.96 standard deviations of the mean.

Figure 2 – 273

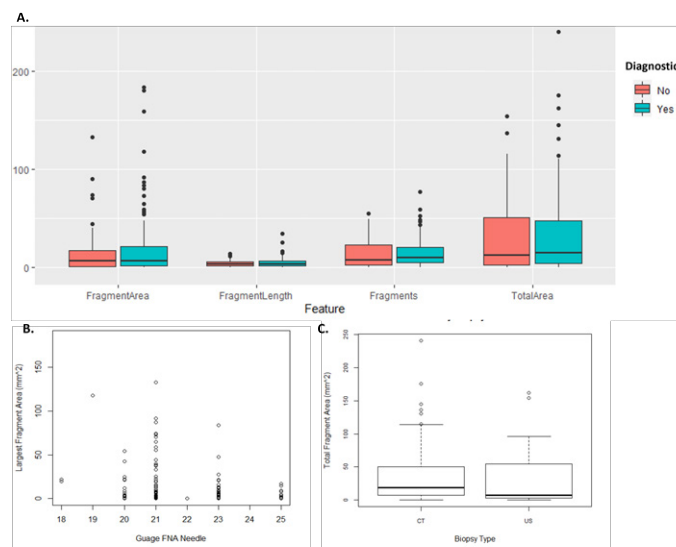


Figure 2. Tissue parameters for diagnostic utility. A) Physical metrics of tissue fragments: area of the largest fragment in mm², FragmentArea; length of the largest fragment in mm, FragmentLength; number of fragments, Fragments; total area of tissue on the slide in mm², TotalArea. B) Area of largest fragment versus gauge of FNA needle used. C) CT or ultrasound guidance versus total area of tissue on the slide.

Conclusions: These findings suggest that physical biopsy characteristics alone are insufficient to determine likely adequacy for the purpose of ruling out transformation in follicular lymphoma, however larger intact fragments may improve diagnostic utility and can be achieved through CT guidance and larger needle bore sizes. Importantly, this cohort is limited in that the majority of specimens were deemed diagnostic. The software described here may be useful when there is a need to identify tissue in SVB specimens.

274 Role of Fine Needle Aspiration for the Diagnosis of Skeletal Lesions: A Large Tertiary Care Center Experience

Carla Saoud¹, Syed Ali²

¹Johns Hopkins Hospital, Baltimore, MD, ²Johns Hopkins Medical Institutions, Baltimore, MD

Disclosures: Carla Saoud: None; Syed Ali: None

Background: Bone lesions represent a wide and diverse disease spectrum. Fine needle aspiration (FNA) is considered the most cost-effective and least invasive sampling technique with fewer complications and high diagnostic accuracy. However, FNA presents several practical challenges including; limited size of sample material, reduced ability to assess the underlying architecture and lack of standardized reporting system for bone cytopathology. The aim of our study is to elucidate the performance, adequacy and accuracy of FNA in the diagnosis of bone lesions.

Design: We performed a retrospective search of cytopathology archives at our institution from January 2015 to September 2021 to identify all bone FNAs. Available data for patient demographics, tumor site, cytopathologic diagnosis and subsequent surgical follow-up were recorded. FNA results were grouped into five cytomorphologic groups: non-diagnostic (ND), benign-non-neoplastic (B-NN), benign-neoplastic (B-N), atypia of undetermined significance (AUS) and suspicious for malignancy/malignant (SFM/M).

Results: A total of 335 cases were identified with slight male predominance: 172 males (51.3%) and 163 females (48.7%). The mean age was 57.2 (range=5-92). The Iliac crest (n=134) was the site most commonly biopsied followed by the spine (n=92). Surgical follow-up diagnosis was available in 288 cases (86%) and surgical specimens included concomitant or subsequent biopsy (84%), resection specimen (14.2%) and curetting specimen (1.8%). The frequency of cytomorphologic groups on FNA were as follows: 21.8% (ND), 17.9% (B-NN), 4.5% (B-N), 11.9% (AUS) and 43.9% (SFM/M). The adequacy of bone FNA sampling was 78.2%. The overall accuracy of FNA for definitive diagnosis was 75.8% and it was highest (95.5%) in the FNAs that were classified as SFM/M followed by those classified as B-N (85.7%). Secondary bone metastasis (33%) was the most common diagnosis on

surgical follow-up while chordoma was the most common primary bone tumor encountered. The overall sensitivity and specificity of bone FNA with regard to nature of the lesions (benign or malignant) were 79.8% and 91.9%, respectively. Table 1 highlights the surgical pathology follow-up diagnosis of the cases.

Table 1. Summary of the follow-up surgical pathology diagnoses for the five FNA reporting groups.

Cytomorphologic Reporting Group (n)	Subsequent surgical pathology diagnosis
Not diagnostic (ND)(73)	Non-diagnostic biopsy (20) Benign (28) <ul style="list-style-type: none"> ● Bone with reactive changes (10) ● Osteonecrosis (4) ● Bone fracture and remodeling (2) ● Osteomyelitis (2) ● Sarcoidosis (2) ● Bone hemangioma (2) ● Paget's disease of bone (1) ● Aneurysmal bone cyst (1) ● Fibrous dysplasia (1) ● Schwannoma (1) ● Myofibroma (1) ● Osteochondroma (1) Malignant (20) <ul style="list-style-type: none"> ● Secondary bone metastasis (11) ● Plasma cell myeloma (3) ● Lymphoma (3) ● Angiosarcoma (1) ● Osteosarcoma (1) ● Clear cell chondrosarcoma (1) No surgical follow-up (5)
Benign-non-neoplastic (B-NN)(60)	Non-diagnostic biopsy (2) Benign (50) <ul style="list-style-type: none"> ● Bone with reactive changes (24) ● Paget's disease of bone (8) ● Osteomyelitis (4) ● Aneurysmal bone cyst (3) ● Giant cell tumor of bone (2) ● Bone fracture and remodeling (2) ● Osteonecrosis (2) ● Sarcoidosis (1) ● Abscess (1) ● Malakoplakia (1) ● Simple cyst (1) ● Calcium pyrophosphate deposition arthropathy (1) Malignant (4) <ul style="list-style-type: none"> ● Secondary bone metastasis (3) ● Clear cell chondrosarcoma (1) No surgical follow-up (4)
Benign-neoplastic (B-N)(15)	Benign (14) <ul style="list-style-type: none"> ● Giant cell tumor of bone (8) ● Aneurysmal bone cyst (2) ● Chondroblastoma (2) ● Chondromyxoid fibroma (1) ● Osteoblastoma (1) No surgical follow-up (1)
Atypia of undetermined significance (AUS)(40)	Non-diagnostic biopsy (3) Benign (10) <ul style="list-style-type: none"> ● Bone with reactive changes (3) ● Osteonecrosis (2) ● Paget's disease of bone (1) ● Enchondroma (1)

	<ul style="list-style-type: none"> ● Osteoblastoma (1) ● Schwannoma (1) ● Fibrous dysplasia (1) <p>Malignant (24)</p> <ul style="list-style-type: none"> ● Secondary bone metastasis (11) ● Chondrosarcoma (6) ● Lymphoma (4) ● Chordoma (2) ● Osteosarcoma (1) <p>No surgical follow-up (3)</p>
Suspicious for Malignancy/Malignant (SPM/M)(147)	<p>Non-diagnostic biopsy (1)</p> <p>Malignant (112)</p> <ul style="list-style-type: none"> ● Secondary bone metastasis (70) ● Chordoma (16) ● Plasma cell myeloma (10) ● Osteosarcoma (7) ● Chondrosarcoma (5) ● Lymphoma (1) ● Angiosarcoma (1) ● Myoepithelial carcinoma (1) ● Epithelioid hemangioendothelioma (1) <p>No surgical follow-up (34)</p>

Table 1. Summary of the follow-up surgical pathology diagnoses for the five FNA reporting groups.

Conclusions: This study elaborates on the overall diagnostic performance of cytopathology and support the use FNA in the diagnosis of bone lesions. A universal and standardized cytopathology reporting system remains strongly needed for better evaluation and classification of skeletal lesions on FNA.

275 Cytologic Accuracy in Identifying High-Grade Dysplasia/Invasive Adenocarcinoma in Histologically Confirmed Intraductal Papillary Mucinous Neoplasms (IPMNs): A Retrospective Study

Serenella Serinelli¹, Kamal Khurana²

¹SUNY Upstate Medical University, Syracuse, NY, ²SUNY Health Science Center, Syracuse, NY

Disclosures: Serenella Serinelli: None; Kamal Khurana: None

Background: Intraductal papillary mucinous neoplasms (IPMNs) may be associated with low-grade dysplasia (LGD), high-grade dysplasia (HGD), or invasive adenocarcinoma. In the current study, we retrospectively analyzed cytologic accuracy in identifying HGD/adenocarcinoma in histologically confirmed IPMNs.

Design: A database search (January 2010 - January 2021) was performed for IPMN resection specimens with endoscopic ultrasound-guided fine-needle aspiration (FNA) performed within the preceding year. Cytology slides were reviewed for the presence of benign, atypical, or malignant cells, and necrosis. Histologically, IPMNs were classified as benign (LGD) or malignant (HGD or adenocarcinoma).

Results: There were 41 patients with IPMN; 24 malignant and 17 benign. Sixteen of the 24 malignant IPMNs were accurately classified as malignant on cytology. There were 8 false negatives and 1 false positive. Cytology yielded a sensitivity of 67% and a specificity of 94%. Among the 16 true positives with FNA diagnosis of adenocarcinoma, 7 were IPMNs with HGD, and 9 had invasive adenocarcinomas on histology. Necrosis was identified on cytology in one case of HGD (1/7) and three adenocarcinomas (3/9). Cellular morphology and absence or presence of necrosis did not help distinguish HGD from adenocarcinoma on cytology ($p > 0.5$). Sampling errors (5) and interpretative errors (3) resulted in false negative cases. The false positive case (suspicious for adenocarcinoma) did not show any evidence of HGD or adenocarcinoma in the resected IPMN.

Conclusions: Cytology is usually accurate in recognizing IPMN with HGD/adenocarcinoma. However, heterogeneity in areas of IPMN with HGD/adenocarcinoma may result in sampling errors yielding false negative cases. HGD and invasive adenocarcinoma

are difficult to distinguish on cytology. To improve communication of cytopathology results to the clinicians for patient management, we suggest using the terms “High-grade dysplasia, cannot exclude invasive adenocarcinoma” in all IPMNs considered malignant on cytology.

276 Role of p16 Immunohistochemistry (IHC) on Cell Block (CB) from Fine Needle Aspiration (FNA) from Metastatic Lesions in the Diagnosis of High Risk-Human Papilloma Virus (HR-HPV) Related Head and Neck Squamous Cell Carcinoma (HNSCC)

Krithika Shenoy¹, Mena Mansour²

¹Barnes-Jewish Hospital/Washington University, St. Louis, MO, ²Washington University Medical Center, St. Louis, MO

Disclosures: Krithika Shenoy: None; Mena Mansour: None

Background: HR-HPV related HNSCC have favorable prognosis compared to HR-HPV negative HNSCC. The College of American Pathologists advocate the use of p16 IHC as a surrogate for HR-HPV with cutoff of >70% nuclear and cytoplasmic staining of moderate to strong intensity for a positive result on surgical specimens. FNA is used as a first-line diagnostic tool for sampling metastatic lesions and may be the only specimen available for testing. In this study, we assess the performance of p16 IHC on CB and derive a cutoff for positive result from FNA of metastatic HNSCC.

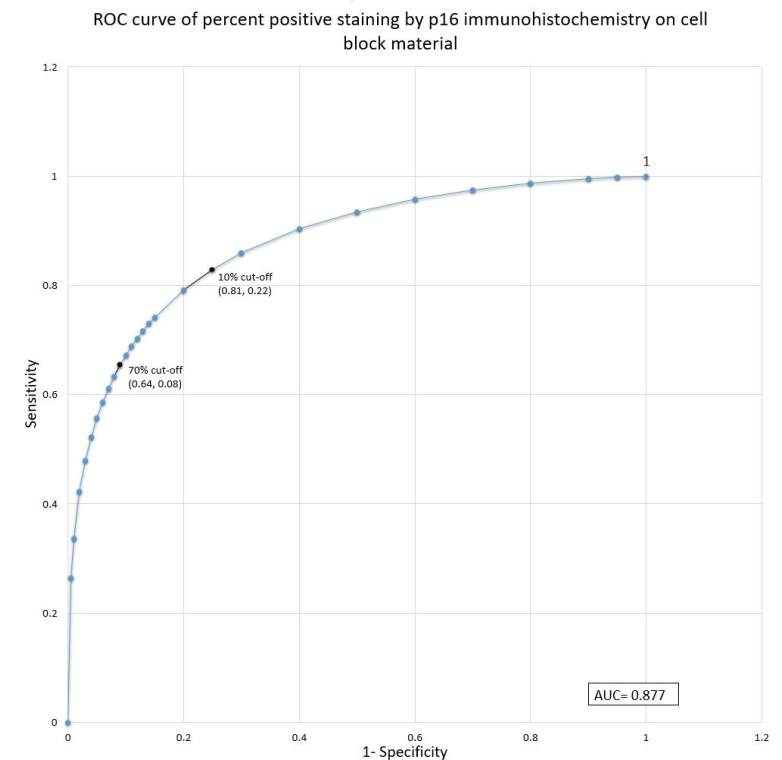
Design: FNA specimens (2016-2020) of metastatic HNSCC with p16 IHC on CB were identified. The p16 stained CB was assessed for distribution of cells (single cells vs. clusters), number of clusters (single; multiple), cluster size (small with < 50 cells; large with > 50 cells), pattern of staining (nuclear; cytoplasmic; both), percent positive staining (in increments of 5% when <15%; increments of 10% when >15%) and intensity of staining (weak; intermediate; strong). Receiver operator characteristic curve analysis was used to assess performance of p16 IHC on CB in correlation with p16 IHC on the corresponding surgical pathology specimens.

Results: Seventy-three cases were identified and included metastatic lesions with primaries in oropharynx (63 cases), nasopharynx (1 case) and unknown primary site (8 cases). Mean age was 59.53 years (range: 34-79 years); 67 were men. There were 60 cases where malignant cells were distributed as cohesive clusters (large clusters- 43; small clusters- 16), 11 cases were exclusively composed of single cells and 2 cases keratinous debris only (Table 1). After rereview of p16 IHC on cell block using our criteria, 8 equivocal cases were reclassified as positive and one equivocal as negative. One positive case was reclassified as negative and one negative case as positive. ROC curve showed a cut-off of 10% staining to have a sensitivity of 81.5%, and specificity of 77.1%. Raising the cut-off to 70% reduced the sensitivity to 64.9% and increased the specificity to 91.3% (Figure 1). There were 10 false negative cases (5 cases with single cells only, 1 case with keratinous debris, 3 cases with ≥1 small clusters, 1 case with > 2 large clusters) and two false positive cases (1 case with > 2 large clusters and 70% strong intensity staining; 1 case with single cells only and weak intensity staining in 70% of cells).

Table 1: Cell block characteristics in correlation with percent positivity of p16 immunohistochemistry on cell block

Cell block characteristics (N = 73)	p16 immunohistochemistry percent positive staining on cell block on review			
	0% (n)	1-10% (n)	10-70% (n)	>70% (n)
Cell distribution ($p = 0.016$)				
Clusters	10	2	9	39
Single cells	5	1	4	1
Keratinous debris	1	1	0	0
Cluster size ($p < 0.001$)				
Large	3	0	5	35
Small	7	1	4	4
No clusters	6	3	4	1
Number of clusters ($p = 0.002$)				
Numerous	8	1	8	37
Single	2	0	1	2
No clusters	6	3	4	1
Stain intensity ($p < 0.001$)				
Strong	0	4	10	38
Intermediate	0	0	2	2
Weak	0	0	1	0
No staining	16	0	0	0

Figure 1 - 276



Conclusions: A lower cutoff value for p16 IHC on CB may be required to attain optimal sensitivity and reduce false negative rate compared to surgical specimens.

277 Assessment of the Diagnostic Accuracy of Cytology in Pleomorphic Adenoma: A Retrospective Single Institutional Study

Hardik Sonani¹, Imran Ajmal¹, Varsha Manucha¹
¹University of Mississippi Medical Center, Jackson, MS

Disclosures: Hardik Sonani: None; Imran Ajmal: None; Varsha Manucha: None

Background: Pleomorphic adenomas (PA) account for 70-80% of benign salivary gland tumors (SGT) and affect the superficial lobe of the parotid gland, making them also the most common SGT diagnosed on cytology. As per the Milan system for reporting salivary gland cytology (MSRSGC), PA is categorized in the group of “benign neoplasm”, with a proposed risk of malignancy (ROM) of <5%. The aim of this study was to first, evaluate the ROM and diagnostic accuracy of PA diagnosed on cytology, and second, to determine the MSRSGC categorization of PAs diagnosed on histology.

Design: The laboratory information system was searched over a period of 3 years (2017-2020) for all the cases that were diagnosed as PA on fine-needle aspiration (FNA) and a separate search for cases that were diagnosed as PA on histology. The surgical follow-up of FNA cases and the preceding cytology of resected PA were recorded. Cases that had both cytology and surgical pathology were included in the study. The age, gender, and site of all the PAs diagnosed on surgical resection were noted. The ROM, risk of neoplasm (RON), and diagnostic accuracy PA was calculated (Figure 1).

Results: There were 74 PA diagnosed on cytology, of which 53 cases had a surgical follow-up. There were 64 cases diagnosed as PA on surgical resection, of which 56 had preceding cytology. In the entire cohort, there were 63 cases with paired cytology-histology. The average age was 51.5 years (range, 12-86); male: female ratio (0.65:1). The most common site was parotid (76%), followed by submandibular (19%) and other sites (5%) including hard palate, parapharyngeal, and neck. Of the 63 paired cases, 46 PA were accurately diagnosed on cytology, while 8 PA were placed in SUMP category and 2 were non-diagnostic. There were 7 additional cases that were diagnosed as PA on cytology, but the surgical resection showed 3 benign neoplasms other than PA, 3

malignant, and 1 non-neoplastic (Figure 2). All lacked fibrillary matrix as a diagnostic component. The RON/ROM for diagnosis of PA on cytology is 98.1%/5.6%. The diagnostic accuracy is 82.1%.

Figure 1 - 277

$$\text{RON (\%)} = \frac{\text{Number of neoplastic cases (52)}}{\text{Total number of cases (53)}} \times 100 = 98.1\%$$

$$\text{ROM (\%)} = \frac{\text{Number of malignant cases (3)}}{\text{Total number of cases (53)}} \times 100 = 5.66\%$$

$$\text{Accuracy (\%)} = \frac{\text{Number of cases with a definitive diagnosis on FNA (46)}}{\text{Number of cases with a matching diagnosis on surgical resection (56)}} = 82.1\%$$

Figure 1: Method of calculation – RON, ROM, and Diagnostic Accuracy

Figure 2 – 277

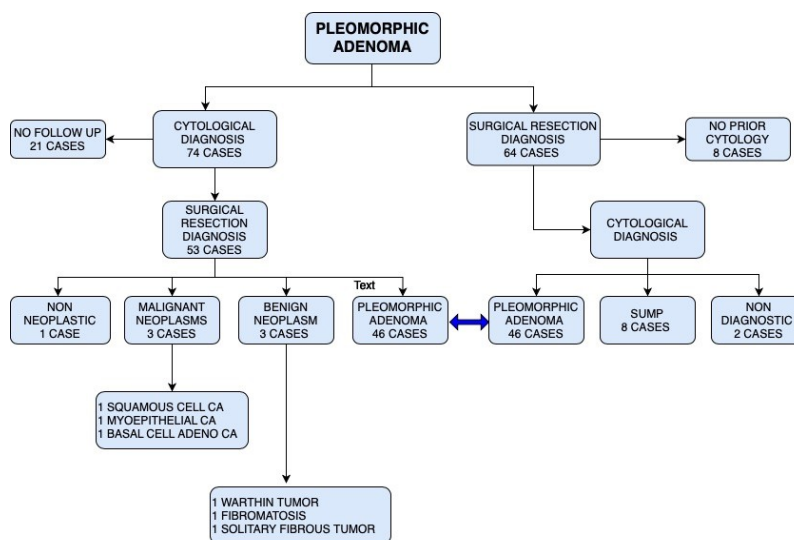


Figure 2: Study design and outcomes

Conclusions: As proposed by MSRSGC, the diagnosis of PA on cytology is highly predictive (98.1%) of a neoplasm but also carries a small risk of malignancy (5.6%). The diagnostic accuracy of 82.1% and 14% probability of categorizing a PA as SUMP, highlights the diagnostic challenge that overlapping cytologic features in salivary gland FNAs present. In the absence of a fibrillary matrix, a diagnosis of PA should be made with caution.

278 The Risk of Malignancy Assessment of the International System for Reporting Serous Fluid Cytopathology in Community Hospital Setting

Tong Sun¹, Minhua Wang¹, He (Peter) Wang²

¹Yale School of Medicine, New Haven, CT, ²Yale University School of Medicine, New Haven, CT

Disclosures: Tong Sun: None; Minhua Wang: None; He (Peter) Wang: None

Background: The International System for Reporting Serous Fluid Cytopathology (ISRCFC) recently was published as a tiered structure to provide standard reporting terminology for serous fluid. Though value of this system has been reported from a few large academic centers, the impact of the ISRCFC in community practice has not been fully explored. Herein, we applied the ISRCFC on reporting peritoneal and pleural fluid in a large retrospective cohort in community hospital setting.

Design: With IRB approval, total 446 peritoneal effusion and 299 pleural fluid specimens from 558 patients in 3 community hospitals over 12-month period were reviewed and reclassified according to the ISRCFC. The patients' demographic characters and follow up information have been summarized in Table 1. Risk of Malignancy (ROM) were calculated based on confirmation of

malignancy by previous and/or subsequent fluid and/or tissue biopsy specimen and/or clinical follow-up from the same anatomic location. Median clinical follow up time was 18 months.

Results: Among peritoneal effusion cases, 14 (3.9%) were nondiagnostic (ND); 277 (77.2%) were negative for malignancy (NFM); 16 (4.5%) were atypia of undetermined significance (AUS); 6 (1.7 %) were suspicious for malignancy (SFM) and 46 (12.8%) were malignant (MAL) after reclassification. Similar category distribution was observed in pleural effusion, there were 12 (5.5%) ND, 168 (77.1%) NFM, 9 (4.1%) AUS, 2 (0.9%) SFM and 27 (12.4%) MAL pleural cases. Calculated ROM was 0% for ND, 1.8% for NFM, 37.5% for AUS, 83.3% for SFM and 100% for MAL in peritoneal cases and 8.3% for ND, 1.2% for NFM, 44.4% for AUS, 100% for pleural cases (Table 2). With a definite diagnosis of absence or presence of malignancy considered, peritoneal fluid cytology had a sensitivity and specificity of 90 % and 100 %, and pleural fluid cytology had a sensitivity and specificity of 93 % and 100 %, respectively.

Table 1. Patients Demographics and Follow Up Information

Variables			
Age	Median, range	68 (18 – 97) years	
Sex	Male	320	(57 %)
	Female	238	(43 %)
Self-reported Ethnicity	Caucasian	394	(71 %)
	African American	98	(17 %)
	Hispanic and other	55	(10 %)
	Asian	7	(1 %)
	Refused	5	(1 %)
Follow-up status	Histological follow up	175	(31 %)
	Ancillary study use	81	(15 %)
	Clinical follow up	503	(90 %)
Total No.		558	(100 %)

Figure 1 - 278

Table 2. Diagnostic Category and Risk of Malignancy Assessment of Serous Effusion Specimen

	Peritoneal fluid (ascites)			Pleural fluid		
	Case No.	Malignant case No.	ROM %	Case No.	Malignant case No.	ROM %
No. of specimen	446			299		
No. of patients*	359 (100%)			218 (100 %)		
Diagnostic category #						
Non-diagnostic	14 (3.9 %)	0	0 %	12 (5.5 %)	1	8.3 %
Negative for Malignancy	277 (77.2 %)	5	1.8 %	168 (77.1 %)	2	1.2 %
Atypia of Undetermined Significance	16 (4.5 %)	6	37.5 %	9 (4.1 %)	4	44.4 %
Suspicious for Malignancy	6 (1.7 %)	5	83.3 %	2 (0.9 %)	2	100 %
Positive for malignancy	46 (12.8 %)	46	100 %	27 (12.4 %)	27	100 %

* Nineteen patients have both pleural and peritoneal fluid collected.

If discrepancy exists in repeated specimen collected from the same patient, the highest diagnostic category will be counted.

Conclusions: To our best knowledge, it is the first large scale study for assessing ISRCFC value in a community practice setting. Compared with literatures from large academic institutes, the ROM of ISRCFC categories was comparable for SFM and MAL in both settings; with significantly lower ROM in ND, NFM and AUS categories in community hospital setting (All 3 categories *P* value for Fisher’s two-sided exact tests < 0.001). Overall sensitivity of serous fluid cytology in community practice setting was significantly higher than that reported in academic setting, with similar excellent specificity.

279 A Heterogeneous Lymphoid Population in Fine Needle Aspiration Specimens is not Synonymous with Reactive/Benign Lymphoid Hyperplasia

Hamza Tariq¹, Ji-Weon Park²

¹Northwestern University Feinberg School of Medicine, Chicago, IL, ²Rush University Medical Center, Chicago, IL

Disclosures: Hamza Tariq: None; Ji-Weon Park: None

Background: Although many pathologists recognize the limitations of Fine Needle Aspiration (FNA) in suspected cases of lymphoma, it remains a commonly used diagnostic test in clinical practice. A “heterogeneous lymphoid population” in FNA is commonly considered by clinicians as being equivalent to a benign etiology, however, many lymphomas by their very nature and biology are heterogeneous. The aim of this study is to highlight that FNA is a suboptimal test for the initial diagnosis and subclassification of lymphoma and to stress that a heterogeneous morphology in FNA does not exclude lymphoma.

Design: We retrospectively analyzed lymphomas that showed a heterogeneous morphology in preceding FNAs suggesting a benign process. Clinical findings, FNA thin preps, cellblocks, immunohistochemistry (IHC), and flow cytometric results were examined.

Results: A total of 10 cases were identified (Table1) including 4 low-grade follicular lymphomas (FL); 3 classic Hodgkin lymphomas (CHL); and 1 case each of marginal zone lymphoma (MZL), chronic lymphocytic leukemia (CLL), and T-cell rich large B-cell lymphoma (TCRBCL). Previous FNAs showed heterogeneous lymphocytes in all 10 cases. Additionally, 2 CHL cases showed non-necrotizing granulomas (Fig1), 1 MZL of submandibular gland showed benign acinar cells suggesting intrasalivary lymph node vs chronic sialadenitis (Fig2), and 1 TCRBCL showed rare large cells. Cellblocks were unsatisfactory for definitive diagnosis in all except 1 case of CHL that showed rare CD30+ large cells. Concurrent flow cytometry was ordered in only 1 case of FL and showed a CD10+ kappa-restricted B-cell population. All 10 cases required a core/excisional biopsy for final diagnosis and accurate classification.

Case #	Age	Gender (M/F)	Site of biopsy	FNA thin prep findings	Cell block findings	Concurrent flow cytometry (Yes/No)	Final diagnosis on core/excisional biopsy
1	66	F	Neck Level II lymph node	Non-necrotizing granulomas in a background of heterogeneous lymphoid cells	Non-necrotizing granulomas and heterogeneous lymphoid cells. AFB, Fite, and GMS special stains negative for organisms	No	Classic Hodgkin Lymphoma with marked granulomatous reaction, nodular sclerosis subtype
2	63	F	Submandibular gland	Heterogeneous population of lymphoid cells and rare acinar cells, suggestive of chronic sialadenitis vs benign intra salivary lymph node	Heterogeneous lymphocytes and rare benign acinar cells.	No	Extranodal marginal zone lymphoma of mucosa-associated lymphoid tissue (MALT)
3	50	M	Neck Level V lymph node	Heterogeneous population of lymphoid cells. Assessment limited by crush artifact and poor preservation	Too few cells for adequate assessment	No	Follicular Lymphoma, grade 1-2
4	54	M	Neck Level V lymph node	Heterogeneous population of lymphoid cells with a necrotic background	Too few cells for adequate assessment	No	Classic Hodgkin Lymphoma, mixed cellularity subtype
5	62	F	Neck Level II lymph node	Overall heterogeneous population of lymphoid cells but a slight predominance of small forms	Too few cells for adequate assessment	No	Atypical CD5+ B cell population, consistent with Chronic lymphocytic leukemia (CLL)/Small lymphocytic lymphoma (SLL)
6	58	M	Neck Level V lymph node	Heterogeneous population of lymphoid cells and scattered histiocytes	Heterogeneous lymphocytes and histiocytes	No	Follicular Lymphoma, grade 1-2
7	71	M	Neck Level Ib lymph node	Relatively heterogeneous population of lymphoid cells with a few larger cells with open chromatin	Heterogeneous lymphocytes with more CD20 than CD3 positive cells	No	Follicular Lymphoma, grade 1-2
8	57	M	Mesenteric lymph node	Heterogeneous population of lymphoid cells	Essentially acellular	Yes. Positive for kappa-restricted B cells	Follicular Lymphoma, grade 1-2
9	69	F	Neck Level V lymph node	Non-caseating granulomas in a background of heterogeneous lymphoid cells	Rare large atypical cells that are CD30+, CD20-, CD3-. Non-specific staining with PAX5 & CD10	No	Classic Hodgkin Lymphoma with marked granulomatous reaction, nodular sclerosis subtype
10	45	F	Neck Level V lymph node	Heterogeneous population of lymphoid cells with necrotic debris and rare scattered larger lymphocytes with prominent nucleoli	Scant material showing scattered heterogeneous CD3+ T-cells and CD20+ B-cells. No large cells seen	No	T-cell rich large B-cell Lymphoma

Figure 1 - 279

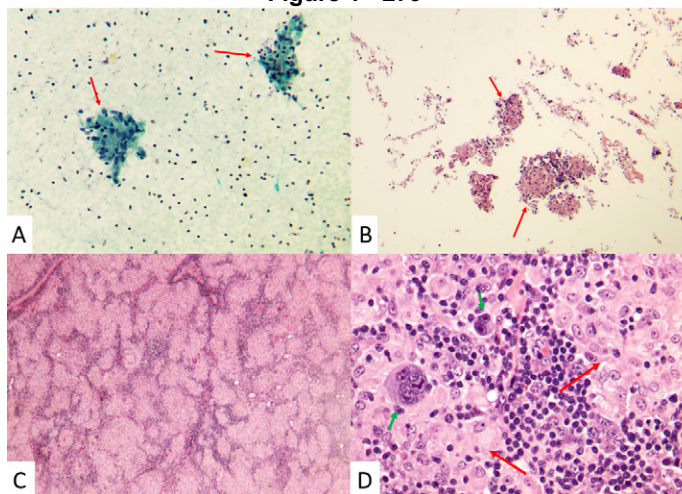
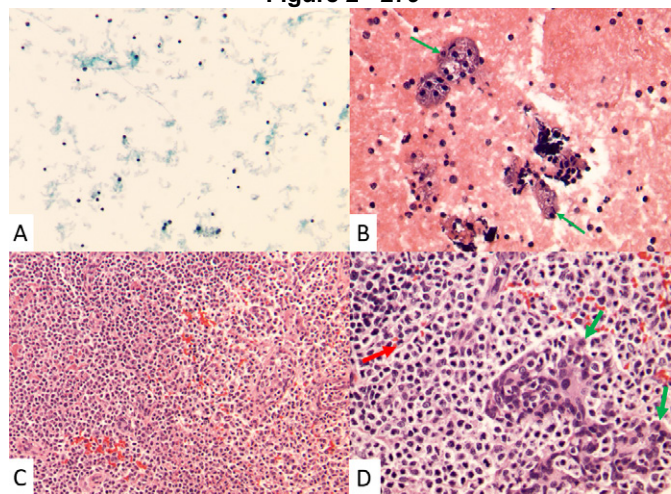


Figure 2 - 279



Conclusions: While heterogeneous lymphocytes in FNA specimens are suggestive of a benign etiology, many lymphomas too are characteristically heterogeneous. These include CHL, NLPHL, low-grade B & T NHLs, and TC/HRLBCL. FNA in suspected cases of lymphoma can be helpful in the initial triage of the specimen, however, it is unable to provide precise diagnosis, grading, classification, and therapeutic guidance. This is due to limitations of FNA that include but are not limited to a significant morphologic overlap between benign and malignant entities on FNA, sampling error, lack of architecture, lack of adequate material for flow cytometry, and inadequacy of cellblocks for IHCs. When evaluating these FNA specimens, we recommend adding a comment to make the clinicians aware of these limitations.

280 Fine Needle Aspiration of Intramammary Lymph Nodes: A Clinical/Cytologic Review

Hamza Tariq¹, Lei Yan², Indu Agarwal², Vijaya Reddy², Paolo Gattuso², Lin Cheng²

¹Northwestern University Feinberg School of Medicine, Chicago, IL, ²Rush University Medical Center, Chicago, IL

Disclosures: Hamza Tariq: None; Lei Yan: None; Indu Agarwal: None; Vijaya Reddy: None; Paolo Gattuso: None; Lin Cheng: None

Background: Intramammary lymph nodes (IMLNs) can occur in any quadrant of the breast and can be detected by palpation or radiographic examination. Recognizing and sampling them may play an important role especially in the clinical management of patients with breast carcinoma. We undertook a retrospective study to evaluate the clinical utility of fine needle aspiration (FNA) in assessing IMLNs.

Design: We performed a search in our database for all IMLN FNA cytology cases from January 2005 to August 2021. The cytologic findings and clinical data were reviewed.

Results: A total of 149 cases were reviewed. All patients were female, ranging in age from 27 to 82 years. 17/149 (11.4%) patients had synchronous breast tumors at the time of the FNA [13 invasive ductal carcinomas (IDC), 1 ductal carcinoma in situ (DCIS), and 3 fibroadenomas]. 16/149 (10.7%) patients had a prior history of breast tumors [9 IDCs, 5 DCIS, 1 lobular carcinoma in situ (LCIS), and 1 fibroadenoma]. Only 2/149 (1.3%) patients had a prior history of lymphoma.

In patients with synchronous IDC, FNA of IMLNs was positive for metastatic carcinoma in 4/13 (30.7%) cases. While in patients with a past history of IDC, all IMLNs were negative for metastatic carcinoma (0/9, 0%). The IMLNs in the remaining 13 patients (6 DCIS, 1 LCIS, 2 lymphomas, and 4 fibroadenomas) were all negative for malignancy. 2/149 cases (1.3%) showed granulomatous lymphadenitis. None of the IMLNs with benign FNA results were surgically excised; while 3/4 IMLNs with malignant FNA results were excised and the diagnosis was confirmed on histological examination.

Conclusions: IMLNs are commonly associated with synchronous/metachronous breast tumors (33/149, 22.1%). Although IMLN FNAs are positive for malignancy in only 2.7% (4/149) of all patients, the incidence of positive IMLN FNA in patients with synchronous invasive breast carcinoma can be as high as 30.7% (4/13). FNA of IMLNs in conjunction with clinical presentation and

radiologic findings is a highly sensitive and specific technique that allows to triage patients for appropriate clinical management and avoids additional unnecessary surgical procedures.

281 Immunohistochemistry for SS18-SSX and SSX is Highly Sensitive and Specific for Synovial Sarcoma in Cytology and Core Needle Biopsy Specimens

Emily Towery¹, Jeffrey Mito¹, Jason Hornick², Vickie Jo²

¹Brigham and Women's Hospital, Boston, MA, ²Brigham and Women's Hospital, Harvard Medical School, Boston, MA

Disclosures: Emily Towery: None; Jeffrey Mito: None; Jason Hornick: *Consultant*, Aadi Biosciences; *Consultant*, TRACON Pharmaceuticals; Vickie Jo: *Stock Ownership*, Merck and Co

Background: The diagnosis of synovial sarcoma (SS) is challenging on cytology and core needle biopsy (CNB). Confirmation of SS18-SSX fusions is diagnostic; however, molecular genetic testing is costly and not widely available and conventional TLE1 immunohistochemistry (IHC) is only moderately specific for SS. Recent studies have shown that IHC using both an SS18-SSX fusion-specific antibody and an SSX C-terminus antibody is highly sensitive and specific for SS on resection specimens. We evaluated the diagnostic utility of these markers in distinguishing SS from other spindle cell neoplasms on cytology and CNB samples.

Design: In total, 83 cases of cytology cell blocks (n=33) and CNBs (n=50) of spindle cell neoplasms were investigated. Tumor types included: SS (12: 3 biphasic; 4 monophasic; 5 poorly differentiated, including 1 post-treatment), malignant peripheral nerve sheath tumor (11), dedifferentiated liposarcoma (12), cellular schwannoma (1), solitary fibrous tumor (6), leiomyosarcoma (14), sarcomatoid carcinoma (4), gastrointestinal stromal tumor (12), unclassified spindle cell sarcoma (5), spindle cell/sclerosing rhabdomyosarcoma (3), and fibrosarcomatous variant of dermatofibrosarcoma protuberans (3). For 6 SS cases, SS18 rearrangement was confirmed by fluorescence in situ hybridization (5) or karyotype analysis (1). IHC for SS18-SSX and SSX was performed, and nuclear staining was scored for extent (0; 1+, 1-25%; 2+, 26-75%; 3+, >75%) and intensity (weak, moderate, strong).

Results: Nuclear SS18-SSX staining was present in all cases of SS (4 cell blocks, 8 CNBs). Positive cases showed weak (2), moderate (3), or strong (7) intensity of staining, with 3+ (7) or 2+ (5) extent. SSX IHC on 9 SS cases showed weak (1), moderate (2), or strong (6) intensity, with 3+ (5) or 2+ (4) extent. For SS cases with both SS18-SSX and SSX IHC, staining extent was concordant in all 9 and intensity was concordant in 7. All other tumor types were negative for SS18-SSX IHC (0/71). While most mimics were negative for SSX IHC, 3 unclassified spindle cell sarcomas showed 1+ weak (1) or moderate (2) staining (3/39).

Conclusions: IHC using the SS18-SSX fusion-specific antibody has remarkably high sensitivity (100%) and specificity (100%) for SS in cytology specimens and CNB; SSX IHC shows similar findings (sensitivity, 100%; specificity, 92.3%). These are reliable diagnostic markers in small biopsy specimens and may serve as surrogates for molecular genetic testing, especially in cases with limited material.

282 Is Histologic Confirmation Underestimating the Absolute Risk of Malignancy Estimates of Bone and Soft Tissue Tumors Involving Serous Cavities?

Swikrity Upadhyay Baskota¹, Pooja Srivastava², Daniel Martinez Coconubo², Samer Khader³

¹Columbia University Irving Medical Center, New York, NY, ²University of Pittsburgh Medical Center, Pittsburgh, PA, ³University of Pittsburgh Medical Center Presbyterian Shadyside, Pittsburgh, PA

Disclosures: Swikrity Upadhyay Baskota: None; Pooja Srivastava: None; Daniel Martinez Coconubo: None; Samer Khader: None

Background: Malignant bone and soft tissue (BST) tumors are aggressive tumors that rarely involve serous cavity fluids (SCF), and when they do, it usually happens in the setting of widespread disease. Oftentimes, it is difficult to achieve histologic confirmation of involvement of SCF because of patients' intolerance to an invasive procedure, and the management decisions are mostly based on clinical and radiologic findings in addition to SCF cytologic evaluation. We conducted this study to calculate the risk of malignancy (ROM) of cytologic diagnosis of "atypical" and higher categories in cases with or without histologic confirmation based on clinical, and radiologic findings.

Design: A query of pathology database from 2016-2020 yielded 35 cases with a history of BST malignancy and clinical suspicion of SCF involvement. Patient demographics, anatomic site, volume collected, clinical and radiologic impression, ancillary studies, the presence or absence of histologic confirmation, the presence or absence of widespread disease (defined as 1 or more body site involvement other than SCF), and follow-up status were documented; also, ROM was calculated.

Results: There were 29 pleural, 5 peritoneal and 1 pericardial effusion case. Average volume submitted for evaluation was 114 mL (range 1mL-1400mL). Ancillary studies were performed on 24 (68.6%) cases. 21 (60%) cases were atypical, 7 (20%) were suspicious and 7 (20%) were positive for BST malignancy. The most common sarcoma was leiomyosarcoma 14.2% (N=5), followed by pleomorphic sarcoma and liposarcoma 11.4% (N=4) each. One case was lost to follow-up. 12 (34.3%) cases had histologic confirmation of involvement of SCF. Only 2 (5.7%) cases were clinically and radiologically considered benign/reactive. 26 (82.9%) cases had a widespread disease. 26 (82.9%) patients were deceased at the time of data collection (Table 1). The absolute ROM with histologic confirmation was 34.3%. The calculated ROM with integrated clinical, radiologic and cytologic findings was 97% (33/34).

Table 1: Clinical Burden, Radiologic, Cytologic and Histologic Findings and Follow-Up of The Bone and Soft-Tissue Malignancies Involving Serous Cavity Fluids (SCF)

Diagnoses	Total	Cytology	Clinically Malignant	Radiologically Malignant	Histologic Confirmation	Follow-up	Widespread Disease*
Leiomyosarcoma (including de-differentiated)	5 (14.2%)	1 Atypical	Y	Y	N/A*	Alive	Y
		2 Atypical	Y	Y	N/A (1) Y (1)	Alive (1), Deceased (1)	Y (1) N (1)
		1 Suspicious	Y	Y	Y	Deceased	Y
		1 Positive	Y	Y	Y	Alive	Y
Pleomorphic/ High-Grade Sarcoma	4 (11.4%)	2 Atypical	Y (2)	Y (2)	Y (2)	Deceased (2)	Y (2)
		1 Suspicious	Y	Y	N/A	Deceased	Y
		1 Positive	Y	Y	Y	Deceased	N
Liposarcoma (Including de-differentiated)	4 (11.4%)	3 Suspicious	Y (3)	Y (3)	Y (2) N/A (1)	Deceased (3)	Y (3)
		1 Atypical	Y	Y	N/A	Deceased	Y
Epithelioid Hemangioendothelioma	3 (8.5%)	2 Atypical	Y (2)	Y (2)	N/A (2)	Deceased (2)	Y (2)
		1 Positive	Y	Y	N/A	Deceased	Y
Chondrosarcoma (including de-differentiated)	3 (8.5%)	2 Atypical	Y (2)	Y (2)	N/A (2)	Deceased (1), Alive (1)	Y (2)
		1 Positive	Y	Y	N/A	Deceased	Y
Ewing's Sarcoma	3 (8.5%)	1 Atypical	N	N	N/A	Deceased	N
		1 Atypical	Y	Y	N/A	Deceased	N
		1 Suspicious	Y	Y	N/A	Deceased	N
Angiosarcoma	2 (5.7%)	1 Atypical	Y	Y	N/A	Deceased	N
		1 Atypical	N	N	N/A	LTFU	N/A
Extraskeletal Osteosarcoma	2 (5.7%)	2 Atypical	Y (2)	Y (2)	N/A (1) Y (1)	Deceased (2)	Y (2)
Malignant Solitary Fibrous tumor	1 (2.9%)	Atypical	Y	Y	Y	Deceased	Y
Desmoplastic Small Round cell tumor	1 (2.9%)	Atypical	Y	Y	N/A	Deceased	Y
Myxofibrosarcoma	1 (2.9%)	Atypical	Y	Y	N/A	Deceased	Y
Pleomorphic Rhabdomyosarcoma	1 (2.9%)	Suspicious	Y	Y	Y	Deceased	N
Clear Cell Sarcoma	1 (2.9%)	Positive	Y	Y	N/A	Deceased	Y
Synovial Sarcoma	1 (2.9%)	Atypical	Y	Y	N/A	Deceased	Y
High-Grade Endometrial Stromal Sarcoma	1 (2.9%)	Atypical	Y	Y	N/A	Deceased	Y
Pulmonary Artery Intimal Sarcoma	1 (2.9%)	Atypical	Y	Y	N/A	Alive	N
Others	1 (2.9%)	Positive	Y	Y	Y	Deceased	Y
Total	35 (100.1%)	21: Atypical; 7 Suspicious 7: Positive	Y: 33, N: 2	Y: 33, N: 2	N/A: 23, Y: 12	Deceased (29), Alive (5), LTFU (1)	Y : 26, N: 8, N/A: 1

*Defined as >1 body site involvement other than SCF
 **Concurrent positive cytology sample
 Abbreviations Used: N: No, Y: Yes, N/A: Not available, LTFU: Lost to Follow-Up, (:): Number of cases

Conclusions: Our study demonstrates that ROM estimation by using histologic confirmation for aggressive tumors like BST malignancies might underestimate the true risk of these malignancies involving SCF. Our findings support international system for serous fluid cytopathology (TIS) recommendation of incorporating clinical and radiologic findings for the assessment of true ROM for aggressive tumors, where histologic confirmation is often not possible due to the clinical burden of disease.

283 An Institutional Clinicopathologic Correlation of Fine Needle Aspiration (FNA) and Surgical Resection of Thyroid Nodules with *DICER1* Mutation

Charitha Vadlamudi¹, Osman Yilmaz¹, Sandra Cerda²

¹Boston Medical Center, Boston, MA, ²Boston University Medical Center, Boston, MA

Disclosures: Charitha Vadlamudi: None; Osman Yilmaz: None; Sandra Cerda: None

Background: *DICER1* mutations are considered innocuous in thyroid nodules. Recent studies, however, demonstrated a relationship of *DICER1* mutations with papillary and follicular carcinoma (on limited samples sizes) raising awareness of a more ominous association. We interrogate if there is distinctive 1)cytologic and morphologic features in FNA and resections, 2)clinical and demographic features, and 3) association with malignancy.

Design: 8 FNAs of thyroid nodules with *DICER1* mutation were identified (2014-2021) at our institution. 3 cases (one patient with 2 nodules) had corresponding surgical resection. Clinical and demographic features were reviewed. Cytologic evaluation included colloid assessment, cellularity, architecture, and nuclear features. Histologic evaluation also included capsule assessment, and degenerative changes.

Results: All patients were females between 28-42 years. 5 patients (5/7) were Hispanic. Of the 8 FNAs 7 were diagnosed Bethesda 3 and 1 Bethesda 4.

Cytology: 6 cases (6/8) had marked cellularity, all cases had mixed micro/macrofollicular patterns and 2 cases demonstrated tridimensional structures (2/8), and 4 cases (4/8) had abundant chunky colloid (Fig 1). 2 cases showed banal nuclear features (2/8), while 6 cases showed focal nuclear atypia including: nuclear overlap (6/8), nuclear enlargement (3/8), and irregular nuclear membranes (2/8). **Histology:** All cases (4/4) were benign encapsulated follicular adenomas. The capsular thickness ranged from 0.2 mm to 1.5 mm. All specimens demonstrated a macrofollicular pattern of growth with 3 of 4 demonstrating frequent papillary infoldings (Fig 2). Degenerative changes, including fibrosis and inflammation, were present in all cases. No nuclear atypia seen in all cases.

All cases showed *DICER1* mutation by Thyroseq V3 Genomic Classifier. 2 cases showed an identical mutation.

Figure 1 - 283

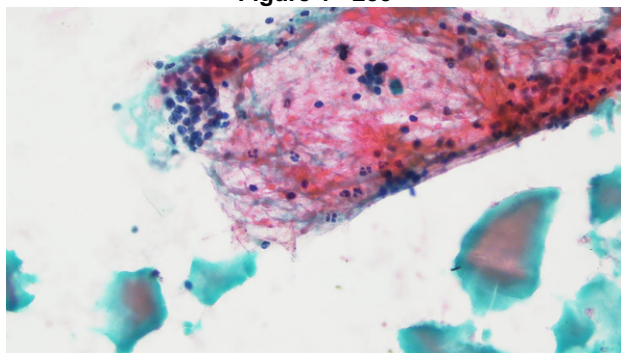
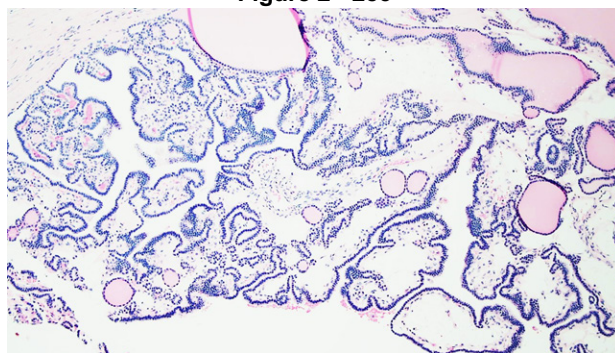


Figure 2 - 283



Conclusions: Cytology showed a spectrum of characteristics. Curiously, one observed pattern exhibited abundant colloid, macro/microfollicles with minimal atypia; this pattern could be categorized as benign suggesting that *DICER1* mutated tumors is underdiagnosed. Histologic evaluation revealed a macrofollicular pattern with occasional papillary infoldings and degenerative changes that could be misinterpreted as nodular hyperplasia or post FNA changes. As seen in prior studies, all patients were female and, in our cohort, 5 of 7 were of Hispanic decent; unlike prior studies, all examined patients have stable follow up imaging or benign final pathology.

284 Diagnostic Discrepancies in the Clinical Workup of Follicular Lymphoma Using Small Volume Biopsies: A Multi-Institutional Collaborative Study

Ashley Volaric¹, Oscar Lin², Sara Zadeh¹, Srishti Gupta³, Daniel Reed⁴, Megan Fitzpatrick⁵, Amy Ly⁵, Robert Hasserjian⁶, Ronald Balassanian⁷, Annabel Frank⁷, Steven Long⁷, Roberto Ruiz-Cordero⁷, Linlin Wang⁷, Kwun Wah Wen⁷, Yi Xie⁷, Joshua Menke⁸, Yasodha Natkunam¹, Dita Gratzinger⁹

¹Stanford Medicine/Stanford University, Stanford, CA, ²Memorial Sloan Kettering Cancer Center, New York, NY, ³University of Virginia, Charlottesville, VA, ⁴Wake Forest Baptist Health, Winston-Salem, NC, ⁵Massachusetts General Hospital, Boston, MA, ⁶Massachusetts General Hospital, Harvard Medical School, Boston, MA, ⁷University of California, San Francisco, San Francisco, CA, ⁸Stanford Health Care, Stanford, CA, ⁹Stanford University Medical Center, Stanford, CA

Disclosures: Ashley Volaric: None; Oscar Lin: *Consultant*, Hologic; *Consultant*, Jansen; Sara Zadeh: None; Srishti Gupta: None; Daniel Reed: None; Megan Fitzpatrick: None; Amy Ly: None; Robert Hasserjian: None; Ronald Balassanian: None; Annabel Frank: None; Steven Long: None; Roberto Ruiz-Cordero: None; Linlin Wang: None; Kwun Wah Wen: None; Yi Xie: None; Joshua Menke: None; Yasodha Natkunam: None; Dita Gratzinger: None

Background: Despite the increasing use of small volume biopsy (SVB) in the clinical workup of hematolymphoid neoplasms, most studies to date have been from single institutions across a range of diagnoses. Through a multi-institutional collaboration, we evaluated all consecutive SVB of follicular lymphoma cases over a 5-year period to determine the rate and type of diagnostic discrepancies.

Design: A total of 676 biopsy workups of follicular lymphoma from six academic institutions were analyzed (1/1/2012-12/31/2016). The initial biopsy in all cases was an SVB, defined as fine needle aspiration (FNA) and/or cell block or core biopsy performed for clinical indications of initial diagnosis, ruling out transformation, or ruling out recurrent disease. Within this cohort, 182 biopsy workups required a subsequent biopsy (SVB or surgical biopsy) performed less than 3 months from initial biopsy and to answer the same clinical question. The subsequent biopsy served as the gold standard for comparison. Data obtained from electronic medical records at each institution were entered into a shared REDCap database with IRB approval.

Results: Across all clinical indications, there were no cases in which a lymphoma diagnosis was downgraded on subsequent biopsy. The most common outcome of a subsequent biopsy as part of the same clinical workup was a more specific diagnosis (61%), followed by cases resulting in complete agreement with the SVB (13%) (Table 1). Initial biopsies consisted of 41% FNA + cell block (74/182), 37% FNA only (68/182) and 22% core biopsy +/- FNA (40/182). In contrast, 73% of subsequent diagnostic workups consisted of surgical (incisional/excisional) biopsies (133/182) (Figure 1). Lack of flow cytometry at initial biopsy was associated with benign or non-diagnostic diagnoses (Figure 2).

Table 1. Diagnostic Discrepancies in Clinical Workup of Follicular Lymphoma.

	Initial Diagnosis	Rule Out Recurrence	Rule Out Transformation	All Workups
<i>Discrepancy Category</i>				
Benign to Malignant	13/131 (10%)	2/25 (8%)	2/26 (8%)	17/182 (9%)
Non-diagnostic to Diagnostic	11/131 (8%)	3/25 (12%)	7/26 (27%)	21/182 (12%)
Malignant to Benign	0	0	0	0
Change in Lymphoma Diagnosis	1/131 (1%)	0	3/26 (12%)	4/182 (2%)
Change in Lymphoma Grade	2/131 (2%)	1/25 (4%)	2/26 (8%)	5/182 (3%)
More Specific Diagnosis	92/131 (70%)	13/25 (52%)	6/26 (23%)	111/182 (61%)
Agreement (Between Initial and Final Diagnoses)	12/131 (9%)	6/25 (24%)	6/26 (23%)	24/182 (13%)
Total	131	25	26	182

Figure 1 - 284

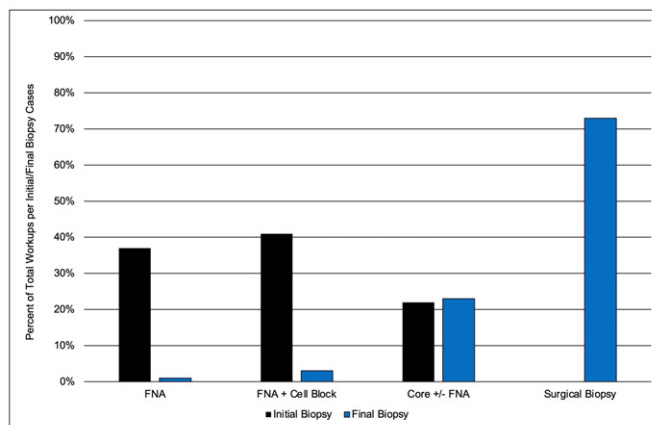


Figure 1. Biopsy Type in Diagnostic Workup of Follicular Lymphoma. Majority of initial biopsies consist of FNA+ cell block or FNA only, while most of the final biopsies are surgical (incisional/excisional) biopsies.

Figure 2 – 284

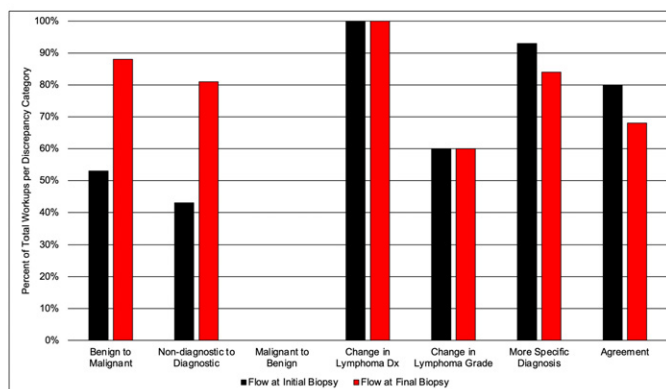


Figure 2. Use of Flow Cytometry in Relation to Diagnostic Discrepancy of Follicular Lymphoma. Flow cytometry is performed in the majority of cases at both the initial and final biopsy and across most categories of discrepancy. Notably, a lower rate of flow cytometry at initial biopsy was seen in the subgroups with non-diagnostic or benign initial diagnoses.

Conclusions: The diagnostic workup of follicular lymphoma using SVB is challenging but can be a very specific method to detect malignancy. Among the repeat biopsy group, no cases of overdiagnosis of lymphoma on SVB were detected (100% specificity), and there was 79% sensitivity for a diagnosis of lymphoma (9% initial benign and 12% initial non-diagnostic biopsies). Flow cytometry appears to increase the sensitivity of SVB for the diagnosis of follicular lymphoma.

285 Ki-67 Index Evaluated on the Fine-Needle Aspiration Specimens of Gastrointestinal Stromal Tumor: The Potential Predictive Value For Histologic Grade

Xi Wang¹, Rita Abi-Raad², Haiming Tang³, Guoping Cai⁴

¹Yale School of Medicine, Yale New Haven Hospital, New Haven, CT, ²Yale School of Medicine, New Haven, CT, ³Yale New Haven Hospital, Yale School of Medicine, New Haven, CT, ⁴Yale University, New Haven, CT

Disclosures: Xi Wang: None; Rita Abi-Raad: None; Haiming Tang: None; Guoping Cai: None

Background: Gastrointestinal stromal tumor (GIST) is the most common mesenchymal tumor of the gastrointestinal tract. It has been increasingly diagnosed by endoscopic ultrasound (EUS)-guided fine needle aspiration (FNA) due to its unique intramural/submucosal location. The WHO has adopted a mitotic rate-based risk assessment of GIST on resection specimen. Whether this risk can be predicted preoperatively on cytology specimens remains unknown. We aimed to determine whether Ki-67 index evaluated on cytologic material can correlate the histologic grade in surgical specimens in an attempt to predict the risk of GIST.

Design: FNA specimens of GIST with adequate cell block material and follow-up surgical specimens were retrieved from the pathology archives. The specimens containing less than 300 tumoral cells on cell block sections were excluded. Ki-67 immunostaining was retrospectively performed on cell block specimens and the Ki-67 index was assessed on the “hot spot” areas of the tumor.

Results: The study cohort included 47 cases from 29 female and 18 male patients with a mean age of 66 years. The most common location was in the stomach (93.6%), followed by duodenum (4.3%) and distal esophagus (2.1%). The tumor size ranged from 1.5 cm to 14.5 cm (mean = 5.6 cm). Based on the histologic grading evaluated on the follow-up surgical specimen, 37 cases (79%) were low grade (LG) and 10 cases (21%) were high grade (HG). The spindle cell type, epithelioid type and mixed type accounted for 63.6%, 11.4% and 25%, respectively. Ki-67 index counted on cell block sections correlated well with the mitotic rate evaluated in surgical specimens ($R=0.76$) (Figure 1). The mean Ki-67 index was 4.4% (range, 0.2%-12.7%) in the HG group and 1% (range, 0-3%) in the LG group. The receiver operating characteristic (ROC) curve of using the Ki-67 index to predict histological grading was further achieved. Using a cut-off (threshold) of 2.8% yielded a sensitivity of 70% at 95% specificity. The AUC (area under the curve) was 0.84 (Figure 2).

Figure 1 - 285

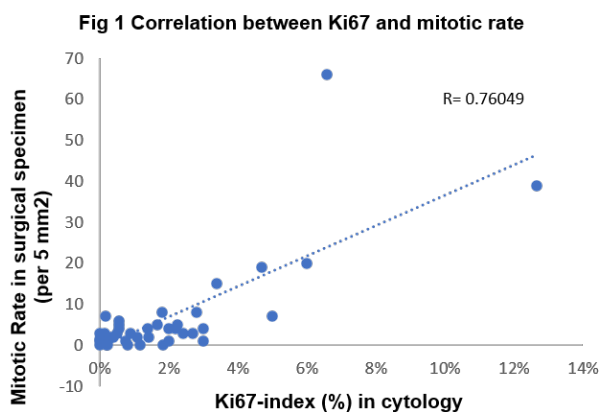
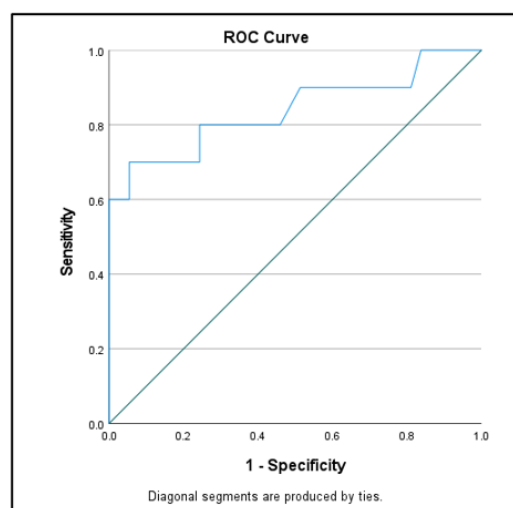


Figure 2 - 285

Fig 2 ROC curve analysis of Ki67 and histology grading



Conclusions: While it is difficult to count mitoses among the limited cell block material, Ki-67 index may offer a promising approach to potentially predict the risk of GIST. Our data demonstrated a good correlation between the Ki-67 index on cytology samples and mitotic rate in subsequent surgical specimens. In addition, ROC analysis showed a good predictive value for histologic grading.

286 Utility of International System for Reporting Serous Fluid Cytopathology for Pericardial Fluid: Cytohistological Correlation and Assessment of Risk of Malignancy

Minhua Wang¹, Tong Sun¹, He (Peter) Wang²

¹Yale School of Medicine, New Haven, CT, ²Yale University School of Medicine, New Haven, CT

Disclosures: Minhua Wang: None; Tong Sun: None; He (Peter) Wang: None

Background: The International System for Reporting Serous Fluid Cytopathology (ISRSFC) has been recently proposed for standardizing pathological reporting of fluid cytology. Its application in pericardial fluid has not been thoroughly evaluated with limited rigorous studies available to date. This study aims to investigate the utility of ISRSFC in categorizing pericardial fluid and assess the diagnostic performance and risk of malignancy (ROM) for each of the diagnostic categories.

Design: All pericardial fluid cases at our institution between 01/01/2019 and 12/31/2020 were reviewed. The diagnoses of these cases were reclassified into 5 categories according to the ISRSFC system: nondiagnostic (ND), negative for malignancy (NEG), atypia of uncertain significance (AUS), suspicious for malignancy (SFM) and malignant (MAL). For calculating ROM and

performance parameters of each category, the absence of malignancy was confirmed by clinical-radiological and/or histopathological follow-ups, while the presence of malignancy was confirmed by subsequent positive fluid and/or flowcytometry and/or malignant histopathological follow-ups from pericardial fluid/pericardium.

Results: The study included 225 pericardial fluid cases. After reclassification, the cases in each category were as follows: ND 0, NEG 171 (76%), AUS 14 (6.2%), SFM 7 (3.1%), and MAL 33 (14.7%) (Table 1). Confirmatory follow-ups were available for 158 NEG (92.4%), 12 AUS (85.7%), 4 SFM (57.1%) and 16 MAL cases (48.5%). The ROM for each category was 0.6% for NEG (1/158), 25% for AUS (3/12), 100% for both SFM (4/4) and MAL (16/16). With MAL and SFM cases considered as positive, while NFM and AUS as negative, the diagnostic performance is as follows: sensitivity 83% (20/24), specificity 100% (166/166), positive predictive value (PPV) 100% (20/20), negative predictive value (NPV) 97.6.4% (166/170), and diagnostic accuracy 97.9% (186/190).

Table 1 Diagnostic categories according to the ISRSFC system and Risk of malignancy (ROM) assessment of pericardial fluid

Diagnostic category	Case #	Case # with confirmatory follow-up	Malignant case #	ROM
Nondiagnostic (ND)	0	N/A	N/A	N/A
Negative for malignancy (Neg)	171 (76.0%)	158 (158/171, 92.4%)	1	0.6%
Atypical of undetermined significance (AUS)	14 (6.2%)	12 (12/14, 85.7%)	3	25%
Suspicious for malignancy (SFM)	7 (3.1%)	4 (4/7, 57.1%)	4	100%
Positive for malignancy (MAL)	33 (14.7%)	16 (16/33,48.5%)	16	100%
Total	225 (100 %)	190/225 (84.4%)	24	

Conclusions: ISRSFC is a highly useful system for pericardial fluid reporting and risk assessment, offering high sensitivity, specificity, PPV, NPV and diagnostic accuracy. The application of this system may help better categorize pericardial fluid, facilitate standardization of cytopathology reporting, and more efficiently convey diagnostic information to improve patients' management.

287 Utility of p53 Immunostaining in Atypical Category in Pancreatic Cytology Specimens

Yan Wang¹, Omid Savari², Hector Ferrer¹, James Gemind¹, Stephen Ganocy³, Caroline Abramovich¹, Santhi Ganesan⁴
¹MetroHealth System, Case Western Reserve University, Cleveland, OH, ²Memorial Sloan Kettering Cancer Center, New York, NY, ³Case Western Reserve University, Cleveland, OH, ⁴MetroHealth Medical Center, Cleveland, OH

Disclosures: Yan Wang: None; Omid Savari: None; Hector Ferrer: None; James Gemind: None; Stephen Ganocy: None; Caroline Abramovich: None; Santhi Ganesan: None

Background: The Papanicolaou Society of Cytopathology System for Reporting Pancreatobiliary Cytology (PSCSRPC) introduced categories to unify diagnoses of pancreatic cytology samples. Among the PSCSRPC categories, the atypical category is problematic and usually results in a repeat procedure to achieve a more definitive diagnosis. However, there is no data about utilizing P53 immunohistochemistry (IHC) in the atypical diagnosis in pancreatic cytology samples.

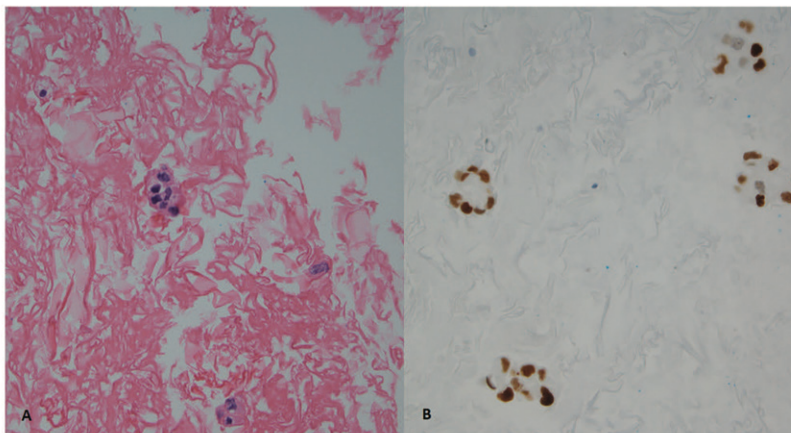
Design: We conducted a retrospective study to review all the endoscopic ultrasound-fine needle aspiration (EUS-FNA) samples of pancreas between 2014 and 2019 in a county hospital. We reclassified them using the PSCSRPC classification system. P53 IHC (BP-53-11, commercially available mouse monoclonal antibody) was applied on formalin fixed, paraffin-embedded sections from the cell blocks of atypical category. Strong nuclear staining in at least 10% of tumor cells was considered as positive.

Results: 47 out of 181 cases (26%) were categorized into the atypical group over a five-year period. In the atypical group, cell blocks were available in 26 cases (55%) out of which 15 cases contained stainable cellular material, and 7 cases were positive for P53 (47% of the stainable cases) (one case's H&E shown in Fig. 1A, its P53 staining result shown in Fig. 1B). All P53 positive atypical cases turned out to be malignant on follow up. Further, the sensitivity and specificity of P53 IHC to identify malignancy in atypical cases are 50% and 100% respectively. The positive predictive value and negative predictive value of P53 IHC to identify malignancy in atypical cases are 100% and 12.5%. On follow up (Table 1), 17 cases of the atypical category had surgical specimens (biopsy or resection), which were diagnosed as malignant in 15 cases, and benign in 2 cases. The P53 stain status of the 15 atypical cases with malignant surgical follow up showed 56% (5 cases) to be positive and 44% (4 cases) negative. P53 was not performed in the remaining 6 cases due to lack of cell block preparation or insufficient cellular material in the cell block.

Table 1. P53 status of the atypical cases with surgical follow up

Category	Follow up #	Follow up	count	p53 positive	p53 negative	P53 not performed
Atypical	17 cases	malignant	15	5	4	6
		benign	2	0	0	2

Figure 1 - 287



Conclusions: In the atypical category, P53 IHC test shows high specificity and high positive predictive value. P53 IHC positivity may help to further refine the atypical category to a suspicious/malignant diagnosis if stainable cell block material is available.

288 Diagnostic Yield of SharkCore Fine-Needle Biopsies and Fine-Needle Aspirations for Pancreatic Ductal Adenocarcinoma

Tiffany Yin¹, Raul Gonzalez¹, Liza Quintana²

¹Beth Israel Deaconess Medical Center, Harvard Medical School, Boston, MA, ²Beth Israel Deaconess Medical Center, Boston, MA

Disclosures: Tiffany Yin: None; Raul Gonzalez: None; Liza Quintana: None

Background: Endoscopic ultrasound-guided fine needle aspiration (EUS-FNA) is currently the standard method used to obtain diagnostic tissue for pancreatic lesions. EUS-FNA is a sensitive procedure, but downsides include lack of architecture and ability to perform ancillary testing. EUS-guided fine needle biopsies (EUS-FNB) have recently seen increased popularity. This study aimed to evaluate the diagnostic accuracy for pancreatic lesions suspicious for pancreatic ductal adenocarcinoma (PDAC) sampled via SharkCore-FNB (SC-FNB) and FNA.

Design: We retroactively searched our departmental archives for cases from patients with a high clinical suspicion for PDAC who had samples taken via concurrent EUS-guided SC-FNB and FNA, spanning from January 2015 to March 2019. Diagnoses rendered by both SC-FNB and FNA were compared. Additional case information including patient demographics, lesion size and location by imaging, and ultimate patient diagnosis were obtained via electronic medical records. Diagnostic results by SC-FNB and FNA were compared using Fisher's exact test and McNemar's Test, with significance set at $P < 0.05$.

Results: We identified 158 cases from 146 patients (73 men and 73 women, with mean age 68 years) with lesions concerning for PDAC that underwent concurrent SC-FNB and FNA. A final clinicopathologic diagnosis of PDAC was made for 118 of these cases (75%). Among these, a diagnosis of PDAC was made on 86 SC-FNB (73%) and 76 FNA (64%). FNA was 64% sensitive and 88% specific in diagnosing PDAC; SC-FNB was 73% sensitive and 88% specific ($P = 0.11$). In 21 cases (18%), SC-FNB was diagnostic but not FNA; out of these 4 were suspicious, 4 neoplastic, 10 atypical, 2 negative and 1 nondiagnostic. In 11 cases (9%) FNA was diagnostic but not SC-FNB. Both modalities were diagnostic in 65 cases (55%). FNA and SC-FNB accuracy in diagnosing PDAC did not differ by site (head/neck vs. body/tail, $P = 0.15$ for FNA and $P = 0.39$ for SC-FNB). Both were more accurate in diagnosing lesions ≥ 2 cm rather than < 2 cm ($P = 0.0008$ for FNA, $P = 0.021$ for SC-FNB), but neither diagnostic modality was statistically superior at this size cutoff.

Conclusions: Samples obtained from pancreatic lesions via SC-FNB and FNA show relatively good concordance. While both methods performed better with larger lesions as expected, differences in diagnostic rates based on lesion location were not statistically significant. Diagnosis of PDAC can be difficult and while SC-FNB has a better diagnostic yield overall, FNA led to a more definitive evaluation in 9% of our cases. As such, our large series suggest that both methods should be utilized to maximize diagnostic yield.

289 Accuracy of Fine Needle Aspiration in the Diagnosis of Non-Pulmonary Mediastinal Lesions, a Single Institutional Experience

Mitchell Zhao¹, Farnaz Hasteh², Jingjing Hu¹

¹University of California, San Diego, San Diego, CA, ²University of California, San Diego, La Jolla, CA

Disclosures: Mitchell Zhao: None; Farnaz Hasteh: None; Jingjing Hu: None

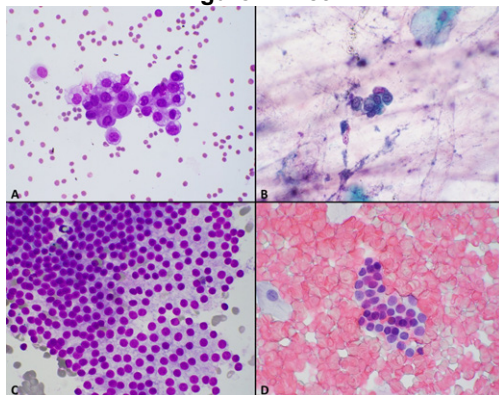
Background: The mediastinum can give rise to a diverse population of mass-like lesions ranging from benign to malignant processes. However, direct surgical management and sampling can pose difficulties given the compartment’s proximity to the heart and lungs. Fine needle aspiration (FNA), performed either transbronchially or endoscopically with ultrasound guidance, is a technique that allows for less invasive sampling to establish a pathologic diagnosis that can guide further management. At this time, there are no standardized systems for reporting mediastinal cytology. Here, we discuss our experience with the accuracy of mediastinal FNA in the diagnosis of non-pulmonary related mediastinal lesions.

Design: Our anatomic database was reviewed for mediastinal FNA cytology cases ranging from 1999-2020 with either concurrent or subsequent surgical pathology. Cases were excluded if there was significant clinical, radiologic, or pathologic evidence of a primary pulmonary malignancy. To evaluate accuracy, the surgical pathology diagnosis was used as the gold standard. Discrepant cases were retrospectively reviewed.

Results: A total of 82 mediastinal FNA cytology cases were identified with 42 cases having an associated surgical diagnosis. One case was excluded in further analysis due to having non-diagnostic surgical pathology. In the 41 remaining cases, a concordant diagnosis was established in 38 cases (92.7%, Table 1). Of the discrepant cases, 1 had a false negative diagnosis due to inadequate sampling. In the other two, the cytology was falsely positive, diagnosed as tumor cells (Figure 1A-B) and atypia (Figure 1C-D) with the final surgical diagnoses resulting as benign, reactive mesothelial cells and normal thymus tissue.

Accuracy of Mediastinal FNA in the Diagnosis of Non-Pulmonary Mediastinal Lesions by Category			
Category	Total Cases	Cases with Concordant Cytology	Accuracy (%)
Non-neoplastic	8	6	75
Thymoma	9	9	100
Peripheral nerve sheath tumor	4	4	100
Lymphoma	6	6	100
Neuroendocrine carcinoma	2	1	50
Other carcinoma	4	4	100
Germ cell tumor	3	3	100
Sarcoma	2	2	100
Neoplasm, other	3	3	100
Overall	41	38	92.7

Figure 1 - 289



Conclusions: Overall, FNA is a useful technique with good accuracy when used for the diagnosis of non-pulmonary mediastinal lesions for both benign and malignant pathology. We propose to imitate and establish a standardized system for reporting cytology in the mediastinum to minimize false positive and false negative diagnoses. Adequate sampling is important to avoid a missed diagnosis. Reactive mesothelial cells continue to serve as a diagnosis pitfall in the evaluation of cytology cases, and pathologists should be wary of their presence in mediastinal cytology.

290 Cytologic Features of Angiosarcoma: A Comparison of Fluid, Fine Needle Aspiration and Imprint Samples from 20 Cases

Zitong Zhao¹, Sangeeta Mantoo¹

¹Singapore General Hospital, Singapore

Disclosures: Zitong Zhao: None; Sangeeta Mantoo: None

Background: Angiosarcoma is an uncommon malignant vascular neoplasm. Cytologic features of angiosarcoma have been well described in fine needle aspiration (FNA) specimens, but rarely reported in fluid or imprint samples.

Design: A search of the laboratory information system for angiosarcoma in cytology in our institution between January 2005 and June 2021 was performed. All pathology reports and available archived slides were reviewed. Cytology features of angiosarcoma were analysed, with cytology-histology correlation.

Results: A total of 20 cytology specimens from 10 patients were identified, including 7 fluid, 11 FNA and 2 imprint samples. Slides from 8 samples were available for review, including 5 fluid, 1 FNA and 2 imprint cases. The majority of patients had a known history of angiosarcoma from skin, heart and breast, except that one patient had ascitic fluid sampled before primary hepatic angiosarcoma diagnosed. The mean age was 67.4 years (range: 59 - 82 years). There was a male preponderance (male:female ratio of 4:1).

All samples showed a variable amount of spindle to epithelioid malignant cells arranged predominantly as singly dispersed cells with some small clusters. Tumour cells exhibited enlarged eccentric nuclei, coarse chromatin and prominent nucleoli. Intracytoplasmic vacuoles were described in 40% (8/20) of cases. Background elements present depended on the sampled site, and were haemorrhagic or necrotic. The cellularity of malignant cells was generally higher in FNA than fluid and imprint samples. Architectural features suggestive of vasoformation, including rosette-like structures, cell whorling and nuclear hugging, were more frequently seen in fluid (100%, 5/5) compared to FNA and imprint (33.3%, 1/3) samples. The cytoplasm of tumour cells was more abundant and dense in FNA samples, while being delicate and wispy in the fluid. Intracytoplasmic vacuoles were slightly more commonly observed in FNA and imprint (66.7%, 2/3) than in fluid (60%, 3/5) samples. Immunocytochemical confirmation was achieved in the cell block preparation of most fluid specimens.

Cytologic features	Fluid	FNA	Imprint
Cellularity	Mostly low to moderate	Moderate to high	Low to moderate
Background	Mesothelial cells, inflammatory cells, maybe haemorrhagic	Sample site dependent elements, maybe haemorrhagic or necrotic	Sample site dependent elements, maybe haemorrhagic or necrotic
Cellular arrangement	Mostly singly dispersed cells, some small clusters	Mostly singly dispersed cells, some small clusters	Mostly singly dispersed cells, some small clusters
Whorls	Often	Sometimes	Rarely
Rosettes, including nuclear hugging	Often	Sometimes	Rarely
Cytoplasm	Little to moderate, delicate	Moderate to abundant, dense	Moderate to abundant, dense
Intracytoplasmic vacuoles	Sometimes	Sometimes	Sometimes
Nuclei	Eccentric	Eccentric	Eccentric
Chromatin	Coarse	Coarse	Coarse
Nucleoli	Prominent	Prominent	Prominent

Figure 1 - 290

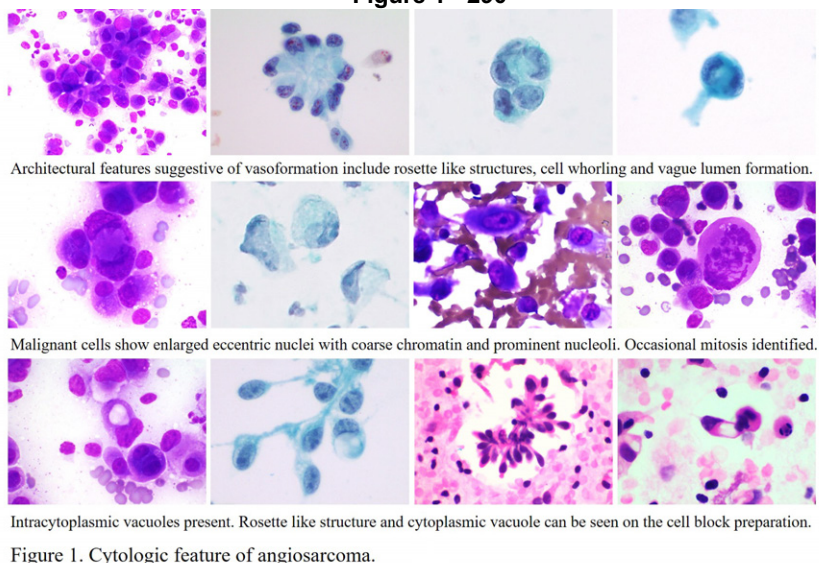
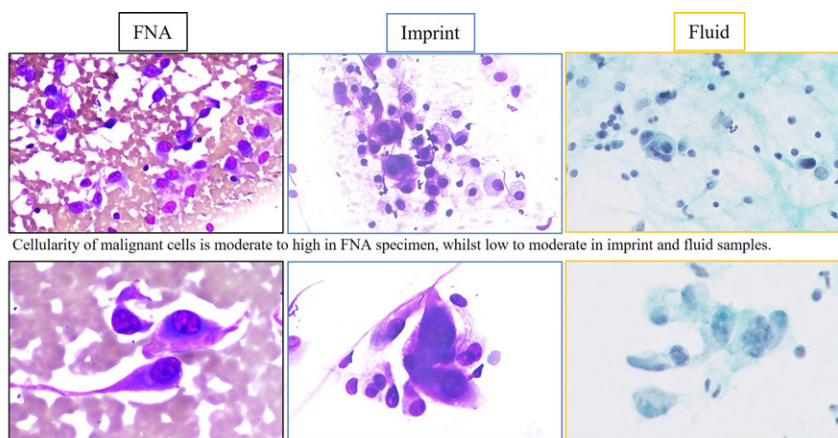


Figure 1. Cytologic feature of angiosarcoma.

Figure 2 – 290



Cellularity of malignant cells is moderate to high in FNA specimen, whilst low to moderate in imprint and fluid samples.

Cytoplasm is dense in FNA and imprint samples, while relatively delicate and wispy in the fluid sample. Nuclear features are similar throughout, with enlarged eccentric nuclei, coarse chromatin and prominent nucleoli.

Figure 2. Comparison of cytologic features in FNA, imprint and fluid samples.

Conclusions: Cytologic features of angiosarcoma in the fluid samples closely mimic those of metastatic adenocarcinoma, which can be treacherous without a known history. Well recognition of different features of angiosarcoma in various cytology specimens can help with the correct diagnosis.

291 SOX6 Expression Distinguishes Mesothelioma from Reactive Mesothelium and Metastases in Pleural Fluid Cytology

Melissa Zhao¹, Edward Richardson², Jason Hornick², Marina Vivero¹

¹Brigham and Women's Hospital, Boston, MA, ²Brigham and Women's Hospital, Harvard Medical School, Boston, MA

Disclosures: Melissa Zhao: None; Edward Richardson: None; Jason Hornick: *Consultant*, Aadi Biosciences, TRACON Pharmaceuticals; Marina Vivero: None

Background: Mesothelioma is a challenging diagnosis to make on cytology specimens due to morphologic overlap with reactive mesothelium and other malignancies. Commercially available antibodies that reliably distinguish mesothelioma from reactive mesothelial cells and metastatic tumors are lacking. Differential expression of SOX6 (SRY-box transcription factor 6), a tumor

suppressor gene, has recently been shown to distinguish mesothelioma from lung adenocarcinoma. We aim to study the utility of SOX6 expression in pleural fluid cytology for the diagnosis of mesothelioma versus reactive proliferations and other metastatic malignancies.

Design: Immunohistochemistry (IHC) for SOX6 was performed on 80 archival formalin-fixed paraffin-embedded pleural fluid cell blocks, including 32 mesotheliomas (including biphasic and epithelioid subtypes), 17 reactive mesothelial proliferations, and 31 metastatic carcinomas including lung, breast, esophageal, and Mullerian adenocarcinomas. Percentage of cells positive for SOX6 was recorded for each case. Intensity of staining was scored as absent (0), weak (1+), moderate (2+), or strong (3+). The sensitivity and specificity of SOX6 according to the scores were analyzed using receiver operating characteristic (ROC) curves. Hierarchical clustering was performed on all four scoring percentages. Intraclass correlation coefficients (ICC) were calculated to assess scoring concordance between two raters. All statistical analyses were performed using R 4.1.1.

Results: Among all four measures of intensity scoring for SOX6, percentage of cells negative and 3+ positive for SOX6 showed the best performance in distinguishing mesothelioma from all other samples (ROC 0.83, 0.79) and from reactive mesothelial cells (ROC 0.73, 0.79). A higher percentage of SOX6 negative cells is associated with non-mesothelioma samples. Hierarchical clustering revealed a cluster of samples with high degree of 3+ SOX6 positivity (>50%) comprising mesothelioma samples only, and highlights that a high degree of 1+ and 2+ SOX6 positivity (>50%) is only seen in 2/49 non-mesothelioma specimen types. ICC coefficients between two raters for degree of 0, 1+, 2+, and 3+ SOX6 staining are 0.83, 0.13, 0.70, and 0.94, respectively.

Conclusions: SOX6 immunohistochemistry may be a useful component of an IHC panel to help differentiate mesothelioma from other processes in pleural fluid cell block preparations. Intensity scoring is concordant between raters, particularly for percentage of absent and strong SOX6 staining.